UNIVERSITY OF CALIFORNIA,
IRVINE

Laminated Microfluidic Coupon Systems for Biological Applications
DISSERTATION

Submitted in partial satisfaction of the requirements
for the degree of

DOCTOR OF PHILOSOPHY

in Electrical Engineering

by

Sara Saedinia

Dissertation Committee:
Assistant Professor Mark Bachman, Co-Chair
Professor G. P. Li, Co-Chair
Professor Fadi Kurdahi

2014

DEDICATION

To

My mom

My family and my loved ones

Without you this wouldn't have been possible!

A river cuts through a rock not because of its power but its persistence.
"Anonymous"

A little more persistence, a little more effort, and what seemed hopeless failure may turn to glorious success.
"Elbert Hubbard"

TABLE OF CONTENTS

LIST OF FIGURES/GRAPHS/TABLES

Chapter 1.

Chapter 2.

Chapter 3.

Chapter 4.

Chapter 5.

Chapter 6

Chapter 7

ACKNOWLEDGMENTS

Starting, working and finishing a Ph.D. is not just getting another degree. It is a lifestyle and it changes one's mindset for the rest of her life. It is a journey filled with a lot of hard work, experiences, and countless number of failures and at the end the success. This journey was not though possible without guidance, advise, inspiration and experience of others. For me this journey was made possible with the guidance of Professor Mark Bachman. I would like to express the deepest appreciation to my committee chair, Professor Bachman who did not just helped me finished this journey but he has taught me not to be just a one-dimensional person and be more than just a Ph.D. He has taught me to be a good researcher as well as an entrepreneur. He continuously pushed me, and conveyed a spirit of adventure and excitement in me. He taught me not to be afraid of failures and more importantly he believed in me.

I also, have my utmost respect for my other adviser professor G.P. Li who has always been there for me during my hardships and failures to give me spirit, advise and to give me the courage to keep on going. His guidance has always given me the hope to see the light at the end of the tunnel.

A special thank goes to Dr. John Krolewski, and Dr. Kent Nastiuk for introducing my main project and for always pushing me in the right

direction. Their valuable guidance has helped me learn so much about biology and chemistry side of my research as an engineer.

I am grateful to my past and present colleagues at the Li-Bachman/ MIDAS/Resonance lab for creating a stimulating and at the same time friendly environment to work at. They have become not only colleagues but also my friends who helped and taught me many lessons and inspired me to come up with new ideas. I like to specially thank my mentor and my friend Dr. Lily Wu who held my hand when I started working in this lab and also excited me about the field of microfluidics. I would like to thank Sarkis Babikian for being my teammate for the microfluidic microvalve system. He has become a close friend that I can rely on and a teammate that was countable and extremely helpful in resolving some of the challenges we encountered during the development of microvalve system. I also like to mention Jason Luo whom I have spent many hours in the lab with and appreciate his sense of humor, which has helped me to go through long nights of working on research experiments. I also like to mention other people in the lab and INRF group for their help and support including Michael Klopfer, Nuthan Hegde, Kevin Limtao, Tina Tom, Renee Pham, Richard Chang, Aki Muranami, Spencer Chang, Sun Vu, Dr. Mark Merlo, Dr. Minfeng Wang, Dr. Peyton Paulick, Dr. Lifeng Zheng, Jonas Tsai, Dr. Sungjun Kim, Dr. Nizan Friedman, Dr. Arthur Zhang, Jason Park and Brittany Gray.

I am also so grateful for having my friends supporting me through these years and helped me get through this journey by their continuous encouraging words. I would like to specially thank Anahita Fazl, Ruja Kia, Dr. Hamid Towhidian, Shahrzad Tavakol, Maryam Moghadam, Dr.Parastoo Derakhshanian, Dr. Mitra Hooshmand, Dr. Shabnam Moobed, Donna Ghalambor, Dr. Nader Kalantari, Dr. Alireza Hodjat, Dr. Amirali Kia, Dr. Darya Mohtashemi, Dr. Artin Der Minassian, Azar Eshraghi, Sara Sedaghat, Dr. Mahshid Fardadi, Dr. Mehryar Rahmatian, Dr. Ali Azadani, Dr. Reza Miraghaie, Omid Koohi, Dr. Solmaz Torabi, Dr. Amin khajeh, Maryam Shakib, and Gelila Solomon.

Lastly, I would like to express my gratitude for the ones that are dearest to my heart and who have loved me unconditionally. I would like to dedicate this doctoral degree to my mother, Sibel Sahebjamei, who has sacrificed her life, her comfort and has gone through many hardship to bring my sister and I to the United States and raised us here on her own. I thank her for believing in me and being my backbone all through my life. She has taught me persistence and hard work. Her continuous support has given me the drive to get through the time of frustration and difficulties. I like to acknowledge my dad for his wisdom words. I would like to thank my Sister Shadi Saedinia and my brother-in-law Peter Melnyk, my nephews Cyrus and Soren who have brought joy and inspiration to my life. My family has given

me the strength, the wisdom, unconditional love and trust to finish this chapter of my life successfully and forever I am grateful to them.

Sara Saedinia

October 22, 2014

CURRICULUM VITAE

SARA SAEDINIA. Ph.D.

2414 Verano Pl. Irvine, CA 92617 | Phone: (619) 602-3645 |email: saedinia.sara@gmail.com

PROFILE

- 8 years of combined experience in research and engineering in the field of electrical engineering and biomedical engineering.
- Energetic, focused and resourceful team player with proven abilities in research, analysis, communications, projects design and implementation.
- Excellent written and oral communications skills and a strong leader who can work independently and in a team. Detail-oriented and a self-starter. Published peer-reviewed articles and have given presentations to technical and non-technical audience.
- Hands-on experience in multi-disciplinary research field to bring engineering solutions to solve complex biological processes.

EDUCATION

University of California, Irvine
Ph.D. Electrical Engineering 2009-2014
(National Science Foundation Graduate Research Fellow)
M.S. Electrical Engineering 2007-2009

University of California, Berkeley 2002-2004
B.S. Electrical Engineering

PROFESSONAL WORK AND RESEARCH EXPERIENCE

UNIVERSITY Of CALIFORNIA, IRVINE

Research Assistant 2009-2014

- Managed and lead a team of researchers in multiple collaborations and mentored undergraduate students.
- Developed and implemented a novel approach for microfluidic chip production aimed for rapid, low-cost manufacturing, and integration of multi-material systems resulted in fabrication and testing a protein analysis assay, and a microvalve system.
- Results of the research have been published in a highly ranked peer review journal "Biomicrofluidics" and multiple times at professional conferences.

Teaching Assistant
2008/2009/2012

- Developed leadership skills by managing a class of over 200 undergraduate students.
- Developed communication skills by lecturing and presenting complex concept to students.
- Organized discussion sessions and designed homework and examination test problems in electronics design, discrete time signal and systems and network analysis courses.

BROADCOM INC.

Intern 2008-2009

- Helped with design characterization and testing of an Analog to Digital Converter.
- Responsible for creating a GUI software using Visual Basic for testing toners in an Analog lab.
- Worked closely with the designers and other test engineers to test the functionality of toners.

ANALOG DEVICES INC.

Applications Engineer 2006- 2007

- Responsible for writing datasheets, application notes, and PSpice modeling for the new product releases.
- Prepared and presented technical presentations to other engineers as well as customers.

- Participated in defining the new standard amplifiers, voltage references and ASSP products.
- Traveled and visited domestic and international customers to understand their needs and provided extensive technical support for their design decision making using Analog Devices products.

Product Engineer 2005-2006

- Team leader and responsible for the new product evaluation, characterization, qualification, and release.
- Responsible for all aspects of assigned manufacturing devices from release to production in order to meet the scheduled deadline.
- Responsible for datasheet graphs and working closely with the applications engineer for creating the datasheet specifications.

Summer Intern 2004

- Built hardware and software solutions for calibrating a voltage regulator.
- Worked on a solution for connecting any remote diode sensor to a thermal diode for thermal evaluation purposes.
- Worked with and tested the EEProm on a new ADI part.
- Helped to find an optimum solution for a frequency to resistance converter.

SKILLS

COMSOL, SolidWorks, LabView, Cadence, MATLAB, Freehand, Adobe Illustrator, Verilog, Visual Basic, Scheme, JAVA, C, MIPS, HTML, PSpice, HSpice, and Microsoft office. Knowledge of lithography, micromashining, laser cutting techniques, microfluidic design and fabrication techniques such as hot embossing, injection molding, lamination and electrochemical etching.

SELECTED AWARDS & SCHOLARSHIPS

- ARCS Foundation Scholarship
- National Science Foundation IGERT LifeChips Fellowship
- National Science Foundation GAANN Fellowship
- Excellent presentation Award in the FLINT-CIBI Conference
- San Diego Mesa College, Class of 2002: Valedictorian Commencement Speaker
- Associated Student Community Service Scholarship
- Associated Student Leadership Scholarship
- Board of Trustee Scholarship
- Alpha Gamma Sigma Scholarship
- Women in Technology International: Member

PUBLICATIONS/CONFERENCE PROCEEDINGS/PRESENTATIONS

1. S. Saedinia, K. Nastiuk, J. Krolewski, G.P. Li, M. Bachman "Laminated microfluidic system for small sample protein analysis", Biomicrofluidics, 8 (2014).
2. S.Saedinia, Kevin Limtao, Kent Nastiuk, John Krolewski, G.P. Li, M. Bachman "Laminates for Miniaturized Integrated Bioelectronic Protein Analysis Systems", Electrical Components and Technology Conference Proceedings, USA, 2013.
3. S. Saedinia, K. Limtao, K. Nastiuk, J. Krolewski, G.P. Li, M. Bachman "Micro-scale immunoblotting for small sample protein analysis". CADMIM Meeting, Poster, USA, 2013
4. S. Selimovic, S. Saedinia, M. R. Dokmeci and A. Khademhosseini, " Research Highlights", *Lab Chip*, 2012, 3217-3220.

5. S. Saedinia, K. Nastiuk, J. Krolewski, G.P. Li, M. Bachman "Micro-scale immunoblotting for small sample protein analysis" MicroTotal Analysis Systems Conference Proceeding. Japan, 2012.
6. S. Saedinia, K. Limtao, K. Nastiuk, J. Krolewski, G.P. Li, M. Bachman "Small Sample Protein Preconcentration Utilizing Photo-patterned Tracked-etched Membrane" Biomedical Engineering Society Conference. USA, 2012.
7. 3rd International Symposium on LifeChips , " Micro-scale immunoblotting for small sample protein analysis". Poster, USA 2012
8. S. Saedinia, K. Nastiuk, J. Krolewski, G.P. Li, M. Bachman Lab Automations Conference 2011, " Micro-scale immunoblotting for small sample protein analysis". Poster, USA, 2011
9. MF3 Conference, " Micro-scale immunoblotting for small sample protein analysis". Poster, USA, 2010.
10. ASME 2010, Frontiers in Biomedical Devices, " Micro-scale immunoblotting for small sample protein analysis". Oral Presentation, USA, 2010.

ABSTRACT OF THE DISSERTATION

Laminated Microfluidic Coupon Systems for Biological Applications

By

Sara Saedinia

Doctor of Philosophy in Electrical Engineering

University of California, Irvine, 2014

Assistant Professor Mark Bachman, Co-Chair
Professor G.P. Li, Co-Chair

The complexity of current microfluidic systems and the need for costume-designed fabrication, which leads to costly manufacturing, are obstacles in microfluidic technology. These complications have kept this technology from becoming commercially available like semiconductor technology.

This dissertation describes a novel technology based that is based on lamination, which allows for the production of highly integrated 3D devices suitable for performing a wide variety of microfluidic assays. This approach uses a suite of microfluidic coupons ("microfloupons") or in short "μFloupons" that are intended to be stacked as needed to produce an assay

of interest. Microfloupons may be manufactured in paper, plastic, gels, PCBs, or other materials, in advance, by different manufacturers, and then assembled by the assay designer as needed. To demonstrate this approach, this dissertation explains different practical applications of this technology. First, we designed, assembled, and characterized a microfloupon device that performs sodium-dodecyl-sulfate polyacrylamide gel electrophoresis (SDS-PAGE) on a small sample of protein. This device allows for the manipulation and transport of small amounts of protein sample, tight injection into a thin polyacrylamide gel, electrophoretic separation of the proteins into bands, and subsequent removal of the gel from the device for imaging and further analysis. The microfloupons are rugged enough to handle, and can be easily aligned and laminated, allowing for a variety of different assays to be designed and configured by selecting appropriate microfloupons. In the second application, a microvalve system is described, which is actuated by electromagnetic force and is manufactured in paper-polymer structures. The microvalve has latching capability, which makes it suitable for low-power applications.

This approach provides a convenient way to perform assays that have multiple steps, relieving the need to design highly sophisticated devices that incorporate all functions in a single unit, while still achieving the benefits of small sample size, automation, and high speed operation.

CHAPTER 1

Introduction

1.1 Microfluidic systems and μTAS in biology

A major vision in the field of biological and medical sciences is to precisely and accurately determine relevant parameters in a short amount of time.[1,2] However, many conventional laboratory methods and techniques in the area of biology and chemistry require fluid handling which involves time-consuming and repetitive manipulation tasks.

A great number of biochemical tests and corresponding detection systems/devices have been developed to allow the detection of those parameters for DNA and protein analysis, drug discovery, diagnostics and environmental sciences.[3–7] Over the last thirty years the development of such systems is becoming more and more focused on trying to fully integrated analysis of complex samples, i.e. human whole blood, with minimal manual handling steps and reduced reagents consumption that can be achieved by miniaturization.

For this reason, the area of microfluidics, also known as lab-on-a-chip (LOC) or micro-total-analysis-system (μTAS) has gained considerable attention in recent decades. Microfluidics enables the manipulation of very small volumes of fluids with the dimension of tens to hundreds of micrometer devices[8] and

has the potential to significantly change the way modern biology is performed. The basic idea of μTAS is to increase the performance of an analysis system by downsizing.

Inspired by the success of commercial semiconductor industry which benefits tremendously by miniaturization of the integrated circuits, numerous activities in this field have been focused on silicon integrated circuit manufacturing, leading to the high number of actual available products, like processors, memories, cell phone components and many others. With time, these technologies provided the basis for micro-scale systems and devices in silicon as well as in other types of materials, like glass, plastics, polymers etc. Since the 1990's, representative mass market Microelectromechanical Systems (MEMS) products have emerged, such as digital optical switches[9], physical parameters sensing like acceleration[10], pressure sensors[11], inkjet printer nozzles[12] and microactuators[13].

Subsequently, these market breakthroughs have induced the development of chemical, biosensing, diagnosis and biomedical microsystems: the benefits associated with miniaturization of bioanalytical techniques include the potential for shorter reaction times, ultra- low reagent consumption, higher throughput, portability, versatility in design and the possibility of integration with other systems.[14–20]

Advances in microfluidics technology offer exciting possibilities in the realm of enzymatic analysis (e.g., glucose and lactate assays), deoxyribonucleic

acid (DNA) analysis [e.g., polymerase chain reaction (PCR) and nucleic-acid sequence analysis], proteomic analysis involving proteins and peptides, immunoassays, and toxicity monitoring. An emerging application area for microfluidics-based biochips is clinical diagnostics, especially immediate point-of-care diagnosis of diseases.[21]

To achieve these goals, many fabrication methods have been introduced.

Microfluidic fabrication depends on the material employed. Early devices were made mainly of silicon and glass substrates using standard photolithographic and etching techniques[22,23] Due to high manufacturing costs of microfluidic devices in glass and silicone, disposable polymer materials are of increasing interest. Several polymers, including poly(methylmethacrylate) (PMMA)[24–26], poly(dimethylsiloxane) (PDMS)[27–30], polycarbonate (PC)[31,32], polyester[33,34], polystyrene (PS)[35,36] and poly(ethyleneterephthalate) (PET)[37], have been employed[38]. Using different manufacturing techniques and different materials, certain microfluidic commercial products are now available on the market such as Agilent 2100 along with its cell assay extension[39], and Mobidiag's DNA based detection of sepsis-causing bacteria.

In the following sections, I will present overall conventional microfabrication techniques of the mostly common materials used to fabricate microfluidic and μTAS devices. These materials are categorized into two groups: conventional and non-conventional materials.

1.2 Conventional microfluidic fabrication materials/techniques

1.2.1 Silicon

Silicon is one of the early materials employed to fabricate microfluidic systems. A motivating force behind choosing silicon material was the field of microelectronics. The initial expectation of microfluidics was that photolithography and associated technologies that had been so successful in silicon microelectronics and microelectromechanical systems (MEMS), would be directly applicable to microfluidics.[8] Batch type microfluidic fabrication similar to microelectronics industry was another goal. Similar to microelectronic fabrication, photolithographic patterning of layer structures on the surface of silicon wafers was used to produce microchannels. The steps to create microchannels were identical to those in microelectronic systems. First a thin film coated the silicon layer by thermal deposition, spin coating, photoresist deposition, physical vapor deposition (PVD), sputtering, etc. A layer of photoresist was then spin coated on top of the silicon oxide layer. In the next step, a mask was placed on top of the wafer. A photo-mask was a stencil used to transfer a desired pattern or geometry to a resist. Photolithography techniques were used to transfer a layout pattern from mask onto the photosensitive film using UV, x-ray or electron beam lithography. Then the channels were etched using wet chemical process or as a plasma process. The process of micromachining microfluidic channels is shown in figure 1.

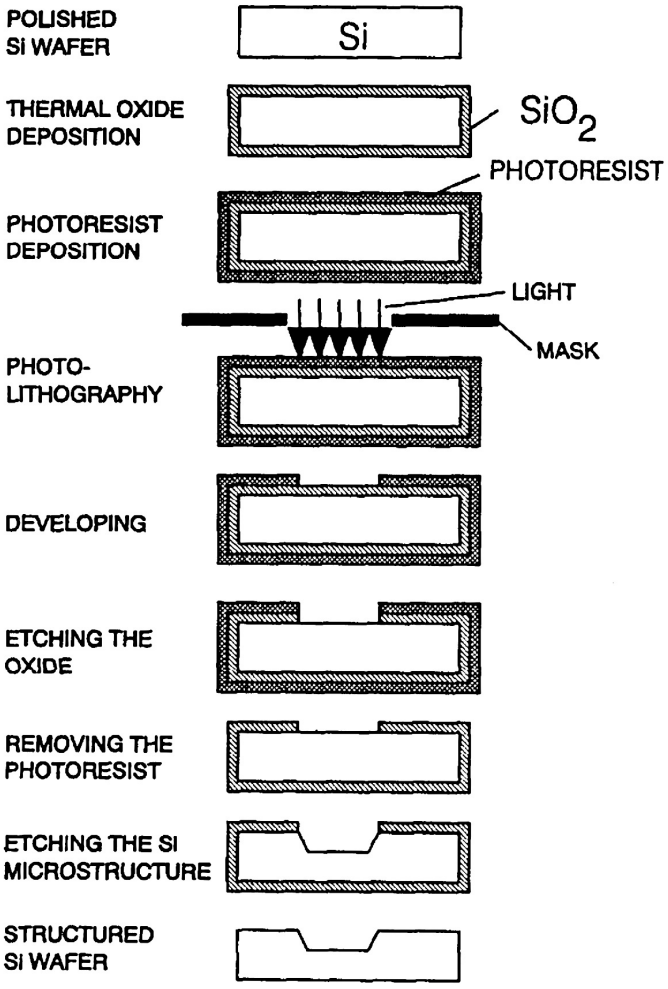

Figure 1. Process steps of a standard one-mask micromachining procedure to etch a channel structure into silicon.[40]

After the channels were fabricated, bonding, which refers to the assembly of structures whether it would be silicon-to-silicon, silicon-to-oxide, silicon-to-glass, or some other combination of materials, was performed. Different techniques such as anodic bonding technology[40] or hydrophilic fusion bonding technology[41] were employed. Due to the planarity of the surfaces used, bonding usually led to fusion of the assembled structures and a perfectly tight seal.[42]

However, for analyses of biological samples in water, devices fabricated in silicon were usually unnecessary or inappropriate. Silicon is expensive, and opaque to visible and ultraviolet light, so it cannot be used with conventional optical methods of detection. It is easier to fabricate the components required for micro-analytical systems — especially pumps and valves — in elastomers than in rigid materials. Additionally, the properties of silicon are not compatible with living mammalian cells.[8] Due to these drawbacks in today's microfluidic technology, silicone is no longer an appropriate material of choice to fabricate microchannels.

1.2.2 Glass

One of the widely used materials that is still employed today for fabrication of microfluidic systems is planar glass substrate. Electrokinetic pumping became the method of choice for transporting liquid samples in microchannels and various glass materials took the place of silicon, since the conductivity of silicon at high voltages was problematic for electroosmotic flow.[43] In electroosmotically driven systems, it is critical that the substrate provides an electrical insulating environment so the voltage drop occurs across the fluid-field channel rather than the substrate. Since silicon is a poor insulator, glass became the material of choice. Various types of glass, especially fused silica glass (SiO2) and Pyrex, are significant in microfluidics due to the inertness against heat and chemicals as well as high optical

transmission range (180-2500nm) and low optical absorbance. Many researchers have developed various methods to fabricate microchannels in glass.[38,44,45] Among those, photolithography, wet-chemical etching[45], dry etching, laser ablation and thermal fusion bonding are the common operations for the fabrication of planar microfluidic elements. In general, this process involves masking a glass substrate with a metal layer, followed by lithographic patterning of the metal mask. The exposed glass is then etched with an HF- based solution to produce channels in the glass, and the mask is then removed.

There are two techniques for etching the glass substrate: wet and dry etching. In the wet etching technique, the process occurs on an exposed glass surface, so the walls of the channels are not parallel to each other. As the channels etch deeper, the walls also get etched. As a result, the channels become wider at the top than at the base. One of the difficulties associated with the fabrication of these devices is the etching process used to produce the microchannels. It is difficult to produce narrow channels with reasonable depths due to the isotropic nature of the etching, resulting in severe mask undercutting. In contrast, dry etching techniques such as deep reactive ion etching, or laser ablation produce deep channels with parallel sides. Problems with the dry etching technique, however, are the low etching rate and the low etching selectivity between glass and photoresists. Using mechanical tools is less common among methods of fabricating patterns on

the glass substrate. Laser ablation and mechanical processes lead to a rough surface and fabrication of the smooth surface as it is shown in figure 2 is difficult. To overcome these obstacles, Shoji et al., have recently introduced a new method of glass fabrication where first they make an inverse pattern of the design on silicon mold and then vacuum seal borosilicate glass to silicon. The glass-silicon is heated to 1100 to pass through the glass transition and melt the glass to create the patterns on the glass. With this method, they produced microchannels up to 50μm in depth.[46]

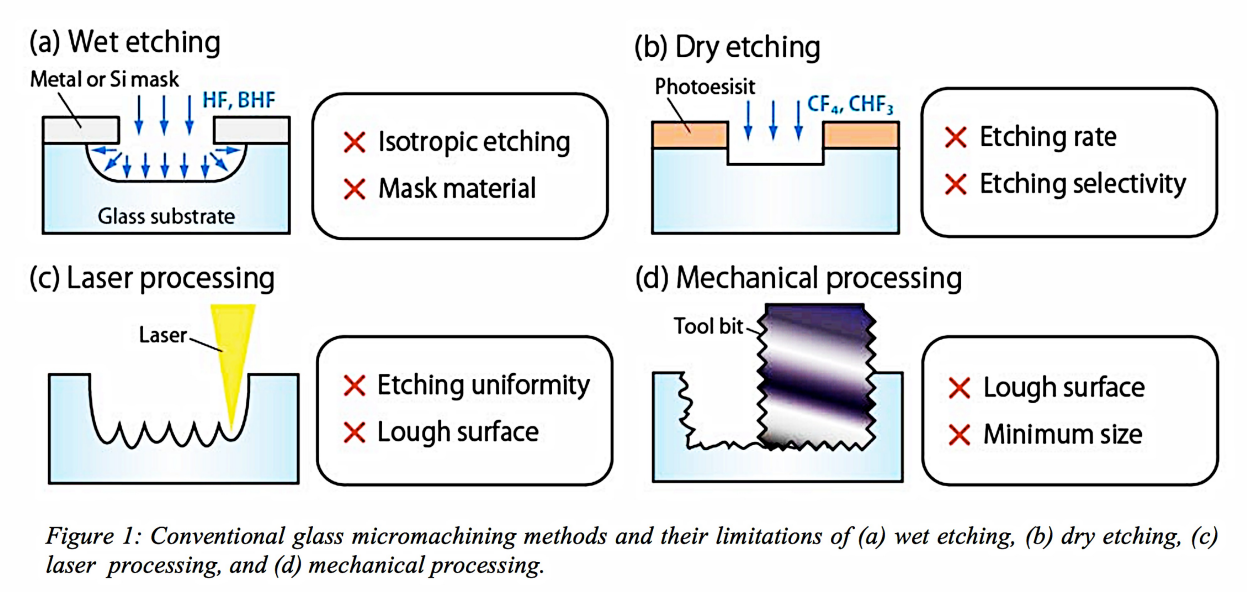

Figure 1: Conventional glass micromachining methods and their limitations of (a) wet etching, (b) dry etching, (c) laser processing, and (d) mechanical processing.

Figure 2. Conventional glass micromaching methods and their limitations of (a)wet etching (b) dry etching (c) laser processing and (d) mechanical processing.[46]

After channel's microfabrication, the device must be assembled enclosing the channel networks or microstructures to allow fluids to flow through the device. In most cases, a cover glass plate encloses the channels. The procedure for glass-to-glass bonding is not always straightforward. Thus,

various bonding methods such as anodic bonding, silicon fusion bonding and thermal bonding have been developed.[22,47–49]In some studies, melting the top and bottom glass plates of each device together under controlled conditions created thermal bonding. Even after placing steel weights on top and heating over 500°C for a few hours, the process completes overnight, and some regions do not bond properly. In one study, Chiem et al. temporarily bonded the top and bottom glass layer at room temperature by rigorous cleaning, which involved washing and drying the glass layers several times using a high power washer, but they too used thermal bonding when permanent bonding was desired.[48] Nevertheless, each of these techniques require high cost instrumentation, set-up and maintainace.[38] Due to the high-cost, the microfluidic devices are not suitable for disposable applications. In addition, silica-based substrates are a good process to create channels with low aspect ratios due to isotropicity of the etching process. The aspect ratio is defined as a feature's height divided by its width. Typically, aspect ratios for glass channels etched chemically fall in the range of 0.25 to 1. Low aspect ratios limit researchers to simple and shallow trapezoidal channels.

1.2.3 Polymers

Polymers are the most commonly used material of choice for fabrication microfluidic devices. Commercial manufacturers of microfluidic devices see

many benefits in employing plastics that include reduced cost and simplified manufacturing procedures, particularly when compared to glass and silicon. Mass replication technologies such as hot embossing and injection molding as well as fast prototyping such as laser micromachining and casting make polymers an excellent candidate for microfluidic fabrication. Another feature that make polymers so enticing as platforms for microchemical applications is the wide selection of polymers with various physical properties that can be used. Because of the diverse physical and chemical properties of polymers and the ability to effectively machine them, a polymer can conceivably be found to suit any particular application. Careful consideration is necessary choosing a polymer for a particular application.[50]

The first important characteristic in choosing the right polymer for a certain application is its machinability. The chosen material must satisfy the application requirements. Some of these requirements include its rigidness or softness, transparency, UV absorption, biocompatibility. One important property in fabrication of polymers is transition temperature, T_g is the temperature at which a polymer is 'softened' due to the increased movements of amorphous chains within the polymer upon heating. This is an important parameter in polymer fabrication since if the temperature is raised about T_g, the material becomes plastic-vicious making it moldable. At the same time, it is important to cool the polymer down below T_g before de-molding it to ensure proper pattern transfer and geometry stability.[43]

Polymers can be classified into three categories based on their molding behavior: thermoplastic, elastomeric, and duroplastic polymers. Thermoplastic polymers have weak chain molecules. Above T_g they become plastic and can be molded while retaining the mold shape after cooling down. Elastomers have even weaker cross-linked polymer chains, which means the molecules can withstand an outside force and stretch when the force is applied. As soon as the external force is removed, they relax to their original state. They behave the same as thermoplastic against thermal molding. The last category, duroplastics, have strong cross-linked chain that makes them brittle and hard to mold.[43]

One important advantage of using polymers is the promise of low-cost replication. For example, in the mold fabrication technique, a master mold, which is the one time most expensive part of the process, is fabricated and the rest of the replication is done using the master mold.

There are several methods for fabrication of master mold. Micromachining, electroplating, and silicon micromachining are some of the common methods for mold fabrication. With the modern micromachining techniques, structures in the 10 μm range can be made. This is a fast way of producing relatively easy structures without using masks. However, this method is not suitable for high aspect ratio or very small structures. One of the common methods of mold production is electroplating, resulting in a replication master made out of nickel or a nickel alloy. In this method, a metal layer is grown over a

substrate by photolithographic techniques and structures as high as 1 mm can be fabricated. The downside of using this method is the slow metal growth time and the fragility of the structures, which sometimes tend to bent the master. The silicone micromachining is another method in which the silicone wafer is etched away either by wet or dry method using lithographic techniques. The depth of etching is much less than electroplating up to 200μm.[43]

Other techniques for polymer microfabrication include hot embossing, injection molding, casting, and just direct fabrication. Hot embossing is a replication process that has been used extensively in microfluidic applications.[51–54] The technology of hot roller embossing is mainly motivated by the aim of high-throughput production of microstructures. The microstructures are fabricated using either silicon micromachining or LIGA (a German acronym for lithography, electroplating, and molding) processing. In this process, the master mold from nickel or nickel-alloy is fabricated by electroplating over an appropriate photoresist. LIGA is a more desirable technique since higher aspect ratio structures can be produced. After the master mold is fabricated, it is mounted with the substrate polymer material and placed under the vacuum to remove trapped bubbles, which may cause errors in production. Then the temperature of the substrate is raised to above T_g, and the master leaves an impression on the substrate. While the pressure between the master and substrate is still on, the temperature is

slowly brought down to below T_g and the substrate contains and maintains the features.

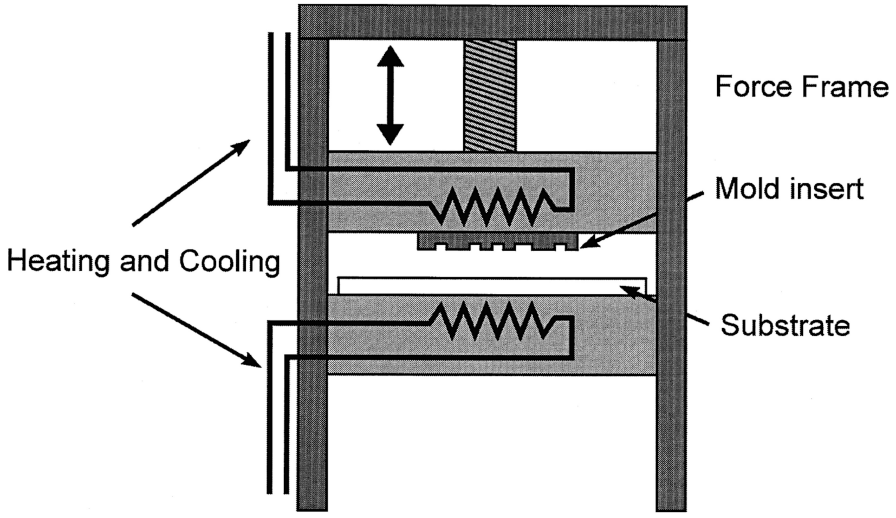

Figure 3. Schematic diagram of hot embossing[43]

Micro-injection molding is a very different process than hot-embossing in that thermoplastic material has to be melted rather than being "softened". After melting the material in a heated barrel, it is forced under pressure inside a mold cavity and subjected to holding pressure for a specific time to compensate for material shrinkage. The material solidifies as the mold temperature is decreased below the glass transition temperature of the polymer. After sufficient time, the material freezes into the mold shape and gets ejected, and the cycle is repeated. A typical cycle lasts between few seconds and few minutes, which makes it a great candidate for rapid and disposable device production.

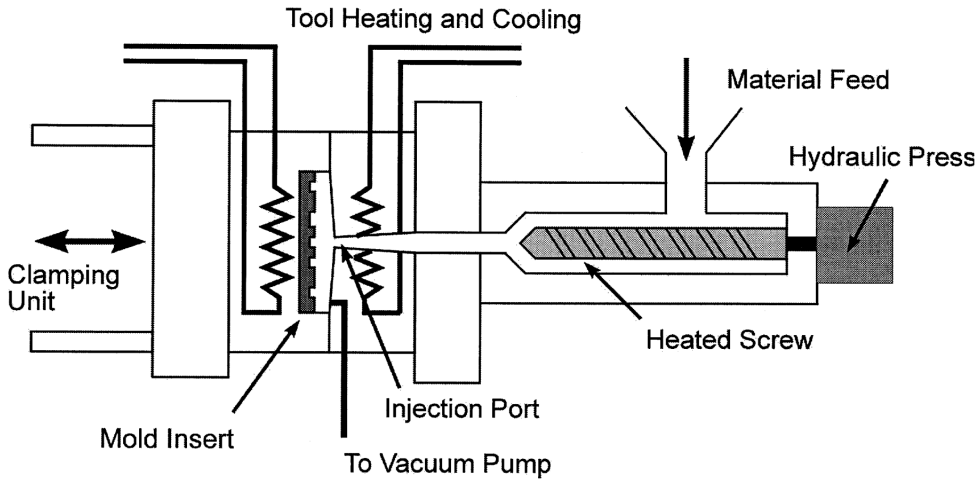

Figure 4. Schematic diagram of injection molding machine.

In general, polymers have the necessary characteristics to be successful platforms for a variety of chemical applications. Most polymers have desirable dielectric strengths, which allow the application of the high electric fields needed in high voltage applications such as electrophoresis. Polymers, however, have thermal conductivities that are somewhat inferior to glass, thereby requiring small channels to prevent significant Joule heating. Joule heating results from the inevitable volumetric heating when an electric field is applied across conducting media such as electrolyte.[55] Another concern is that polymers are typically opaque in under UV light and thus may generate background fluorescence with laser-induced excitation. Finally, careful consideration must be given to the organic solvent used in the assay and its compatibility with the polymer, whereas in glass, most organic solvents have no detrimental effects on this substrate.

1.3 Non-conventional microfluidic fabrication methods

Since year 2007, besides the conventional microfluidic devices, a new class of passive microfluidic analytical devices were introduced that were fabricated based on paper material and hence are known as μPADs (micro-paper-based analytical devices)[56]. The concept was to build very inexpensive microfluidic devices that could be used as screening or detection techniques in the remote areas and developing countries where people don't have access to proper health care diagnostics. These devices were made as passive microfluidic systems out of inexpensive material, which do not require external supporting equipment or power sources to function. The first device was built by patterning photoresist onto chromatography paper to form defined areas of hydrophobic "walls" or barriers and hydrophilic "channels". These defined areas could guide the fluidic transport through capillary forces in millimeter sized produced channels. This device was used for glucose and protein determination in the urine.

Since the introduction of this class of microfluidics, several groups have introduced different manufacturing techniques to create the "walls" and the "channels" of the μPAD devices both on chromatographic paper and filter paper.[57] They involve polymers (such as SU-8 photoresist, AKD (alkyl ketene dimer), PMMA (poly (methyl methacrylate), PDMS (polydimethylsiloxane), PS (polystyrene)) used in the photolithographic technique[56] and their

solutions used in converted ink plotters[58] and typical ink jet printers[59]. Next group of materials consist a waxes used for commercial printing[60] and screen-printing[61]. μPADs can be also created by using flexographic printing[62], a laser[63] and plasma treatment[64] and finally by cutting knives.[65]

As far as the applications of these systems go, in laboratories, paper is commonly used as basic material for filtration and chromatography. Typical μPADs detection systems are based on colorimetry, electrochemistry, chemiluminescence and electrochemiluminescence, however colorimetric and electrochemical qualitative and quantitative determinations are the most popular. The first diagnostic system involving paper based device was used for colorimetric determination of glucose and protein in urine[56]. In addition, μPADs have been used in environmental studies for detecting heavy metals[66], food quality and in clinical tests for blood analysis and DNA detection.

Although paper-based microfluidic devices provide a low-cost and simple platform for performing multi-analyte detection and semi-quantitative measurement, more complex devices are required where there are multiple steps involved in the analysis/diagnosis, such as the premixing of samples before the final reaction. Under such circumstances, functional elements could be incorporated into the devices for controlling the movement of fluids within paper-based microchannels and for expanding the functions of the devices.[67] In addition, the sample retention (i.e., the ineffective sample

consumption) within paper fluidic channels and the sample evaporation during transport result in the low efficiency of sample delivery within the device. Furthermore, Some hydrophobic agents for patterning devices cannot build hydrophobic barriers strong enough to withstand samples of low surface tension.[67] Moreover, since the detection limit of the traditional colorimetric methods is high, it makes the paper microfluidic devices insufficient for analysis of low concentration samples.

1.4 Overall Research Objective

After looking at different microfluidic technologies, there seems to be a common drawback. A significant problem with this technology is the difficulty in manufacturing and integrating products that have dissimilar materials in a single device, and utilizing 3D designs. Manufacturing microfluidics tends to be monolithic and planar, requiring the development very clever or complex methods for building integrated devices.[28,29,68,69] Indeed, in most cases, additional functionality (such as pumping, filtering, imaging, electronics, etc.) is added externally to the chip since it is too difficult to integrate the required components on-chip.[70–73] Fluids are moved primarily in the plane of the device and assays tend to treat the device as a two-dimensional system. Moreover, chips tend to be completely sealed so that their assays must be predetermined at time of manufacture. They cannot readily accommodate changes at the time of the assay or transport

of material from one chip to another. These types of devices have been used with some success to replicate standard bench-top assays. In many cases, the assays have been cleverly and significantly redesigned so that they may work within the manufacturing limitations of the microfluidic system.[74,75]

This shortcoming in microfluidics manufacturing limits the types of assays that can be readily addressed. Assays that require a variety of different materials, processes, and transfer of analytes are particularly hard. An example of such as assay is the Western blot.[76] This assay starts with proteins prepared in a solution, which are transferred to a gel medium for electrophoretic separation, and then blotted onto a solid membrane for immunochemical analysis. Since this assay is difficult to design and manufacture as a microfluidic system, clever workarounds have been developed such as embedding antibodies within the separation gel. [77–80]

Gel-based separations[81] and blotting may benefit from miniaturization of microfluidic scales. In particular, for applications that produce very small quantities of sample material, a small-sized assay is needed. An ideal Western-style, micro-scale assay would be able to manipulate small volumes of sample, efficiently inject analytes into a very small zone, perform electrophoretic separations, and allow separated species to be immobilized and transferred to another system for further analysis such as immunostaining, high sensitivity imaging, or harvesting. Further, it would be useful if the details of the assay (such as staining antibodies, protocol, gel

density, etc.) could be readily changed without the need for a completely new device.

To address this need, we propose a different approach to the design and production of microfluidic systems. In our approach, we produce micro-gels, microfluidics, and other functional micro-components on thin paper carriers that are then laminated together to form a stack that can perform an assay (see figure 5). We refer to each thin carrier as a "microfluidic coupon" or "microfloupon" for short. Microfloupons are typically manufactured on paper (although any material may be used). Paper is an ideal material for many microfloupons since paper is inexpensive, easy to modify and cut, and has reasonable mechanical strength to enable handling. Moreover, the fibrous, porous nature of paper makes it convenient for embedding materials such as gels or polymers. For specialized functions (such as electronics or optics), microfloupons may be made differently from other materials, such as polymers and metals. In the microfloupon approach, each microfloupon may be manufactured separately (provided by separate manufacturers if appropriate), then stacked together as needed to produce an assay of interest. If needed, the stack may be separated, and one or more of the microfloupons can be transferred to a new stack for further processing.

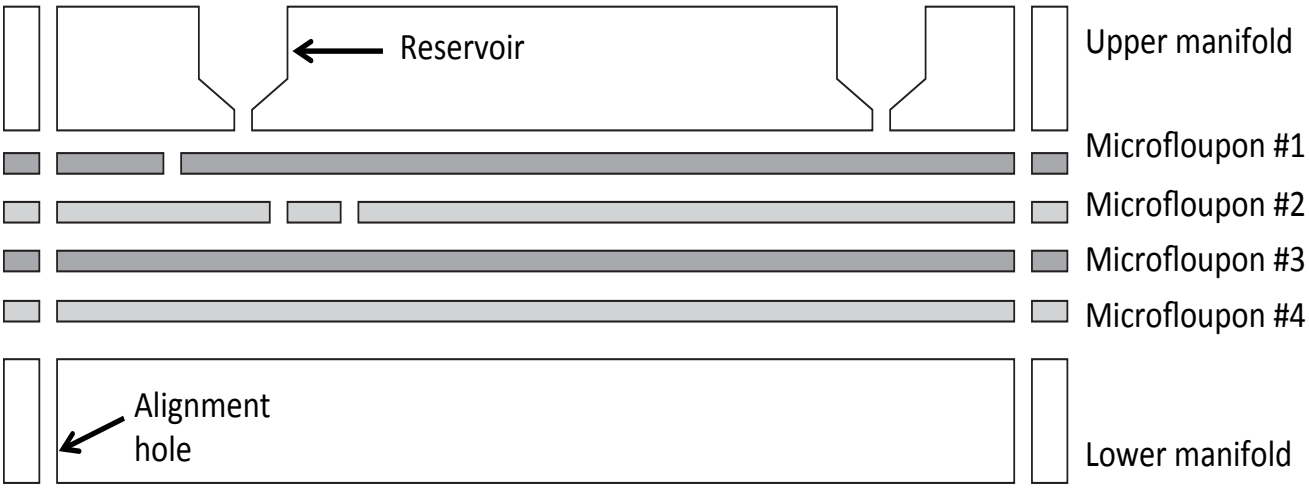

Figure 5. General illustration of μFloupon laminated device. Multiple functional microfloupons form layers in a stack, allowing for 3-D integration of many dissimilar components. Microfloupons may contain microfluidics, thin gels, sieves/filters, electronics, optics, etc. Microfloupons may be mixed and matched as necessary to produce an assay, and may be moved from one stack to another.

To illustrate the potential for microfloupons in microfluidic assays, we demonstrate the first half of a Western blot assay, sodium-dodecyl-sulfate polyacrylamide gel electrophoresis (SDS-PAGE), using small quantities of protein. This demonstration uses microfloupons to

(1) Manipulate a small sample of proteins,

(2) Inject them into a small zone,

(3) Perform gel electrophoretic separation, then

(4) Remove the gel from the system for imaging and further processing.

The demonstration utilizes some features that are difficult to produce using conventional microfluidic technology. These include the use of an externally manufactured thin membrane to filter and hold proteins, the use of the vertical direction as a viable part of the assay, the use of a very thin acrylamide gel slab, and the ability to remove the gel after separation for

further processing of the sample. All microfloupons used in the assay device were inexpensive and easy to manufacture. In the following chapter, microfloupon technology is thoroughly explained and manufacturing of each microfloupon layers are explained which can be applied in several applications in a mix and match format.

Chapter 2

μFloupon Technology

2.1 Introduction

Some of the main applications of microfluidic systems can be found in the field of molecular biology, chemical synthesis and biotechnology and pharmaceuticals. Up to the current time, many novel microchips have been introduced. In the field of DNA analysis, a number of commercial microarrays were introduced to the market place such as GeneChip, DNAarray from Affymetrix[82], DNA microarray from Infineon AG, or NanoChip microarray from Nanogen. However, a majority of these products could not be sustained and were taken off from the marketplace. In the world of academia, there have been several novel, state of the art biochips. A protein array, similar to a DNA microarray, is a miniature array in which a multitude of different capture agents, most frequently monoclonal antibodies, are deposited on a chip surface (glass or silicon); they are used to determine the presence and/or amount of proteins in biological samples, e.g., blood. A drawback of DNA and protein arrays is that they are neither reconfigurable nor scalable after manufacture. Moreover, they lack the ability to carry out sample preparation, which is critical to biochemical applications.[21]

As discussed in the previous chapter, one of the main substrates for fabricated microfluidic devices has been silicon. Silicon substrates lend its technology from the semiconductor industry, and utilize existing standard machines, materials and protocols. However, silicon is not biocompatible nor it is transparent. In addition, because this material is expensive for biochip applications, glass and other polymers have been introduced as the alternative substrate material of choice for microfluidics chip fabrication. Glass has several advantages as a fluidic substrate: i) it is optically transparent over a wide range of wavelengths, ii) its surface is hydrophilic, iii) its surface chemistry is well understood, iv) there are numerous etching methods and v) modification of surface can be performed with various techniques. In most cases, glass is the material of choice for the chemists and biologists, but the isotropic nature of its wet etching makes it difficult to create deep channels in glass. The fragility of this material is an additional issue. [83,84]

The basic idea of microfluidic biochips is to integrate all necessary functions for biochemical analysis onto one chip using microfluidics technology. Current fabrication methods underline the need for external pumps, external valves and external extensive tubing to perform some simple assays making lab on a chip devices rather chip in the lab devices as shown in figure 6.


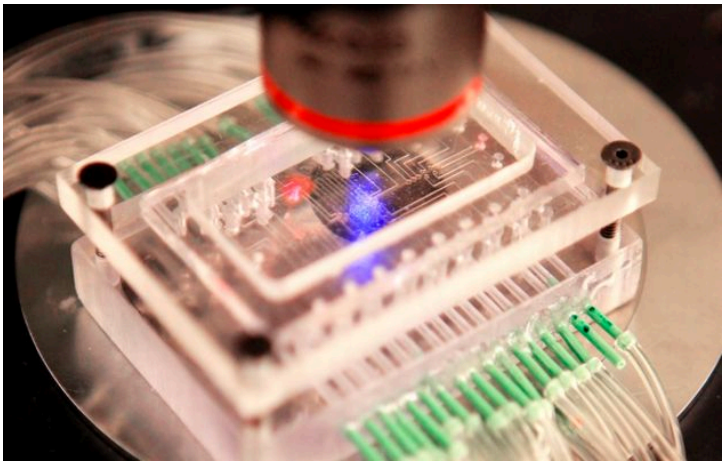

Figure 6. Examples of application specific microfluidic chips. Right : http://www.popsci.com/scitech/article/2009-08/lab-chip-can-carry-out-1000-tests-once?dom=PSC&loc=recent&lnk=7&con=labonachip-can-carry-out-over-1000-chemical-reactions-at-once Left: http://www.timeslive.co.za/scitech/2011/07/31/lab-on-a-chip-may-be-game-changer-in-disease-detection

While these devices are novel and state of the art, their complex manufacturing design makes them ideal for prototyping only. Many external components are needed, so it is nearly impossible to scale up the production making these devices impractical in high throughput scalable production systems.

Another challenge facing microfluidic systems is that the complexity of microfluidic systems is increasing rapidly; sophisticated functions such as chemical reactions and analyses, bioassays, high-throughput screens, and sensors are desired to be integrated into single microfluidic devices.[85–87] Many channels require more complex connectivity than can be generated in a single level, since single-level design does not allow two channels to cross without connecting. Most methods for fabricating microfluidic channels are based on photolithographic procedures and yield two-dimensional (2D) systems.[88] Research groups have conducted a few different attempts to

introduce (3D) microfluidic structures.[86,87,89,90] Nevertheless, the fabrication of 3D microfluidic structures with arbitrary geometries is still challenging, if not impossible, because today's mainstream microfluidic fabrication techniques heavily rely on the well-established 2D planar lithographic approach.

Whitesides and his team were some of the early pioneers in fabricating (3D) devices manufactured by layering several poly(dimethylsiloxane) (PDMS) material together. First, they fabricated bottom master microfluidic systems using photoresist on Silicon by multilevel photolithography. Then, by Two-level Photolithography and Replica Molding , they created the Top Master in PDMS. To make the (3D) structure, they used a method called membrane sandwiching in which one drop of PDMS prepolymer is placed in between a facedown top master and top of the bottom master. The top master slides on the pre-polymer until its tall alignment track falls into the tall alignment tracks of the bottom master and the segments of the channel system from both masters were aligned. Sufficient pressure is applied to the top master so that pre-polymer does not seep between features that were in contact, and the PDMS is heated to 75 °C and cured in place. The PDMS membrane and the top master are peeled off the bottom master. The bottom of the membrane and a flat slab of PDMS were oxidized in air plasma for 1 min and brought into contact to seal. After the top master is peeled off, the top surface of the membrane is sealed to a flat slab, to enclose the channel

system, and trimmed to a convenient size.[87] With this method, they were able to produce very complex (3D) structures. However, this method needs multiple complicated steps involving surface treatment and silicon photolithography techniques, which makes it suitable for prototyping only. In addition, each component is made of PDMS, which cannot be controlled electronically and again, requires external components to design a full μTAS system.

The same group later on introduced another low-cost (3D) manufacturing technique in paper.[86] (3D) microfluidic devices are fabricated by stacking layers of patterned paper and double-sided adhesive tape. Using wax-injected printers, paper is patterned, and by heating the wax hydrophilic channels, hydrophobic walls are created. Double-sided tape is patterned with holes that connect channels in different layers of paper. These devices extend paper-based assays from simple 1D lateral-flow systems to 3D devices for very low-cost analytical systems. The main functionality of this class of devices is based on wicking and capillary action in liquids. There are no physical channels, and integrating much functionality such as optics and valves are difficult to impossible. In addition, non-specific adsorption may occur by using tape in previous 3D designs.

Regarding (3D) designs, to this date with our knowledge, there are no groups that have reported a system in which several layers of different materials are stacked together to make a fully functional device. The design

is either not suitable for mass production or not a general answer to most biological problems. In the next section, the concept of μFloupons is discussed.

2.2 What are μFloupons?

μFloupons, short for microfluidic coupons, are the new class of analytical microfluidic devices made by lamination of several layers. The layers are thin carriers that can be manufactured out of several different kinds of materials. Based on the selected assay, the μFloupons can range from micro-gels to membranes, polymers, or metallic material. After manufacturing different layers of interest, the μFloupons can be laminated to form a stack that performs an assay. Manufacturing of these layers can be done in house or can be provided by outside manufacturers.

As mentioned earlier, each layer can be fabricated form the desired material suited for the assay. If the material is not elastic, such as PDMS or rubber, then a gasket, which is also a μfloupon, is placed between two layers to prevent leakage of fluid into other layers. However, if the desired material is manufactured or impregnated with elastomer polymers, then each layer can act as a μFloupon and gasket as well. The design features on each layer can be made on computer aided design (CAD) software, illustrator, or any other common drawing software, with alignment considerations in mind. The components can then be manufactured using laser cutting machinery,

computer numerical control (CNC) machinery, or an outside manufacturer. To illustrate the laminated layers, figure 7 is provided.

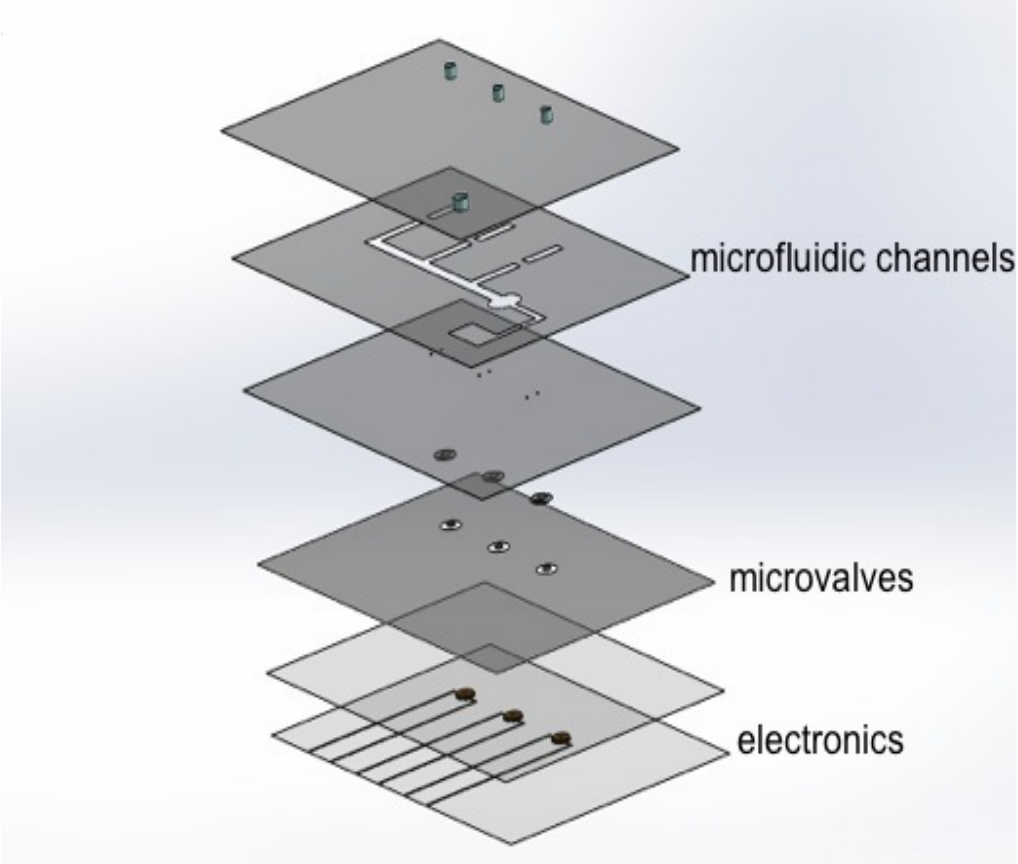

Figure 7. General schematic for μFloupon system

2.3 μFloupon fabrication methods

Since μFloupon systems are comprised of different materials, this section is chosen to explain some of the techniques we used to manufacture them. A variety of polymers has been studied and developed into micro systems to perform biological and chemical experiments.[51,91,92] The techniques and methods explained in this section are the general description of

manufacturing μFloupons. Materials other than the ones mentioned can be produced by similar methods. More applications and specific fabrication methods are explained in the subsequent chapter.

2.3.1 Paper μFloupons

Fibrous materials are important substrates for diagnostics applications and are used in various analytical test strips; also know as lateral flow assays. Cellulosic matrices such as paper are made out of organic pulp in which liquid is moved by capillary action. In this research, we heavily use paper as the material of choice to make μFloupons. Paper has properties that make it an ideal coupon carrier in an assay. Some of these properties are as follows:

1) Paper is widely manufactured from renewable resources and is inexpensive.

2) It is combustible and biodegradable.

3) Paper is also suitable for biological applications since cellulose is compatible with biological samples.

5) Paper surface can be easily manipulated through printing, coating and impregnation and can be fabricated in large quantities.

6) It can be easily stored, transported and disposed.

7) Existing use in analytical chemistry allow for easy transfer of techniques for new applications

8) Paper properties can be easily altered to suit different applications.

Among papers, blot absorbent filter papers are ideal because they are specially made to interact with fluids without wrinkling. Filter papers have a much higher wet strength[93] and repress the swelling of fibers thus inhibiting the separation of fiber. In addition to the above properties, paper is flexible, and can be patterned with a laser-cutting machine or even manually. It is easy to stack up, store and transport. Paper is a great support for other fragile materials such as gel (polyacrylamide, agarose): the gels can impregnate the paper, so thin gels can be handled easily. Since paper comes in different thicknesses from sub μm to mm, it is possible to alter the thickness of the gel or other impregnating materials by choosing the right thickness for the paper. So in this case, paper is used as a support and as a spacer for accomplishing the right thickness as well. More application specific details on gel-paper fabrication technique is given in chapter 4.

In our study, all the paper-based μFloupons were designed on Illustrator, CarolDraw, AutoCAD or Freehand software, with defined channel length and width. As mentioned before, the height of the channel is the thickness of the paper. The design was then transferred to the laser-cutting machine, and the patterns were cut out.

CO_2 Laser machining is rapid prototype technique for meso scale fabrication with 100 - 250 mm resolution that cuts and engraves patterns onto various

substrates. In such systems, the laser beam is guided by several mirrors and focused by an optical lens onto the plastic substrate as shown in Figure 8. Two-dimensional robotic arms direct the focused laser beam to scan over the entire machining area with the substrate motion limited to vertical direction.

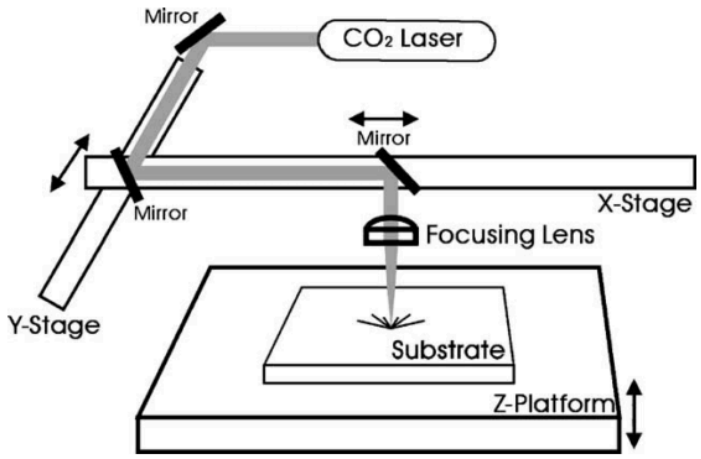

Figure 8. Configuration of a direct-write laser machining system with an X–Y stage

This manufacturing technique is excellent in producing structures in paper, and by adjusting the power setting on the laser machine other μFloupons in different materials could be manufactured in the same way.

Structures that are made with the desired pattern then can be impregnated with various monomers such as polyacrylamide gel, agarose, PDMS, polyurethane or epoxy and polymerized through chemical reaction or any other polymerization technique. By using this technique, we produce thin

layers that can be stacked on top of each other and handled easily. This method allows for handling of fragile thin materials especially soft gels, which are extremely difficult to handle otherwise. It is worthy to notice that this manufacturing technique is different than the μPAD system since in this method actual channels are produced and the liquid can flow and being transported to different places through the channels actively.

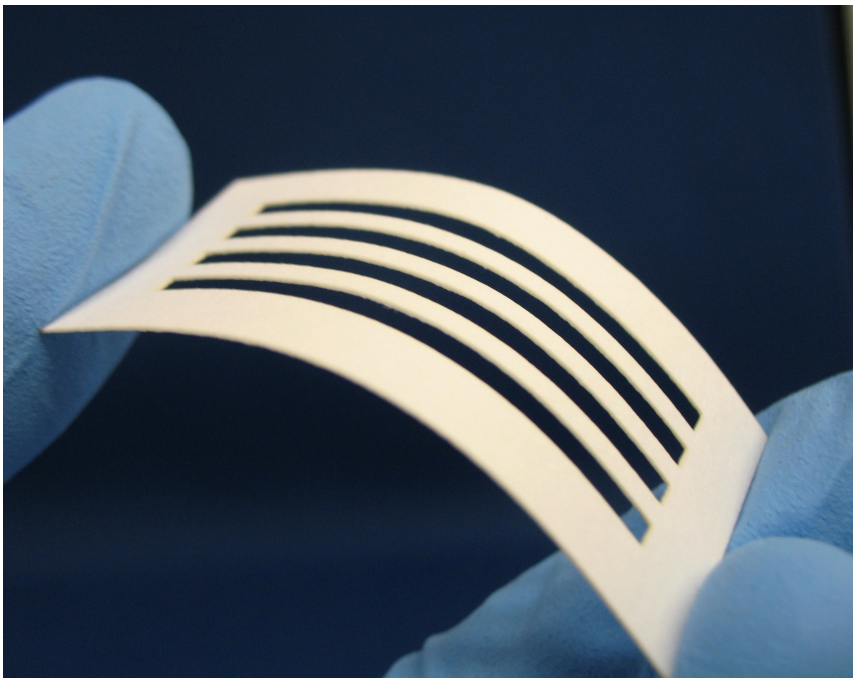

Figure 9. Image of a paper μFloupon

2.3.2 PAPER-PDMS μFloupons

Paper-PDMS μFloupons are another widely used floupon category in our applications. These type μFloupons are a hybrid of Poly (dimethylsiloxane) (PDMS) and paper. The characteristics of this paper/PDMS duality make a

powerful combination that is easy to manufacture and biocompatible and can be used in a variety of applications.

PDMS is a silicon-based organic material used widely in microfluidic devices due to physical properties and ease in fabrication. PDMS posseses many chemical and physical properties that makes it an attractive material: is has a good thermal stability, good transparency,[94] low surface tension, and is environmentally safe[27] and biocampatible. PDMS is also considered an excellent prototype material for fabricating microfluidic devices with the use of biological samples in aqueous solutions.

PDMS used in microfluidic research is typically in a two-part heat curable liquid form (Sylgard 184, Silicone Elastomer Kit, Dow Corning Corporation). The solid PDMS is prepared by crosslinking the pre-polymer and the curing agent at a certain ratio. As a general rule, 10:1 ratio of base to curing agent is applied in most applications. The mixture is then vacuumed to remove the air bubbles. Then it is cured in an oven of 70°C for an hour.

The process of fabricating PDMS-paper μFloupon in each application might be slightly different resulting in different stiffness and different heights. First, the two parts are mixed well together, then degassed and poured on a desired carrier such as paper or a mask, then pressed and cured by raising the temperature. The paper carrier is advantageous since the height can vary with the height of the paper. Using this method, fabrication and handling of very thin μFloupons is possible without the need for cleanroom

facilities. The detailed application specific description of PDMS μFloupon is described in the following chapters.

2.3.3 PMMA μFloupons

Poly(methyl methacrylate) (PMMA), also known as acrylic, is a synthetic polymer that has been used for several years to fabricate microfluidic devices. Although it is not a glass, the substance has been historically called acrylic glass. It is a very popular amorphous thermoplastic polymer that usually can be found in clear hard sheets and flexible films with different thicknesses from sub-microns to millimeter range.

PMMA films/sheets can be machined, pressed and sealed and are hard, durable and optically transparent [95] (92% transmission in the visible region). These are attractive properties for prototyping a microfluidic device. Furthermore, PMMA has a good degree of biocompatibility, which allows biochemical assays to be performed.

Several techniques have been introduced for fabrication of PMMA microfluidic devices[25,26,52,91,96,97]. Some of these methods include injection molding, hot embossing, X-ray lithography, laser ablation and CNC machinery. In injection molding method, the prepolymerized pellets of PMMA are melted and injected under high pressure into a heated cavity. The injected pieces are then cooled and released from the mold. The molten nature of plastic during injection allows for excellent contact with the features of the mold

resulting in a precise replication[97]. In hot embossing method, the patterns are made using a master stamp, pressure and heat to transfer the features from the master to the PMMA sheets. Masters are usually made either in silicon or metals. Silicon wafers are processed using micromachining techniques to create the stamp[51], while metal stamps are either electroplated against micromachined silicon masters or eletroformed using LIGA[98]. With Laser ablation, a laser-cutting machine such as the one shown in figure 8 is used to melt the plastic away. The patterns are usually drawn in a CAD tool such as illustrator or EAGLE then transferred to the laser cutting machine software. By adjusting the power on the laser, the features then can be transferred on to the PMMA sheets. CNC machinery is another method in which patterns are drawn using one of the desired software such as CAD eagle or G-code, and then transferred to the machine. By using the desired end mill as the thickness of the channel, the features can be transferred to the sheets.

In our applications, PMMA materials were used as the hard material to enclose the softer μFloupons. For rapid fabrication, all the features and patterns were made using laser cutting machine and CNC machinery techniques. More details on the application specific fabrication are given in the following chapters.

2.3.4 PCB μFloupons

A printed circuit Board (PCB) is an important layer that can be integrated into the μFloupon device to make a complete lab on a chip device. Integration of microelectronic connection with fluidics is an essential part of a μTAS that should be addressed. Advancements in the PCB fabrication industry have introduced sophisticated manufacturing techniques.[99,100] However, the integration of PCB with microfluidics has remained a challenge. Most researchers attempt to integrate additional functions into their devices by processing them monolithically. This method subjects the entire chip to more manufacturing in order to produce a single function on a small portion of the device. In addition, a lot of times, to support one-function microfluidic chip, several valving, pumping, switches or microcontroller systems might be needed externally. Adding external microelectronic systems to the microfluidic systems, make the lab on a chip unattractive and inefficient to the market since the "lab on a chip" becomes "chip in the lab".

The microfluidic community has recently started to take advantage of PCBs as a substrate for the microfluidic devices.[101–104] Wu et al. have been able to integrate microfluidics systems with circuit boards by using a multi-step process.[101] The key steps to achieving this goal are as follows: After designing and manufacturing the circuit board using CAD tools on FR-4 through standard PCB manufacturing and placing the components on the board, negative 1002F photoresist is applied on the surface. Then the

surface is planarized by using a flat PDMS coated glass and spacers under the hot press. Then selectively the parts that are needed to have access to fluidics or optics are removed by photolithography techniques. This enables optional fluidic connections to the electronics layer below as it is shown in figure 10.

PCB μFloupons are fabricated in a similar manner to allow for mass production. We used different techniques for manufacturing based on the application of the PCB μFloupons. First, the PCB layout is drawn using Eagle CAD software tools, then desired design is built by an outside manufacturer on a regular or thin sheets of FR4 boards. The components are then soldered to the board and a planarization technique similar to Wu's technique was used to make a flat surface.

First, a PCB was mounted to a flat surface using a double-sided tape. Spacers were placed at the ends of the board to accommodate for the height of the highest component. Then degassed PDMS pre-polymer/curing agent was carefully poured onto the PCB and a flat PMMA sheet was placed on top. The whole system was then transferred under the press and it was pressed gently overnight at room temperature. After PDMS was cured, the PMMA sheet was carefully removed from the top leaving a flat plane PDMS surface, on which the microfluidic system could be placed. For applications that

required optical imaging on the bottom of the chip, such as using inverted microscope imaging, μFloupon PCBs were manufactured slightly different.

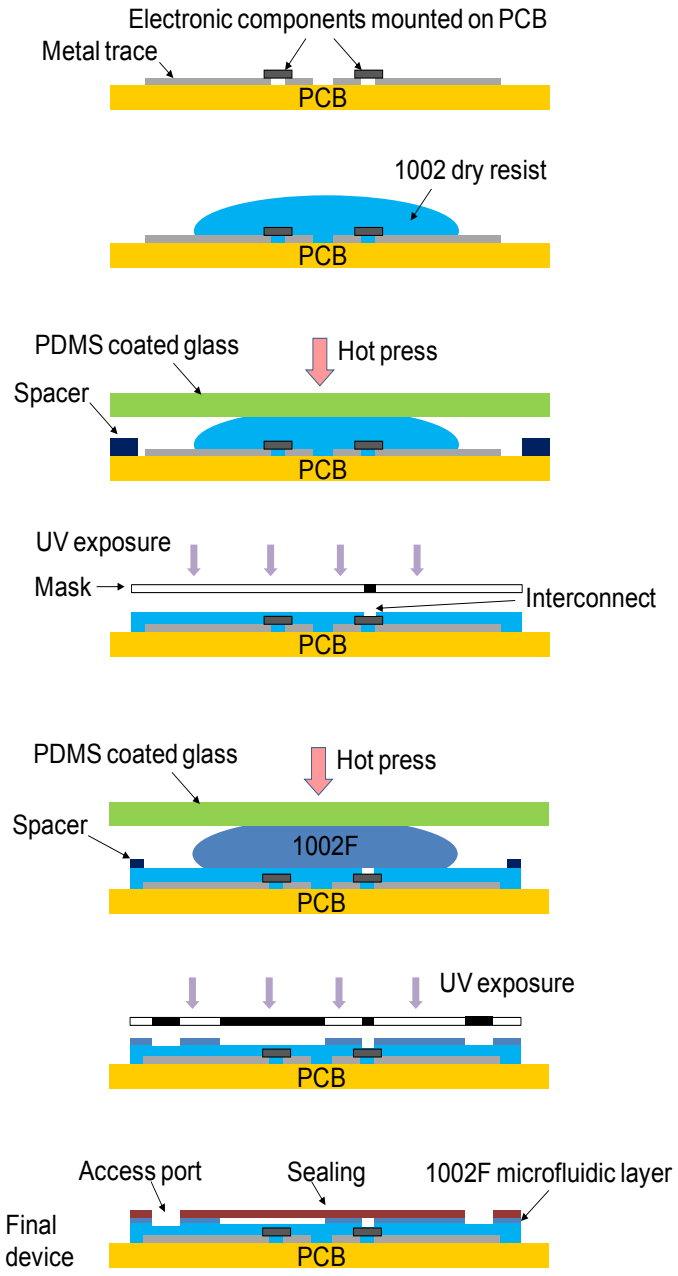

Figure 10. Detailed 1002F fabrication process on PCB using hot pressing and lithography. The steps include surface mounting electronics on PCB, 1002F planarization and encapsulation, 1002F fluidic layer patterning and sealing[101]

The steps to produce a transparent PCB μFloupons are shown in figure 11. First, layout of the circuit board was drawn using illustrator software. For more complex circuit layouts, Eagle CAD software was used and the file was exported to illustrator. Using a laser-cutting machine, the layout of the circuit was then cut out on a piece of silicon dicing tape to make a template for the connections of the routings. This technique produced a stencil that was taped on top of a thin Mylar sheet (50 μm) and silver nanoparticle paint was manually deposited on the mask to fill out the connections. After air-drying the silver paint, the tape mask was removed and components were mounted on top of the board using conductive epoxy. The board was placed in the oven at 70C for 30 minutes for the epoxy to bond and dry. After this stage, the same planarization technique planarized the surface leaving a smooth circuit board layer. This method can be used for other substrate materials as well. Also, we were able to manufacture PCB boards and planarized the process using filter paper.

In the third technique, another printing method was utilized to accommodate direct contact with the biological assays while it was developed on a transparent flexible substrate for imaging purposes. Since silver is not compatible with biological reagents and oxidizes when in contact with conductive buffers due to electrolysis effect, stainless steel was chosen as the tracing material. Stainless steel corrodes at a much slower rate than silver.

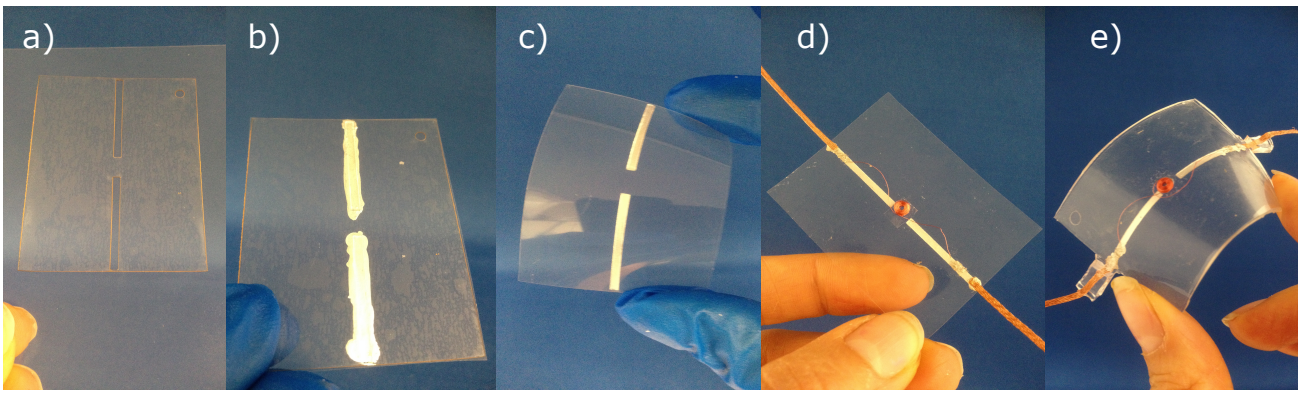

Figure 11. Process of producing a transparent PCB microfloupon. a) A stencil mask is designed and attached to transparent substrate b)silver particles are painted on the traces c)the mask is removed d) the components are attached. e) demonstration of flexible PCB microfloupon**.**

Moreover, because this material is much less expensive than platinum, stainless steel was the best option for making disposable PCB μFloupons.

To manufacture the PCB μFloupons, the board traces were drawn using illustrator. Then, a thin (50μm) stainless steel tape was etched out using laser-cutting machine and then bonded on a surface of Mylar sheet using alignment marks. Then the rest of the tape was removed to leave just the stainless steel traces. This method allowed us to manufacture vias and electronic traces on a single sheet in a very rapid, inexpensive fashion. In this method, to make the connection between the traces and the wires, copper tape was used to avoid any soldering issues such as poor adhesion, and the need for excessive heat in heat soldering process.

2.4 μFloupon Lamination techniques

After manufacturing, the desired layers were laid on top of each other and aligned with alignment pins. The alignment pin locations were designed and incorporated into each μFloupons layer during the design and manufacturing of the μFloupons. If the layers were made out of hard polymers or PCB boards, or the μFloupons were conductive throughout the whole surface, a gasket was needed between the two layers. For example if a μFloupons was out of polycarbonate and the next μFloupon on top of it was made out of paper impregnated with a conductive material such as polyacrylamide gel, a soft thin gasket needed between the two μFloupons to avoid any leakage. The specific gasket that was used in our applications were made in house and were built using thin sheets of paper which were cutout in the middle to make a frame with the thickness of 100μm or less. Then, each cavity of the frame were filled with PDMS monomer and flattened using a flat piece of acrylic. Next, it was cured in the oven with the temperature of 80°C for an hour. In this method, the paper frame was impregnated with PDMS and made a thin gasket. A sharp biopsy punch was used to make the access holes at specific locations between layers where they were needed. In some applications, the temporary adhesion between the PDMS layers was strong enough that lamination is done by placing each layer on top of another without any other extra force. However, in the protein analysis system, in which gaskets were insufficient in creating adhesion between the layers, a

metal frame was built by an outside vendor to screw in the laminated device and hold the layers tightly together as it is shown in figure12. The next chapter explains specific applications of the μFloupon.

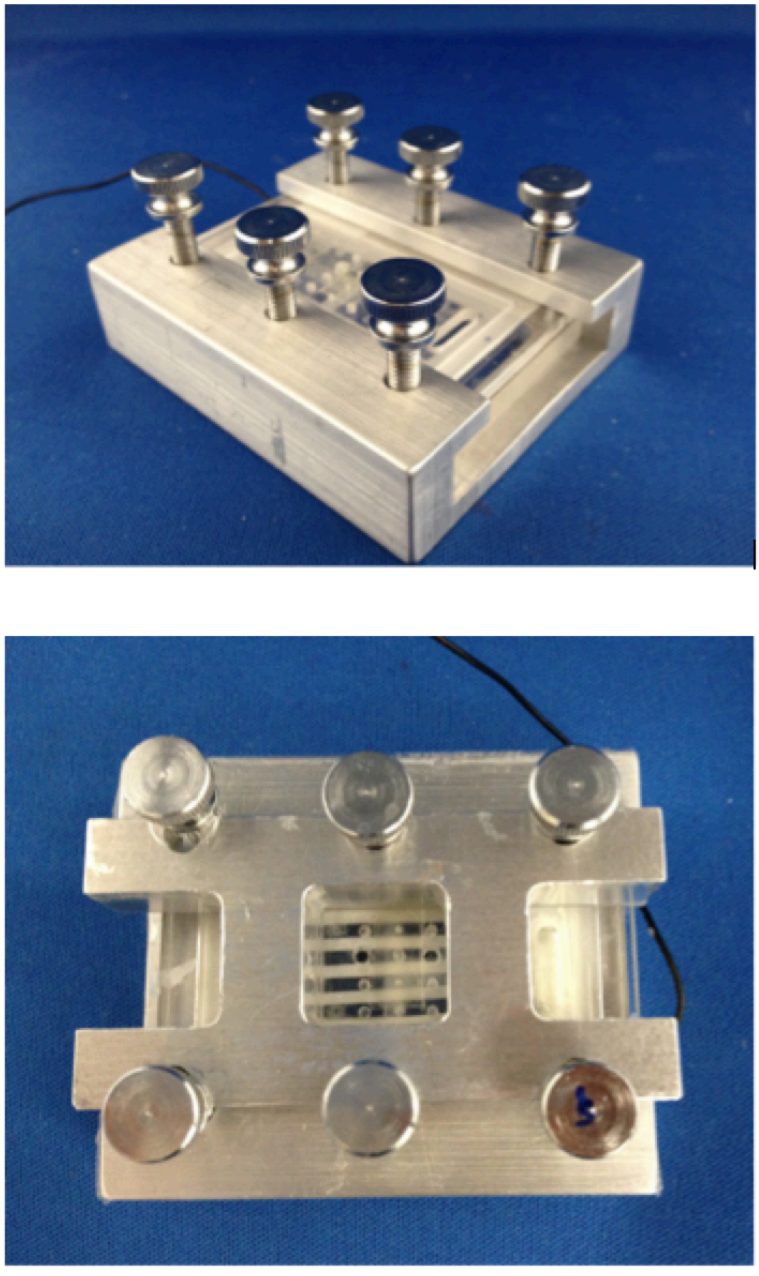

Figure 12. Images of the SDS-PAGE fixture to keep the microfloupons layer together to avoid leakage**.**

Chapter 3

μFloupon Integrated System In A Protein Analysis Assay

3.1 Electrophoretic Protein Separation

Separation of charged molecules in an electric field is called electrophoresis. In biology these molecules can be DNA, RNA, and Proteins. Separation of proteins in an assay is a well-known technique[105] and an important step in biology, which enables the possibility to study its enzymology (the science that deals with the biochemical nature and activity of enzymes), understand its affinity for particular substrates, or dissect its ability to catalyze enzymatic reactions. Such approaches have allowed scientists to understand how biological molecules can act as catalysts in metabolic processes or as transducers that will convert chemical energy into ionic gradients or mechanic forces. This powerful step gives information about the particular activities that resides in a specific protein and data about the function of the protein. In addition, understanding protein expression and protein function is crucial to the identification of new targets for drug development.

Proteins can be separated by exploiting differences in their solubility in aqueous solutions. The solubility of a protein molecule is determined by its amino acid sequence because this determines its size, shape, hydrophobicity and electrical charge. Proteins can be selectively precipitated or solubilized

by altering the pH, ionic strength, dielectric constant or temperature of a solution. There are many methods for protein purification and separation. Here, we will review the sodium dodecyl sulfate polyacrylamide gel electrophoresis since this was the chosen method for the purpose of this project.

3.1.1 SDS-PAGE

Sodium dodecyl sulfate polyacrylamide gel electrophoresis (SDS-PAGE) is the single most widely used analytical technique for researchers working with proteins. Protein separations by SDS-PAGE are commonly used to determine the approximate molecular weights of a protein and the relative abundance of major proteins in a sample. This technique is based on the fact that any charged ion or group will migrate upon the application of electric field. Since proteins carry a net charge at any pH other than their isoelectric point, they will migrate and their rate of migration will depend upon the charge density (the ratio of charge to mass) of proteins concerned; the higher the ratio of charge to mass, the faster the molecule will migrate.[106] In the absence of obstacles, polyelectrolytes with the same chemical nature and different sizes migrate at the same velocity, because the friction and the charge are both proportional to the size.[107] Therefore, the proteins must have a supporting medium to move through to separate based on size.

In order to better understand the mobility phenomenon, we can apply a simple model and use a negatively charged point and the forces that are applied to the charge when it is placed in an electric field as it is shown in figure 13. In such system, there are two forces that are applied to the charged molecule: electrostatic force which pushes the charge towards the cathode and the friction force which keeps the charge away from moving forward. At any time, these two forces are equal. The electrostatic force is proportional to electric field and charge while the friction force is proportional to the shape, viscosity and velocity of migration. Therefore we can have setup the following formulas:

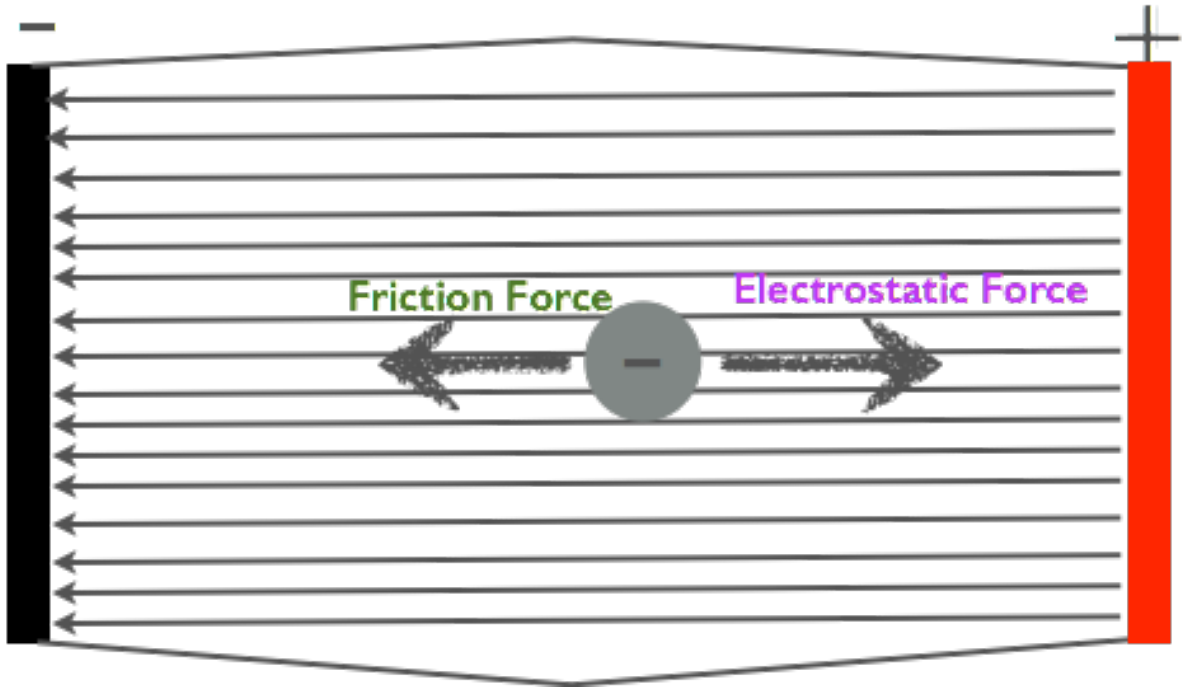

Figure 13. Image of a particle placed in an electric field indicating the forces on a negatively charged particle that is placed in an electric field.

Eq.(1) $$F_e = q.E$$

Eq.(2) $$F_f = 6.\pi.\eta.r.v_{ep}$$

$$F_e = F_f \quad \therefore \; q.E = 6.\pi.\eta.r.v_{ep}$$

Eq.(3) $$v_{ep} = \frac{q.E}{6.\pi.\eta.r}$$

q: charge

r: radius of the charge

η: Viscosity of the solution

v_{ep}: Velocity of migration

F_e: electrostatic force

F_f: friction force

Since electrophoretic mobility, μ_{ep}, is the rate of velocity in an electric field, *E*, we can find the mobility of the molecule as follows:

Eq. (4) $$\mu_{ep} = \frac{vep}{E} = \frac{q}{6.\pi.\eta.r} = const.\frac{q}{r}$$

Therefore, mobility is a relationship between the charge and the shape of the molecules. If the same charge is applied to different molecules, their mobility will just depend on their shape or their size and this is the

fundamental theorem that is used in electrophoresis and separation of particles (in this case proteins) based on their size only.

The two options are either using free solution or a more stabilized medium, and each has its own advantages and disadvantages. Although running the sample in the free solution is a much faster procedure, any heating effects caused by electrophoresis can result in convective disturbance of the liquid column and distortion of the separating proteins. In addition, the effect of diffusion will constantly broaden the protein bands even after electrophoresis has been terminated.[106] To minimize these effects, it is preferred to carry electrophoresis not in a free-solution but instead in a more stabilized supporting medium such as gel. Not only does the supporting medium help with diffusion and joule heating, it also aids researchers in fixing the separated proteins in place for post electrophoresis analysis. In the case of SDS-PAGE, polyacrylamide (PA) gel, a synthetic polymer of acrylamide monomer, is the medium of choice. This gel is formed by cross linked polymerization of two organic monomers, acrylamide and the crosslinking bifunctional compound, N,N'-methylene bisacrylamide (usually abbreviated to bisacrylamide) which reacts to free functional groups at chain termini. The structure of the monomers and the final gel structure are shown in figure 14. This compound has been shown as a suitable medium for electrophoresis[108].

Polymerization of acrylamide is initiated by ammonium persulfate with addition of N,N,N',N'-tetramethylethylenediamine (TEMED) which catalyses

the formation of free radicals from ammonium persulfate and these in turns initiate the polymerization.

This gel is a porous medium, with the pore size in the same order as that of the protein molecules. The effective pore size of polyacrylamide gel is greatly influenced by the total acrylamide concentration in the polymerization mixture. As the concentration of acrylamide increases the pore size decreases. Therefore, the choice of acrylamide concentration is critical for optimal separation of protein content where separation is also dependent on both charge density and size[106].

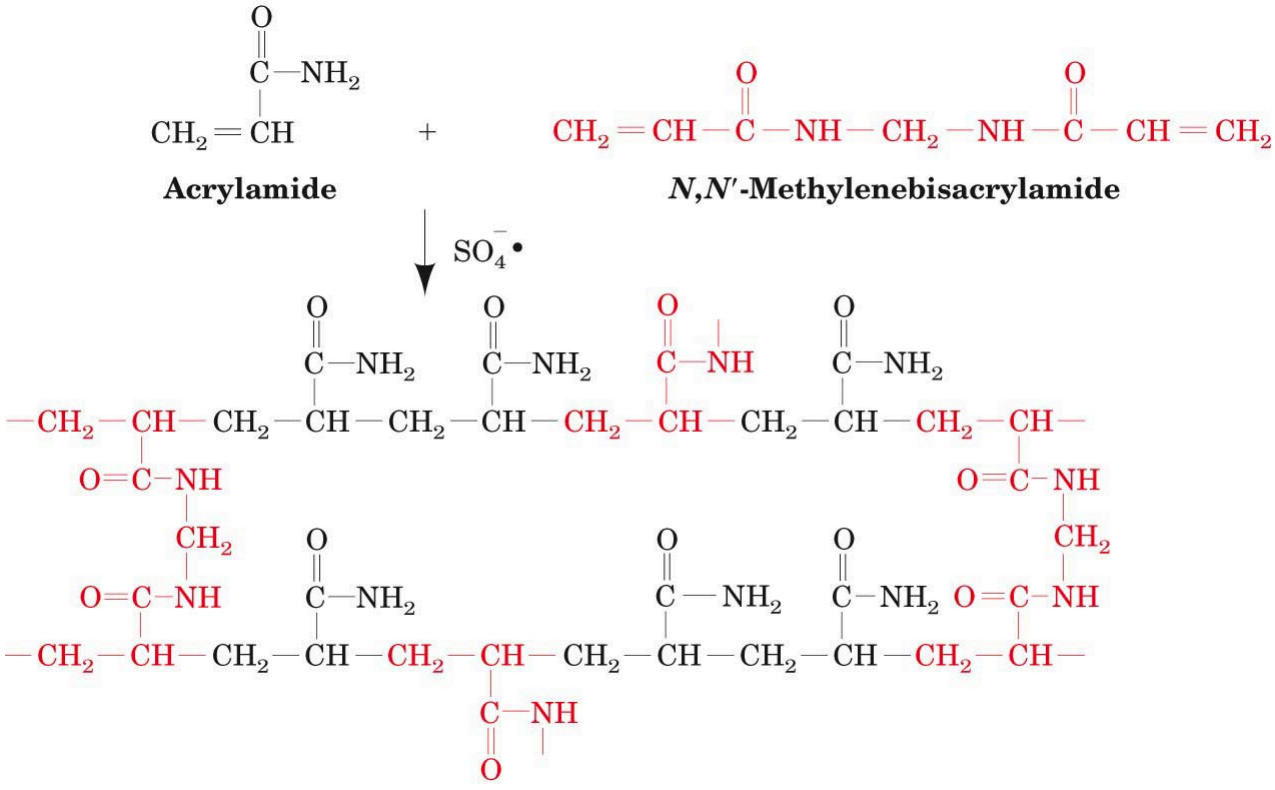

Figure14. The chemical structure of acrylamide, N,N'-methylenebisacryalamide, and polyacrylamide gel.

In conventional SDS-PAGE, a discontinuous vertical buffer system is used with different pH and different concentration of acrylamide in which the proteins are loaded on to the electrophoresis buffer on top of a gel with lower PA concentration which is called stacking gel followed by a gel with a higher PA concentration where proteins separate and is called running or resolving gel. This is done to increase the resolution of protein separation during SDS-polyacrylamide gel electrophoresis. The stacking gel contains chloride ions, the "leading" ions, which migrate quicker through the gel than the protein sample, while the electrophoresis buffer contains glycine ions, the "trailing" ions, which migrate more slowly than the protein sample. The protein molecules are trapped in a sharp band between these ions. When proteins enter the resolving gel, they slow down due to increased frictional resistance (smaller pore size) that allows the following proteins to catch up. This causes the proteins to "stack" at the boundary and as a result all the proteins will start at the similar point and therefore produce tighter band and a higher resolution separation system.

One characteristic of proteins is that they are normally folded up into specific three-dimensional structures, which affect the way they move through the gel. Therefore, both the natural charge of the protein and the shape of the protein will affect the way proteins move through the sieve. In the cases where the study of protein's secondary structure and native charge density are desirable, the proteins are kept unmodified. However, in the case of

SDS-PAGE, it is important to separate proteins based only on their molecular weight. Therefore, it is desirable to eliminate both the natural shape and charge of the protein molecules. In order to do this, a strong solution is added to the sample, causing proteins to unfold. The solubilizing denaturing agents such as sodium dodecyl sulfate (SDS) are widely used in the separation of proteins by gel electrophoresis. SDS has high affinity for proteins and promotes protein denaturation. SDS is anionic detergent that binds to most soluble protein molecules in aqueous solutions over a wide pH range. The amount of SDS bound by a protein and the charge on the complex, is roughly proportional to its size. Commonly, about 1.4 grams of SDS is bound per 1 gram of protein. The proteins are generally denatured and soluble by binding to SDS, and the complex forms a rod of a length roughly proportionate to the protein's molecular weight.

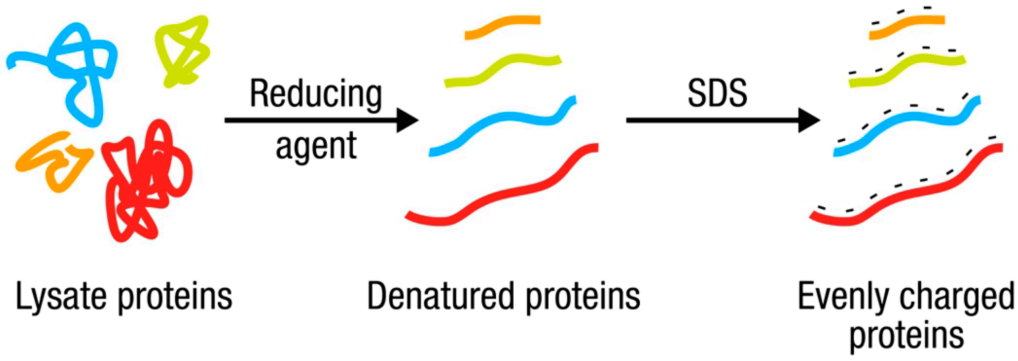

Figure 15. The process of denaturing the folded proteins and attaching SDS molecules on the proteins.

Thus, proteins of either acidic or basic pH, form negatively charged complexes that can be separated on the basis of differences in their sizes by electrophoresis through a sieve-like matrix of polyacrylamide gel.[109] In a gel of uniform pore size, the relative migration distance of a protein is the relative electrophoretic mobility (Rf) and is negatively proportional to the logarithm of its MW.[110] If proteins of known MW are run simultaneously with the unknowns, the relationship between Rf and MW can be plotted, and the MWs of unknown proteins can be determined.[110] This is the basis of polyacrylamide gel electrophoresis, which leads to identification and quantification of specific proteins.

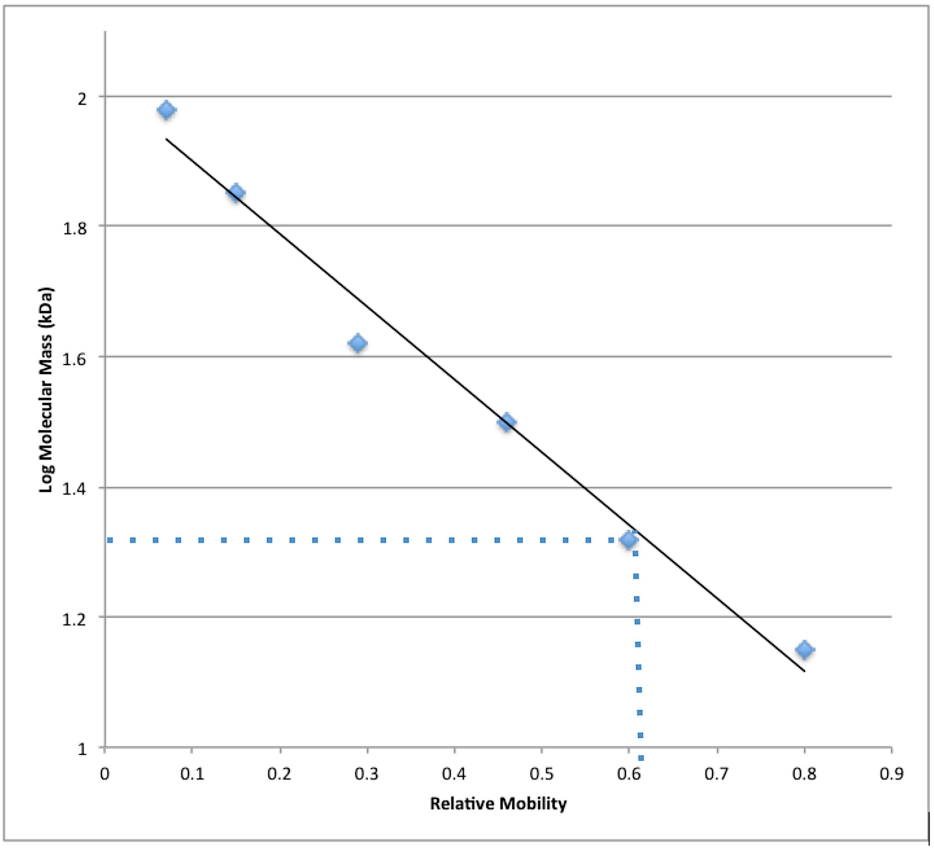

Figure 16. Graph of molecular weight vs. relative mobility of proteins.

3.2 Microfluidic Protein Separation/Analysis Technology

The recent development in protein analysis utilizing microfluidic technology has led researchers to realize new techniques for performing electrophoresis and analysis, which can be much more efficient and sensitive than its conventional benchtop counterpart. Other important benefits of a microfluidic electrophoresis include the ability to work with small protein sample, less reagents consumption, and a much faster experiment time and less laborious work. Electrophoresis can be performed much more efficiently

on microfluidic devices: because of the large surface area, the heat dissipation is much more efficient and the injection plug is significantly shorter via more flexible control. Thus, higher electric field can be applied across a much shorter separation channel and less time is needed to separate the proteins. [111]

As mentioned earlier, here we discuss the microfluidic systems that are gel based rather than using free solution. Incorporation of sieving matrices such as gel into microfluidic electrophoresis technology has yielded enhanced separation efficiency.[78,112,113] Among the various sieving structures explored, including micro/nanomachined structures and functional chemical materials, polyacrylamide (PA) gel is notable. PA gels are a common and powerful separation matrix for conventional benchtop electrophoretic separations of proteins, peptides, DNA and other biomolecules. PA gels are typically used in slab-gel formats including polyacrylamide gel electrophoresis. [77]

Much work has been done by different research groups to fabricate microfluidic devices capable of performing SDS-PAGE in a more efficient and shorter analysis time.[74,75,77,78,113–115] In each of the microfluidic systems, preconcentration of proteins prior to electrophoresis of the sample has been shown. For example, *Hatch et al*, utilized sophisticated photolithography, wet etching, and bonding techniques to fabricate micro- chips from Schott D263 glass wafers. This device employed two polymeric elements one thin (~50 μm) size exclusion membrane for pre-concentration, and a longer (~cm)

porous monolith for protein sizing, which was fabricated in situ using photopolymerization. The size exclusion membrane was polymerized in the injection channel using a shaped laser beam, and the sizing monolith was cast by photolithography using a mask and UV lamp. Proteins injected electrophoretically were trapped on the upstream side of the size exclusion membrane (MW cutoff ~10 kDa) and eluted off the membrane by reversing the electric field. Subsequently, the concentrated proteins were separated in a cross-linked polyacrylamide monolith that was patterned contiguous to the size exclusion membrane. [113]

In another study by Herr lab, a glass microfluidic chamber with supporting microfluidic channel networks was manufactured using wet etching techniques and then several different polyacrylamide gel elements were patterned by photopolymerization techniques to integrate stacking and resolving gel in to the system to mimic the conventional PAGE and subsequent antibody-based blotting. In this work, ultra violet (UV) light had been used to polymerize a different part of the polyacrylamide gel selectively at different times such that stacking occurred; running and blotting gels could be formed at specific regions of a planar, glass microfluidic device. Biotinylated antibody using streptavidin polyacrylamide gel was used to act as the blotting membrane, which allowed for post-separation analysis. [77]

The Agilent 2100 bioanalyzer, developed in collaboration with Caliper Technologies (Mountain View, CA, USA) has become the first fully commercialized implementation of microfluidics technology. [116,117]

The instrument uses semi disposable chips consisting of two glass plates bound together, one layer with microfabricated channels etched into it and another layer with 16 through holes that form the sample and buffer reservoirs and provide access to the channels. The channels are filled with a sieving polymer in order to separate the proteins according to their size, and an intercalating fluorescent dye that stains the proteins. Before the laser induced fluorescence detection of the different proteins, a de-staining step is integrated on the chip. The software automatically evaluates the data and displays a detailed result table containing the size and relative concentration of each protein, as well as the percentage of the total protein content of the sample.[118]

Although the mentioned devices have shown great novelty in the area of protein analysis in microfluidic systems, nevertheless, manufacturing in all of the these microfluidic systems tends to be monolithic and planar, requiring the development very clever or complex methods for building integrated devices. Glass has the advantage of transparency, but is difficult to obtain straight etched side walls. Simplifying the design, cost of manufacturing, and versatility of using the same technique for performing different assays were the main driving forces of this project. The ability to conduct post-

experimental analysis cannot be done in most current devices due to the closed system design. In addition, as mentioned before, one common drawback that can be counted in all of these systems is the lack integration. To run these systems, a lot of supporting elements are needed which makes these systems not "chip in a lab" rather than "lab on the chip". To address these issues, we came up with the μFloupon version of SDS-PAGE system.

3.3 μFloupon protein separation design

The goal of this study was to demonstrate that a μfloupon lamination technique could be used to perform SDS-PAGE analysis on a small sample of proteins. This involves manipulating proteins from a prepared sample, transport of the proteins into a small zone within a very thin polyacrylamide gel, electrophoretic separation of the sample in the thin gel, and removal of the gel with proteins intact for analysis and further processing.

To accomplish this, a stack of μFloupons was designed containing a top and bottom plastic manifold enclosure, and four microfloupons. These were:

(1) a thin polymer gasket/aperture microfloupon,

(2) a paper-gel microfloupon,

(3) a thin track-etched filter microfloupon,

(4) a second paper-gel microfloupon.

The system also included several gaskets in between the microfloupons to avoid and mitigate any leakage problems. The design is shown in figure 17. The manufacturing details of each component are described in the following fabrication section; here we focus on the design and function of the device.

The microfloupon stack was designed for use with a rigid plastic enclosure on the top and bottom of the stack. The enclosure contained machined holes and channels that provided mechanical strength to the system, and allowed for pipetting of reagent and sample into the system, routing of fluidic channels, attachment of electrical connections. During operation, the entire stack (plastic enclosure and microfloupons) was placed in an aluminum fixture to hold everything and press the stack together. Alignment pins were designed into each microfloupon to ensure that the microfloupons were aligned with respect to each other and the enclosure. To simplify the design, the tests were performed and collected initially on one injection site.

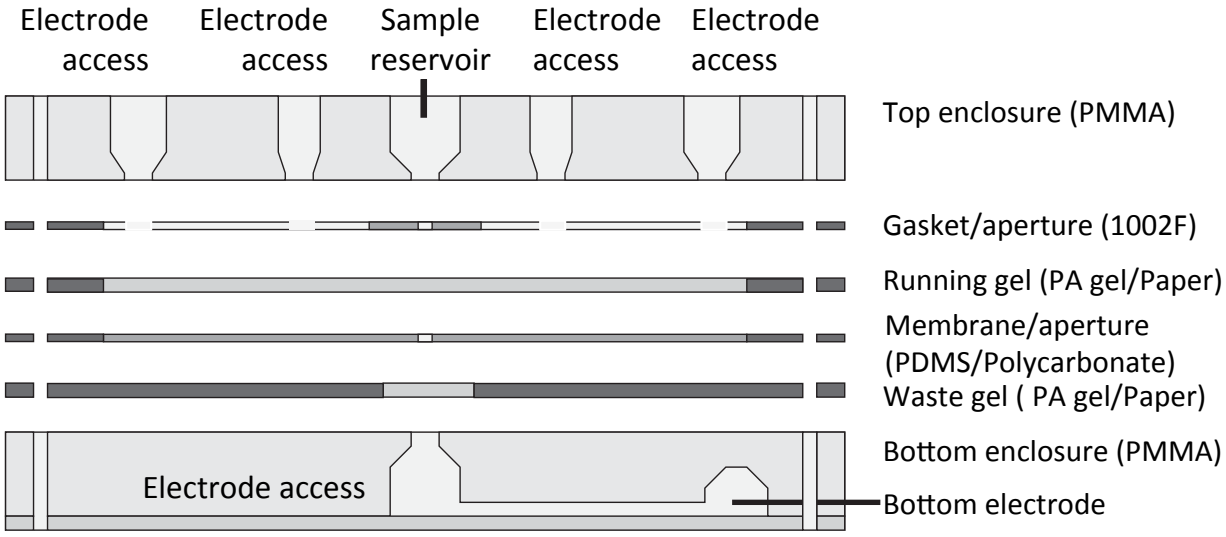

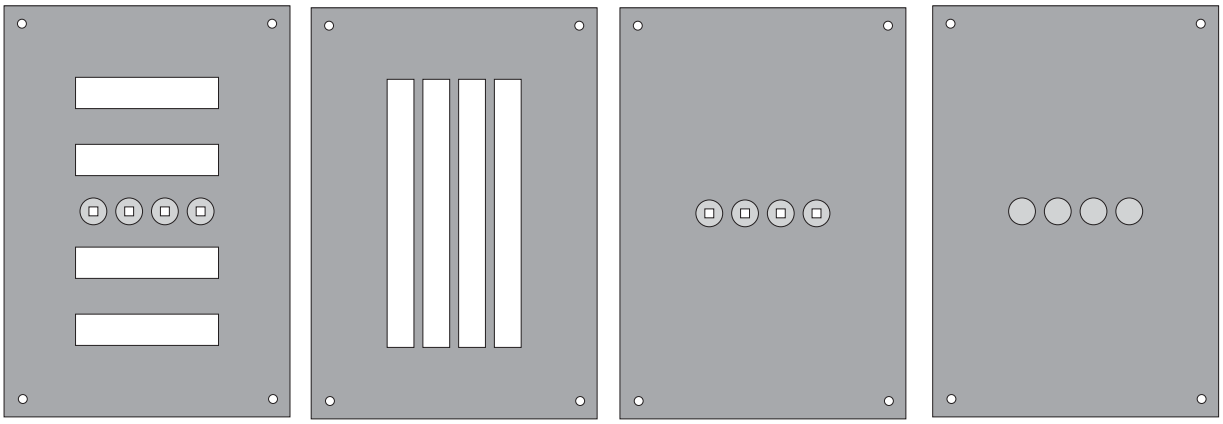

Figure 17. Layout of microfloupons used for this study. The top enclosure has several holes and slots that are filled with buffer to allow electrical connection to the gel. The middle reservoir is used to load the sample, to access the electrode. The bottom enclosure also allows electrical access through a hole and buffer; however, it is sealed to prevent buffer from falling out. The footprint for the entire structure is 4.3 cm x 7.0 cm x 1.5 cm.

The system was designed to work as follows: denatured protein sample was pipetted into the top reservoir in the housing. Voltage was applied to the top and bottom electrodes, forcing the sample to be electrokinetically driven vertically from the reservoir through the top aperture microfloupon:

(1) into the running gel microfloupon (2) the current passed through the running gel, through the track-etched membrane (3), and through the waste gel microfloupon (4) to the bottom of the device where the second electrode was placed. However, if no barrier was used below the running gel microfloupon, then proteins would have just flow from the injection reservoir down to the bottom reservoir and that's where we utilized a polycarbonate membrane. This microfloupon, track- etched membrane, was expected to

trap the proteins. Therefore, stopping and focusing the proteins in the running gel without letting the sample passing through.

After a suitable time, which was determined empirically, the voltage was switched to different electrodes, changing the electric field to a horizontal direction along the length of the running gel, and a standard electrophoresis separation was performed in the running gel. Detection of the sample and qualitative imaging of the system could then be done using standard staining or directly under the microscope using fluorescent-tagged proteins. In the following studies, we have used fluorescent-tagged antibodies to study the behavior of the device.

Successful operation of the device relied on two phenomena: (1) shaping of the electric field lines within the running gel, and (2) trapping the proteins at the surface of the track-etched membrane. For efficient operation, field lines had to be properly shaped to move the proteins into a small region of the gel without allowing dispersion to occur due to diverging field lines. Following focusing and injection of the proteins, the field lines were switched to run parallel to the running portion of the gel to and allow for electrophoretic separation of the proteins.

3.4 COMSOL Simulation Modeling

It is widely accepted that the quality of designs can be verified and improved by the proper use of modeling and simulation tools. Verification of the design

quality can be achieved by simulating the (predicted) performance and showing that it satisfies the demanded performance. Therefore, to better understand and predict the behavior of moving proteins during the injection, concentration and separation COMSOL software was utilized. COMSOL multi-physics is a finite element analysis, solver and simulation software for various physics and engineering applications. It has several modules from AC/DC, acoustic, and heat to MEMS, microfluidics and electromagnetics.

The modeling approach presented here uses a combination of analytical modeling and multiphysics finite element modeling to predict the behavior of μFloupon system for protein concentration upon operation. The results were then compared with an actual test to validate the modeling approach. First, to model the electrophoresis μFloupon system, a simplified model was designed. The original μFloupon design has four parallel lanes for multi-lane protein separation to mimic the macro-scale counterpart. In the simplified version of simulation, only one lane was simulated. Since we were interested in just the behavior of electric field lines, we used AC/DC module, which was sufficient for the design. Using an ammeter, the two currents were measured at an interval of time and the data was calculated to compare the impedances of the two. The impedance of PA impregnated paper was measured to be an average of 1.5X of the gel at relatively any time at a voltage of 330V as shown in Table 1.

The data showed a linear relationship between impedance and time. As time progresses, the resistance of both PA impregnated paper and gel increases due to the depletion of ions from the SDS running buffer.

Time(s)	Current (mA)	Current (mA)	R Paper (kΩ)	R Gel (kΩ)	R (pg)/R(gel)
	Paper+PA	Gel	Paper+PA	Gel	
0	1.86	3.21	177.4193548	102.8037383	1.725806452
15	1.74	2.77	189.6551724	119.133574	1.591954023
30	1.69	2.63	195.2662722	125.4752852	1.556213018
45	1.59	2.51	207.5471698	131.4741036	1.578616352
60	1.55	2.45	212.9032258	134.6938776	1.580645161
75	1.49	2.31	221.4765101	142.8571429	1.55033557
90	1.41	2.17	234.0425532	152.0737327	1.539007092
105	1.38	1.99	239.1304348	165.8291457	1.442028986
120	1.31	1.85	251.9083969	178.3783784	1.41221374
				Average Resistance	1.552980044

Table1. Resistance comparison between the polyacrylamide gel and a soaked filter paper

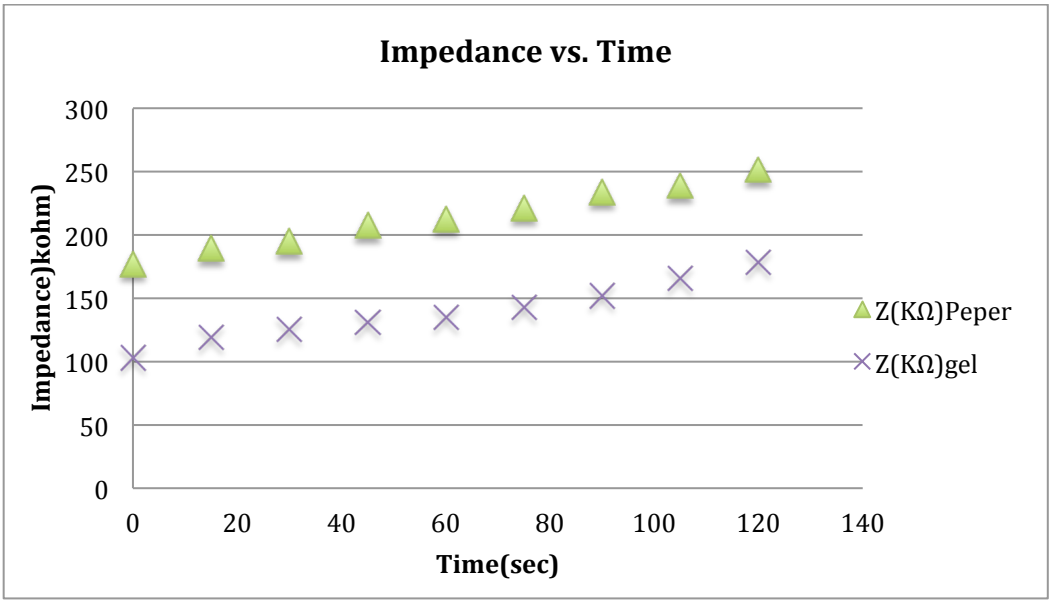

Graph1. Resistance vs. time comparison between gel and paper.

Electric field lines were determined using the location of current sources and drains and the arrangement of conductive and insulating media in the system. Graph 1 shows the side view of one lane indicating the electric field simulations using COMSOL. Two configurations are shown. The first simple design contains a negative electrode in the middle top reservoir for protein injection and a second positive electrode below the gel to drive the proteins from the reservoir into the gel membrane. The second case used three negative electrodes: one electrode in the injection reservoir, two electrodes on each side of the middle reservoir about 1mm apart from the center, and one positive electrode below the gel. In the gel microfloupon, gel was impregnated in both the main component of the paper and in open lanes cut into the paper. As mentioned earlier, the electrical impedance of the gel-filled paper was measured to be 1.5X that of the open gel regions. Thus, wide reservoirs at the electrode ends, and parallel and symmetric design of the gel lanes were needed to ensure that field lines are parallel within these lanes.

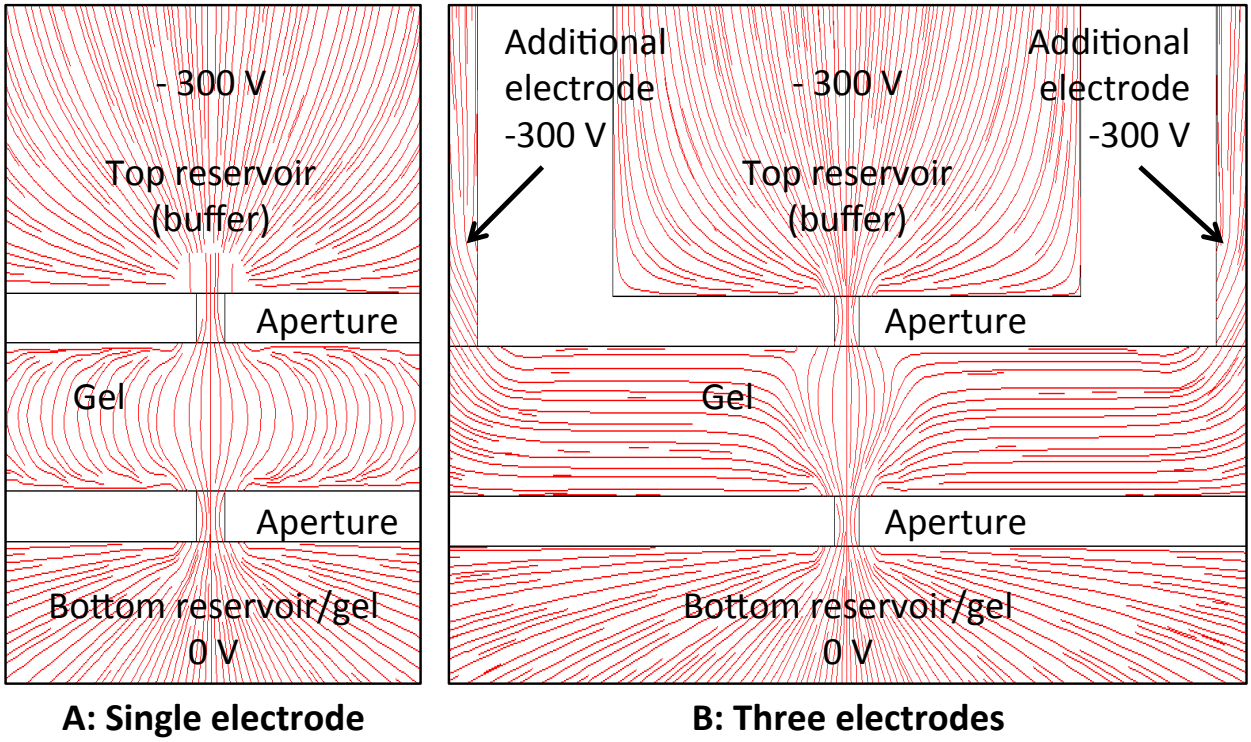

Figure 18 Slice of 3D finite element analysis (COMSOL) simulation of electric fields on a representative electrophoresis device. Image (a) shows simulation results of field lines achieved using one electrode with -300V applied at the top and a grounded electrode at the bottom. Note the diverging of the field in the center of the gel. The second image (b) shows the concentration of electric field lines using three electrodes with -300V applied to the top and sides and a grounded electrode the bottom.

To simulate the design, -300V and ground were applied as the driving forces. The COMSOL simulation indicated that one electrode was insufficient, as the electric field lines show diverging behavior in the gel. As a result, protein sample would be lost, rather than concentrated where the membrane was placed. However, when using three electrodes, the field lines show a tight converging effect, which significantly helped in accumulating and concentrating the protein sample.

This model was compared with an actual experiment and then upon observing the matching result used to do the following experiments that are described in the following chapters.

Chapter 4

Protein Analysis Experimental Method/Setup

4.1 Chemicals, Reagents and Material

Pre-labeled Alexa Fluor 532 goat anti-rabbit IgG (composed of heavy and light chain proteins, 50 kDa and 25 kDa respectively lot#:1241449) and BenchMarkTM fluorescent protein standard (12 kDa, 23 kDa, 33 kDa, 41 kDa, 65 kDa, 100 kDa, 155 kDa lot#:1232327) were purchased from Invitrogen (Carlsbad, CA, USA). Acrylamide/bis-acrylamide solutions (29:1) 30% and 40%, 10x Tris–glycine–SDS buffer (25 mM Tris, 192 mM glycine, 0.1% (w/v) SDS), SDS, tetramethylethylenediamine (TEMED), and ammonium persulfate (APS) were obtained from Sigma-Aldrich (St. Louis, MO, USA). Whatman track-etched membranes (0.1 μm lot#:65691, 0.08 μm lot#:49083, 0.015 μm lot#:54821) were donated by GE Healthcare (Waukesha, WI, USA). To make an appropriate polyacrylamide gel concentration (T), 30% and 40% (w/v) acrylamide-bis acrylamide was diluted with 4x lower Tris SDS electrophoresis buffer and water and when ready to use, a proper amount of TEMED and APS were added to the total volume. For micropatterning work, Shipley 1827 photoresist, SU-8 developer, 1-methoxy-2-propyl acetate, was obtained from Microchem Corp (Newton, MA). To produce 1002F resist, UVI-6976 photoinitiator

(triarylsulfonium hexafluo- roantimonate salts in propylene carbonate) was purchased from Dow Chemical (Torrance, CA), and GPL resin from Sigma Aldrich (St. Louis, MO).

To build the apparatus and other parts of the device, PMMA sheets were obtained from Anaheim Plastics (Anaheim, CA, USA) and PDMS base polymer and PDMS curing agent (Sylgard 184A/B) were purchased from Dow Corning (Elizabethtown, KY). For salinizing the surface of the glass, Sigmacote was purchased from Sigma-Adrich (St. Louis, MO, USA).

4.2 μFloupon Fabrication for Protein Analysis

The device consisted of a top and bottom plastic manifold enclosure, and four microfloupons: (1) a thin polymer gasket/aperture, (2) a paper-gel microfloupon, (3) a thin track-etched polycarbonate filter microfloupon, (4) and a second paper-gel microfloupon.

Figure ba shows Layout of microfloupons used for this study. The top enclosure contains several holes and slots that were filled with buffer to allow electrical connection to the gel. The middle reservoir was used to load the sample, as well as for electrode access. The bottom enclosure also allowed electrical access through a hole and buffer; however, it was sealed to prevent the leakage of buffer. The footprint for the entire structure was 4.3 cm x 7.0 cm x 1.5 cm.

Using computer controlled CO2 laser cutter (Versa Laser Systems, model VL200, Universal Laser Systems, Ltd, Scottdale AZ) and Adobe Illustrator software, the plastic manifold enclosures (top and bottom) were cut and from of slabs of poly methyl methacrylate (PMMA, Anaheim Plastics, Anaheim, CA). Each piece was 4.3 cm x 7.0 cm x 6.35 mm thick. Holes, reservoirs and channels were routed in the plastic using standard computer numerically controlled machining (CNC). Each enclosure had four precision through holes drilled for alignment pins. These were used to align the top and bottom enclosures as well as the microfloupons between them by using mini dowel. The plastic enclosures provided a mechanical-fluidic enclosure, and a flat surface to firmly hold the microfloupons together. They also allowed for easy electronic and fluidic access to the device through embedded the channels and reservoirs. To manufacture the bottom manifold, first a reservoir with the volume of 3mL was cut out using CNC machinery. Then, the bottom manifold was sealed with a thin acrylic sheet to prevent fluid from falling out of the bottom channels. First the bottom manifold and the thin PMMA sheet where cleaned with DI water and air-dried to remove any dust and impurities from the surfaces. Then, few drops of isopropanol were deposited on top of one piece and carefully the other piece was placed on top of it. Then the two pieces were sandwiched between two gaskets and two flat pieces of metals and were placed under the press at 165°C for 1 min to form an irreversible bond. Acrylic was chosen for both

enclosures because it is inexpensive, strong, easy to machine, and transparent in the visible range.[95]

The first microfloupon ("gasket/aperture") consisted of a thin polymer patterned with holes to let protein and electric current pass through from a reservoir in the top manifold to the acrylamide gel below it at a specific location. The polymer was a photo-definable epoxy, Photostructurable Resin PSR 1002F[119], which allowed it to be manufactured as a thin film using standard photolithography. To manufacture the aperture layer, the uncured 1002F epoxy material was spun to a thickness of 100 micrometers on a glass surface. The spin speed was 500 rpm for 10 seconds followed by 30 seconds at 1200 rpm. The resin was then soft baked at 65º C for 30 minutes to evaporate the solvent. Using a computer-generated photomask that defined small open regions (100 μm), the material was exposed to UV light at 6 mW/cm2 for 7 minutes to crosslink the polymer. SU-8 developer (MicroChem, Newton MA) then removed the unexposed areas and developed the pattern as it is shown in figure 19. To ensure proper alignments, alignment points were designed on the mask to indicate where the openings will be placed. The film was removed from the glass surface by soaking it in DI water for 2-3 hours. As the first microfloupon in the stack, the film could be aligned with the manifold by alignment notches placed in the plastic and in the microfloupon. The key feature of the gasket/aperture microfloupon

was a small opening (100 µm x 100 µm) in the PSR 1002F that allowed sample and electric current to pass into the running gel.

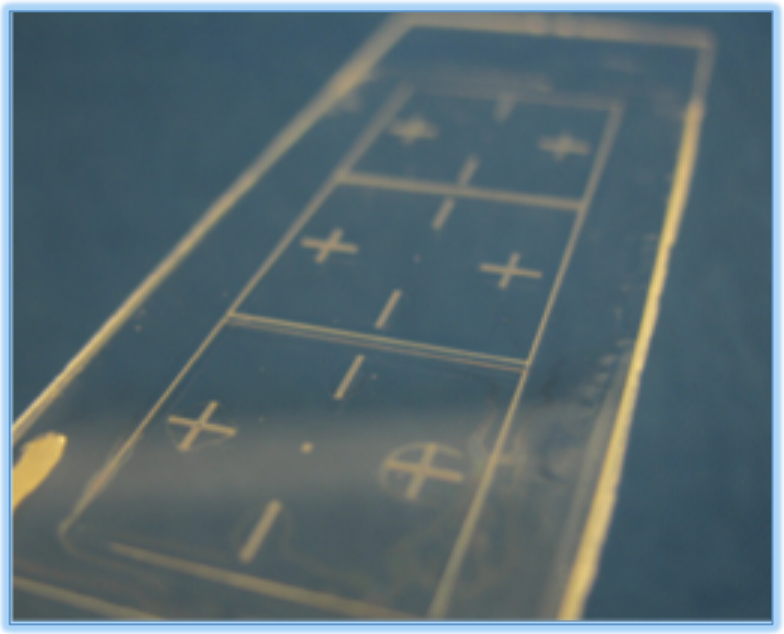

Figure 19. SU-8 pattern on a piece of glass after development

The second microfloupon ("running gel") was a polyacrylamide gel filled paper coupon designed to perform the function of collecting the proteins from the sample, then separating them along the length of the gel slab. This microfloupon was made from blot absorbent filter paper (Bio-Rad, Hercules, CA), 300µm thickness. Four lanes, each 2 mm x 36 mm, were cut in the paper using a computer controlled CO2 laser cutter.

The microfloupon paper and the slots were filled with 12% polyacrylamide gel. First 4x lower buffer was prepared. To make 4x lower buffer of 1.5 M Tris with pH 8.8 and 0.4% SDS, first two liter of the solution was prepared

by mixing 263.3g of Tris with 50mL of HCL and 80ml of 10% SDS and adding nano pure water to bring the volume to 2 liter. Then to make the gel, briefly, 30% acrylamide monomer (667 ml), sodium dodecyl sulfate (SDS) 4x lower buffer (500 µl), nano pure water (825 µl), and chemical initiators TEMED (1 µl) and ammonium persulfate (APS) (25 µL) were mixed together. This mixture was poured onto a paper microfloupon with pre-cut slots and allowed to soak into the paper. To ensure a flat gel of uniform thickness, the saturated paper microfloupon was placed between two clean glass surfaces and the polyacrylamide gel mixture cured. To improve removal of the gel from the glass, the glass was first salinized by dipping in silicone solution (Sigmacote, Sigma-Aldrich, St. Louis, MO) for 15 minutes, rinsing it and allowing it to dry. The result after casting and pressing the polyacrylamide gel in the paper was a smooth, flat paper microfloupon that was impregnated with polyacrylamide gel. The slots contained thin slabs of pure polyacrylamide gel, approximately 300 µm thick, with almost no air bubbles or defects. Moreover, the microfloupon could be handled and easily assembled in the laminate stack without tearing the gel membrane as it is shown in figure 20.

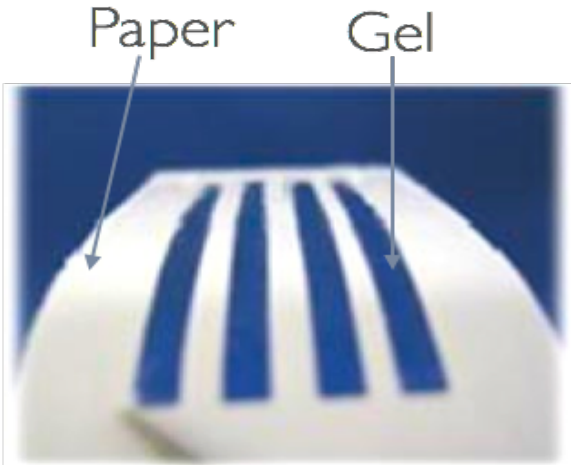

Figure 20. Gel impregnated paper microfloupon

The third microfloupon ("membrane/aperture") was a paper coupon impregnated with silicone polydimethylsiloxane (PDMS) and small openings in the center to allow current and ions to pass through to the bottom layer. A polycarbonate Whatman track-etched membrane, (Whatman, Kent, UK) patterned with photoresist to allow passage of current through a very small region, was placed on the PDMS microfloupon before the PDMS had cured. After curing, it held the membrane securely in place, while providing a good seal against leakage out the bottom and a transparent region for imaging27. The track-etched membranes were 25 mm in diameter, 6 μm thick and contained nanopores 15 nm in size, which appeared to block proteins in laboratory tests. Despite the large pore size of the membrane compared to typical protein size, our results show these to be reasonably effective in blocking the proteins. This may be due to the fact that polycarbonate is known to carry negative surface charge, which repels proteins.[120] The

membrane was prepared in order to produce a tiny region for the electrical current and ions to pass. It was first placed on a silicon wafer and held in place by polyimide tape. The wafer was then spin-coated using Shipley 1827 photoresist (MicroChem Corp, Newton, MA) for 40 seconds at 4000 rpm. After spinning, the membrane was baked at 95 °C on a hot plate for 3 minutes. A negative mask containing a pattern of 100 μm x 100 μm squares was placed on top of the membrane. The photoresist coated membrane was exposed to UV light (365 nm) at 11 mW/cm^2 intensity though the mask for 40 seconds. The membrane was then submerged in Tetramethylammonium hydroxide (TMAH) developer for 40 seconds to develop the resist pattern, resulting in a precise opening that was patterned on the nanoporous membrane. After patterning, the photopolymer was fully cured by baking at 120 °C for 30 minutes. The non-exposed region of the membrane remained covered with the polymerized photoresist, thus sealing the pores everywhere except at the small aperture. To remove the membrane from the wafer, the wafer was soaked in DI water overnight.

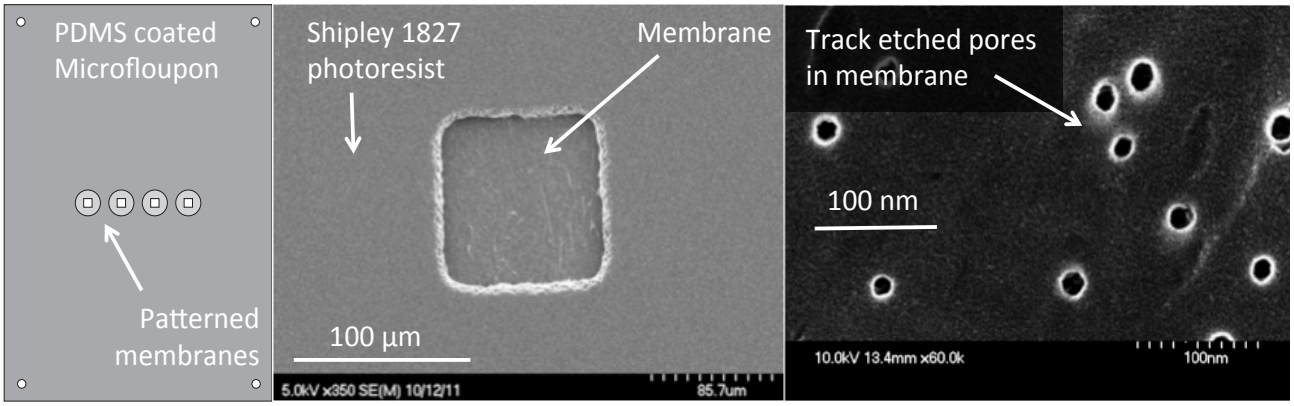

A) Membrane aperture µfloupon

B) SEM of patterned membrane with 100 µm x 100 µm aperture

C) SEM image of nanopores in track etched membrane

Figure 21. Details of track-etched membrane patterned with photopolymer to define small apertures. A) Microfloupon containing four apertures with membranes. B) Scanning electron micrograph of aperture defined by photopolymer, enabling placement of precision opening on the membrane. C) Close-up image of nanopores in the track-etched membrane.

The fourth microfloupon ("waste gel") was a paper coupon with a small opening that held 29% polyacrylamide gel in small openings, 2.5 mm in diameter. The percentage of the polyacrylamide gel was chosen to be over 22% which has the MW cutoff of ~10kDa.[113] The waste gel was chosen to be higher density to significantly slow down the migration of proteins leaving the system, thus allowing them to be imaged. This helped to understand the efficacy of the membrane for filtering the protein sample. This microfloupon also contained a PDMS coating, which was manually applied and cured that served to act as a bottom gasket for the system. The microfloupon provided an electrically conductive path to the bottom enclosure, and captured any proteins that might have passed through the membrane. Both the floupon

and running gel were made in a similar fashion. A small amount of gel solution was pipetted into the holes and allowed to cure using the same protocol as the running floupon. The gel easily impregnated part of the paper, providing a secure holding for the gel after it cured.

The holes drilled into the bottom plastic enclosure figure 23 corresponded with the openings in the waste gel microfloupon. These holes led to a channel that in turn led to a large cavity that contained a platinum electrode, which was inserted and sealed through a hole in the side of the enclosure. At the beginning of each experiment, after assembling the microfloupon system, the cavity with the volume of 3mL was filled with running buffer, providing electrical connection from the microfloupon gel to the electrode. Since bubbles were undesirable at the point of connection between the bottom enclosure and the top microfloupons, the cavity comprised a specific design to prevent the bubbles from moving from the electrode location to the connection point. The dome shape at the electrode side trapped the bubbles from moving along the cavity to the connection side when electrolysis occurred during operation.

At the end, the entire stack, consisting of two plastic enclosures and four microfloupons, was placed in a fixture to press all the layers together, forming a single multi-structured device that could be used to perform loading, concentrating, and electrophoretic separating of proteins as shown in figure 22 and figure 23. A fixture was made out of aluminum, which was

specially designed and fabricated by an outside vendor to provide enough support and enforced a leak-free microfloupon structure. After completing the injection and separation steps, the stack could be separated, and any of the microfloupons removed for further processing.

4.3 Protein Analysis Experimental Setup

To test the device, a standard SDS-PAGE assay was performed using a protein ladder and an antibody with two heavy and light protein bands in one of the four lanes. Two studies were performed, as illustrated in chapter 5. The first study (loading and injection) demonstrated that proteins could be injected into a small region within the acrylamide gel. The second study (separation) demonstrated that proteins could be electrophoretically separated in a thin microfloupon gel and that the microfloupon could be removed from the lamination stack with the gel and protein undisturbed, and that fluorescent analysis could be done on the microfloupon directly.

For both studies, prior to the experiments, the microfloupons were stacked and sandwiched between the plastic enclosures. The top and bottom reservoirs and channels were filled with 1 x SDS buffer (pH 8.3), taking care to avoid formation of bubbles. For the bottom enclosure, a syringe was used to fill the enclosed channel and cavity through a small hole in the side. This hole was also used to insert a bottom platinum electrode wire. Electrodes

were connected to a high voltage power supply HP6209B (Hewlett-Packard, Palo Alto, CA).

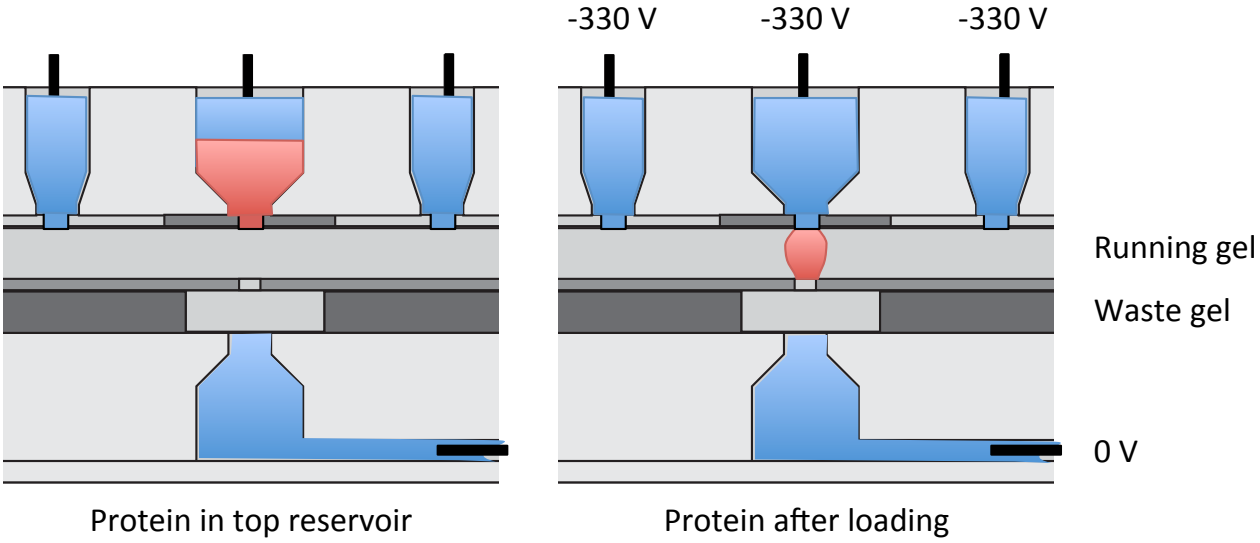

Figure 22 Basic procedure for loading study. Labeled protein sample was loaded into reservoir above gel. After electric field was applied, protein sample was allowed to electrophoretically migrate into the running gel.

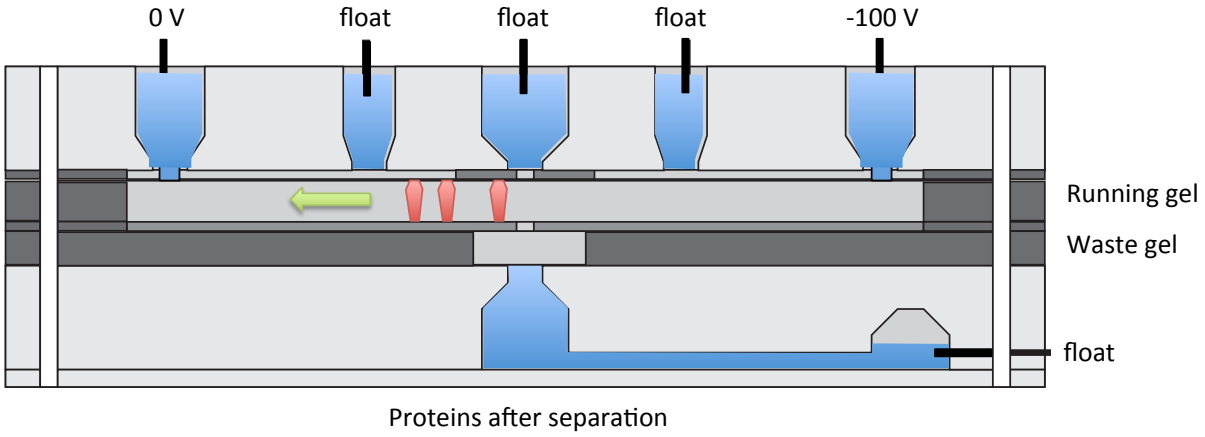

Figure 23 After loading, running gel and waste gel were imaged for proteins. Drawings are for illustration only. Components are not to scale, and gel thicknesses have been exaggerated for clarity.

The first study looked at the protein loading and injection and is illustrated in figure 25 in chapter5. For this study, 10ng Alexa Fluor® 532 labeled goat anti-rabbit IgG(H & L) protein was added to 200 μL of running buffer in the top reservoir. Alexa Flour® 532 is a bright yellow dye with excitation range between 420nm-595nm and emission between 520nm-676nm where the peak of excitation is at 555nm as it is shown in figure 23.

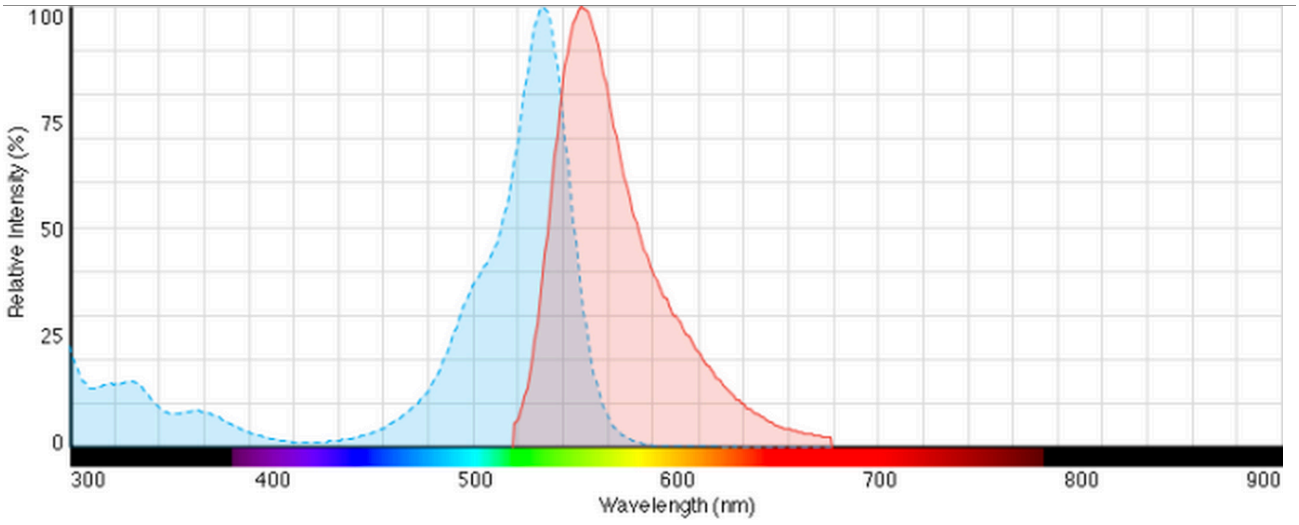

Figure 24 Fluorescence Ex/Em spectra of Alexa Fluor® 532 in pH 7.2 buffer. http://www.lifetechnologies.com/order/catalog/product/A20001

Platinum electrode was placed in the reservoir, as well as two electrodes in the side openings for field shaping purposes. -330 V was applied to the top electrodes with respect to the bottom ground electrode. The electric field was applied for 2 min, 6 min, 8 min, and 12 min allowing the proteins to electro-migrate into the gel layer. After each experiment, the gel microfloupon was removed, and then imaged under an Olympus IX71

inverted microscope equipped with fluorescein isothiocyanate (FITC Ex (494nm)-Em (518 nm)) filter.

In addition, the gel was cut under the microscope where the proteins were imaged using a surgical blade to reveal the cross section of the gel where the migration of the protein was expected. The gel was sandwiched between plastic blocks and turned up for imaging under the same microscope. This procedure allowed cross sectional images to be taken. Together the images indicated the ability of this system to focus proteins into a small plug suitable for electrophoretic separation.

To determine if the loading and injection process was efficient, the same imaging procedure was performed for the waste gel to determine how much of the protein passed through the membrane and left the main gel. Presumably, after some time, proteins may have migrated out of the running gel and passed through the track-etched membrane, thereby reducing the loading efficiency in the running gel. However, those proteins should be trapped within the acrylamide waste gel that was below the membrane, allowing them to be imaged.

In addition, after each experiment, the fluid in the injection reservoir was removed and analyzed for remaining protein. To do this, nitrocellulose (NC) blotting membrane along with filter papers were soaked in Tris-buffered saline and Tween-20 (TBS-T) solution and placed in a Bio-Rad 96 well bio-dot apparatus (microfiltration vacuum blotting device). The apparatus was

sealed using vacuum pressure. As a control, a 10 ng protein sample diluted in 200 μL running buffer was dispensed into one well of the bio-dot apparatus. The liquid samples collected from each experiment were similarly transferred, and all wells were washed with TBS-T solution to ensure that all of the protein in the sample was adsorbed on to the NC membrane. Using vacuum, the liquid contents of the wells was filtered through the NC and the wash repeated three times. The NC membrane was then air-dried in the dark and imaged using a fluorescent microscope (Olympus IX71) to quantitate the amount of protein sample left in the injection reservoir during the loading and injection steps. To account for background noise, the signal derived from an image of a well with no protein sample was subtracted from all of the results, including the control.

The second study examined protein separation and imaging. This proceeded in the same manner as the first study, except that after loading for 12 minutes, the electrodes were moved from the injection and the two site reservoirs and were connected to the ends reservoirs of the device, and the. At this time, -100 V, which was imperially determined, was applied between the first electrode and the second electrode. This initiated electrophoretic migration along the length of the running gel. To do this test, a separation experiment was performed using a "ladder" containing 7 fluorescently tagged proteins ranging in size from 12kDa to 155kDa. The protein ladder was tagged with Alexa Fluor 488®. Alexa Fluor® 488 dye is a bright, green-

fluorescent dye with excitation ideally suited to the 488 nm laser line with the maximum of the dye at 493nm and maximum emission at 516nm as it is shown in figure 25.

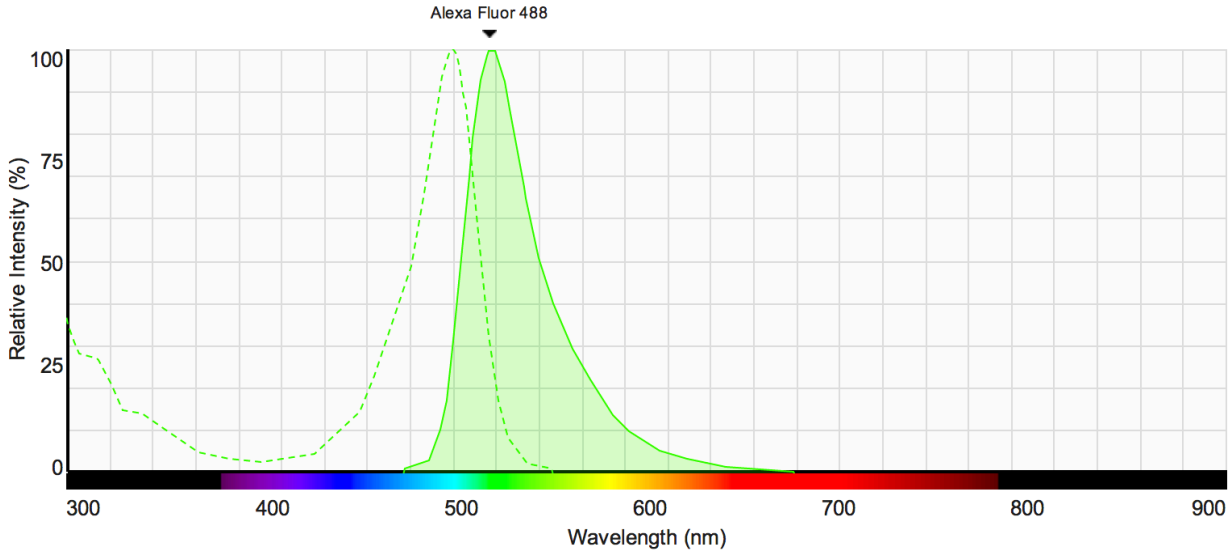

Figure 25. Fluorescence Ex/Em spectra of Alexa Fluor® 488 in pH 7.2 buffer

Chapter 5

Results and Discussion

5.1 Protein Loading And Injection Efficiency

Injection experiments were performed for 2, 6, 8, and 12 min using 10ng of protein in each experiment. The following experiments were performed using Alexa Fluor 532 goat Anit-rabbit IgG with two heavy and light protein bands. A constant voltage of -330 V was applied to force the negatively charged proteins into the gel, and the current consumption was monitored during the injection and separation experiments. The highest power consumption was 67.4 mW and it dropped to 33.7 mW after 12 min. Heating effects were not observed during the trials. Figure 26 shows the imaging results from the loading and injection study.

Cross-sectional images in figure 26 clearly show the movement of the proteins into the running gel, with the highest concentration starting at the top and advancing to the bottom of the gel over time. During injection, the protein front appeared to move in a well-behaved manner, consistent with the known electric field geometry. One can see that the plug shape matches the expected shape from the electric field simulations, as shown in figure 18 in chapter 3. Furthermore, at long injection time (30 min) the proteins appeared to pile up on the membrane at the bottom of the gel. To generate

figure 26, several tests were performed and the result of each test was captured separately and then the images were stitched together using computer software tools to acquire one image comprising top and side view result of each experiment. Refer to chapter 4 for more details on the method of data collection.

After running several tests, we came to the conclusion that most of the protein was driven out of the loading reservoir and into the polyacrylamide gel-paper microfloupon. Results of analysis of the reservoir solution are shown in figure 28. By 8 min, very little of the loaded protein could be detected in the reservoir by quantitation of filtration adsorption (figure 28, lower panel), suggesting that most of the proteins had left the solution.

The system relied on the use of a track-etched membrane to block proteins at the surface, while simultaneously allowing current and ions to pass through. However, since the pores were 15 nm, it is possible that proteins (which are typically smaller than this), would not be stopped by the membrane but rather pass through the pores. Some blocking of the proteins may be expected since the track-etched membrane (polycarbonate membranes) are negatively charged.[120] A 29% polyacrylamide gel microfloupon was prepared by adjusting the concentration of acrylamide solution and using the standard protocol and using the same exact method as described in chapter 4. This microfloupon placed under the track-etched membrane microfloupon to monitor the behavior of the proteins and to

capture proteins that passed through the membrane. Figure 29 shows the results of imaging of these gels after different injection times. After 8 min of injection, the proteins can be seen in the gel indicating that a small amount of proteins had indeed passed through the membrane. Thus, while the track etched membranes may have been effective and slowing down the rate of protein loss, they did allow a small fraction of proteins to pass through. Therefore future assays that wish to use this strategy would need to use smaller pore membranes, other ionic membranes, or use careful timing of the injection step to ensure efficient injection of the proteins into the gel.

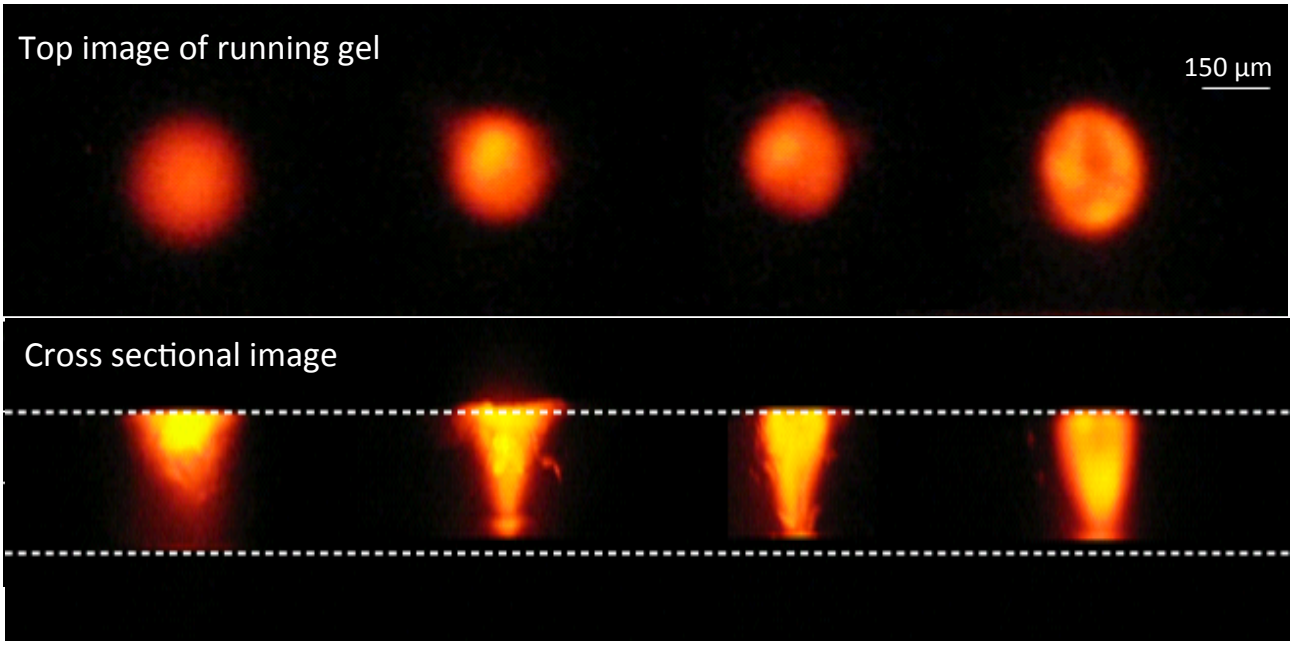

Figure 26. Imaging of protein sample after loading and injection into the running gel. The running gel microfloupon as removed from the stack and imaged after each experiment. Cross sectional images were obtained by cutting the protein gel and imaging the side

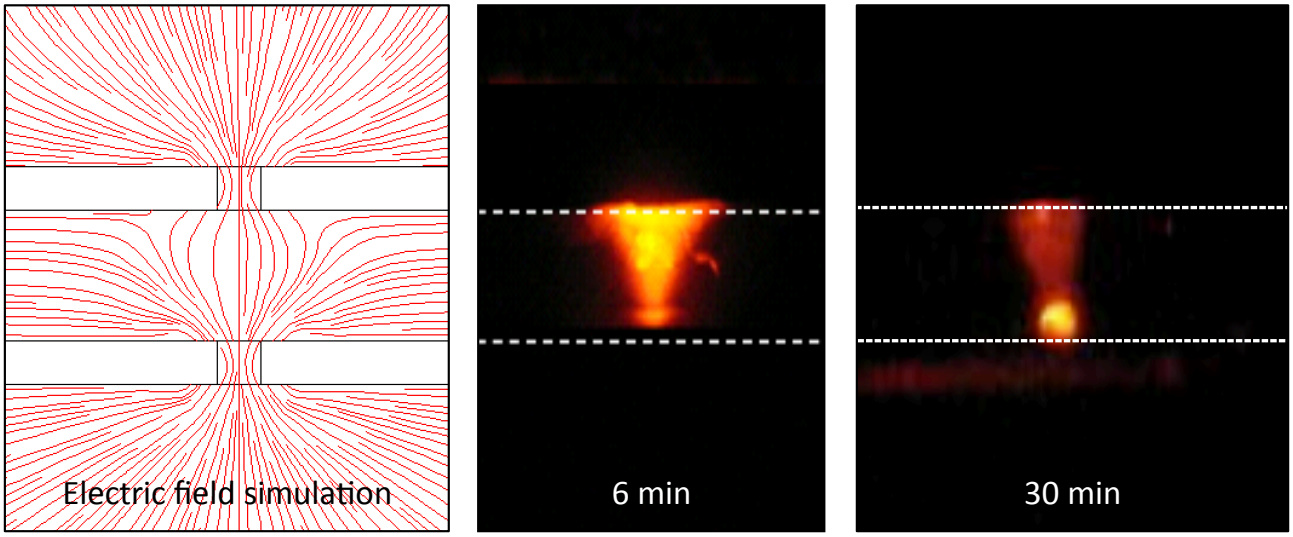

Figure 27. Comparison of finite element analysis of field lines (taken from figure 3) with cross sectional image of proteins during injection. The experimental results indicate the field shaping causes the proteins to pinch together in the gel. Also shown is an image taken after 30 minutes of injection. In this case, most of the protein migrated to the bottom of the gel.

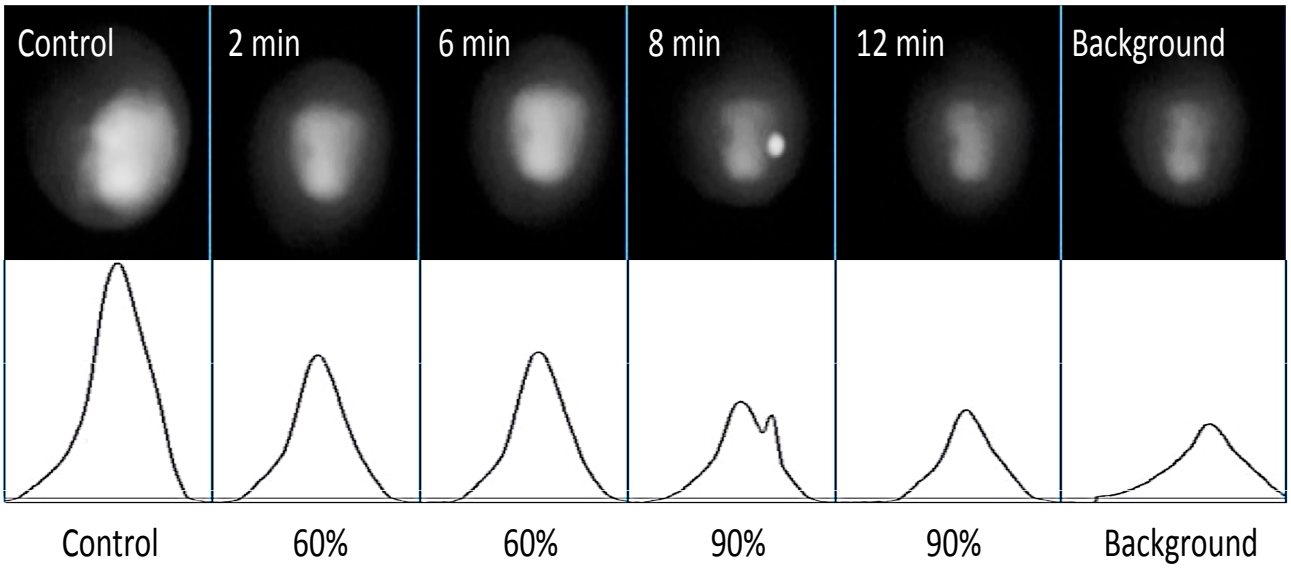

Figure 28. Analysis of fluid remaining in reservoir after loading into running gel. Most of the proteins are missing from the reservoir after 8 minutes of injection (imaging is close to background). These results are qualitative, but indicate that the electromigration of proteins out of the well is efficient

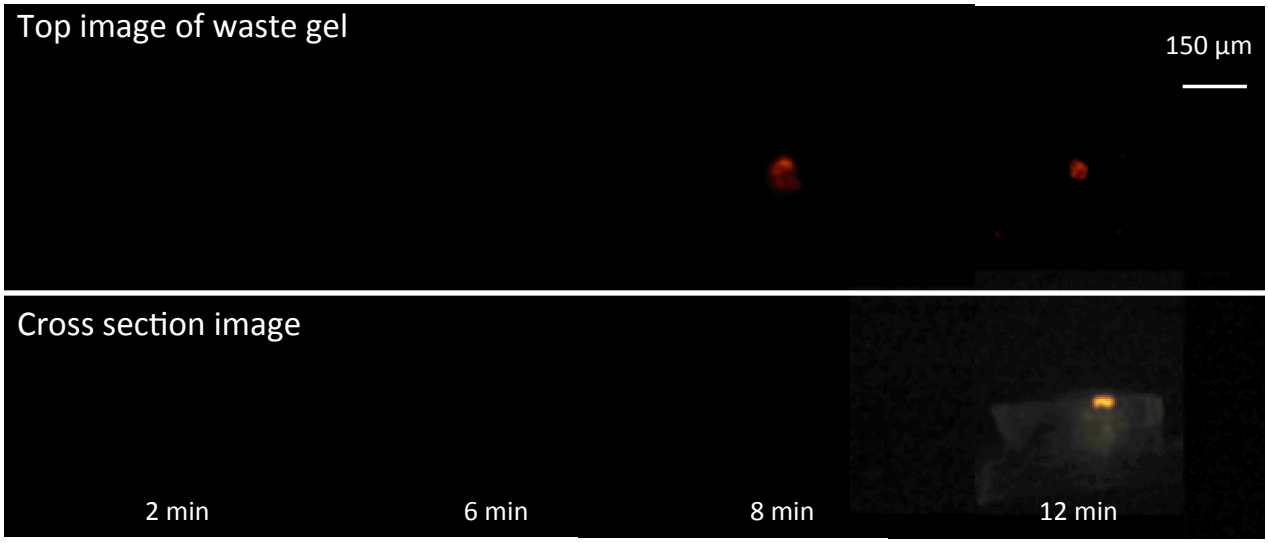

Figure 29. Imaging of waste gel (under track-etched membrane) after loading and injection into the running gel. The waste gel microfloupon was removed from the stack and imaged after each experiment. Cross sectional image was obtained by cutting the protein gel and imaging the side. After 8 minutes, some protein was seen to pass through the membrane into the gel below.

5.2 Protein Separation Analysis

The second study looked at the ability for a microfloupon system to perform a protein separation and to image the proteins in their microfloupon, out of the device. A 500 nl protein sample was loaded into the injection reservoir and injected for 12 min using the method described. Then the voltages on the electrodes were changed, switching the direction of electric field to the horizontal direction, resulting in electrophoresis of the sample. In addition, the voltage was decreased to -100V since higher voltages would have resulted in a very rapid separation and would have caused in lower resolution. During the separation mode, the anode and cathode electrodes were connected to wide conductive paths at each end (figure 28). This

feature, combined with the symmetric and parallel design of the gel lanes, resulted in parallel electric fields along the length of the gel microfloupon, despite the fact that the gel lanes have higher conductivity than the gel filled paper. This was confirmed with full 3D analysis of the electric fields. Thus, no cross-talk in the current between lanes was expected. To proof this fact, a set of tests were run in which two injection reservoirs were filled with the running buffer and 500nL of Alexa Fluor 532 goat-anti rabbit IgG containing 10ng of protein samples were injected in the reservoirs. Then, the microfloupon was taken out of the device and imaged under the microscope. The same size spot were observed on the microfloupon as it is shown in bottom of figure 30. Then the microfloupon was placed back into the device and electrophoresis was performed which showed a parallel field lines as it is shown in the top of figure 30.

The electrophoresis was run for 3 min. After electrophoresis, the running gel microfloupon was removed from the stack and imaged using an inverting microscope. Two sets of experiments were run. One with the Alexa Fluor 532 goat anti-rabbit IgG which contained bands of heavy and light chains at 50 and 25KDa and one experiments with BenchMark ladder with 7 protein bands varying from 155 to 12kDa. The first one was imaged directly under the microscope. However, since the microscope field of view was not wide enough to capture all the protein samples in a single image, in the BenchMark ladder experiment, the microfloupon was imaged at different

points and the images were merged. Figure 31 shows the 7 protein bands of the known standards, indicating that proteins as small as 12 kDa can be collected on the membrane and separated along the gel of the microfloupon, using the SDS-PAGE microfloupon device.

All seven protein bands were clearly identified in the gel, indicating that the system was well behaved and that the protein separation worked according to expectations. Moreover, since the microfloupon was readily removed from the device, it could be readily imaged using conventional imaging tools such as a fluorescent microscope. The gel microfloupon was easy to handle and was not torn or distorted during disassembly or transport, despite being approximately 300 lm thin. For example, the gel microfloupon containing the proteins could be placed on a blotting device, if desired, or placed in a high sensitivity imager.

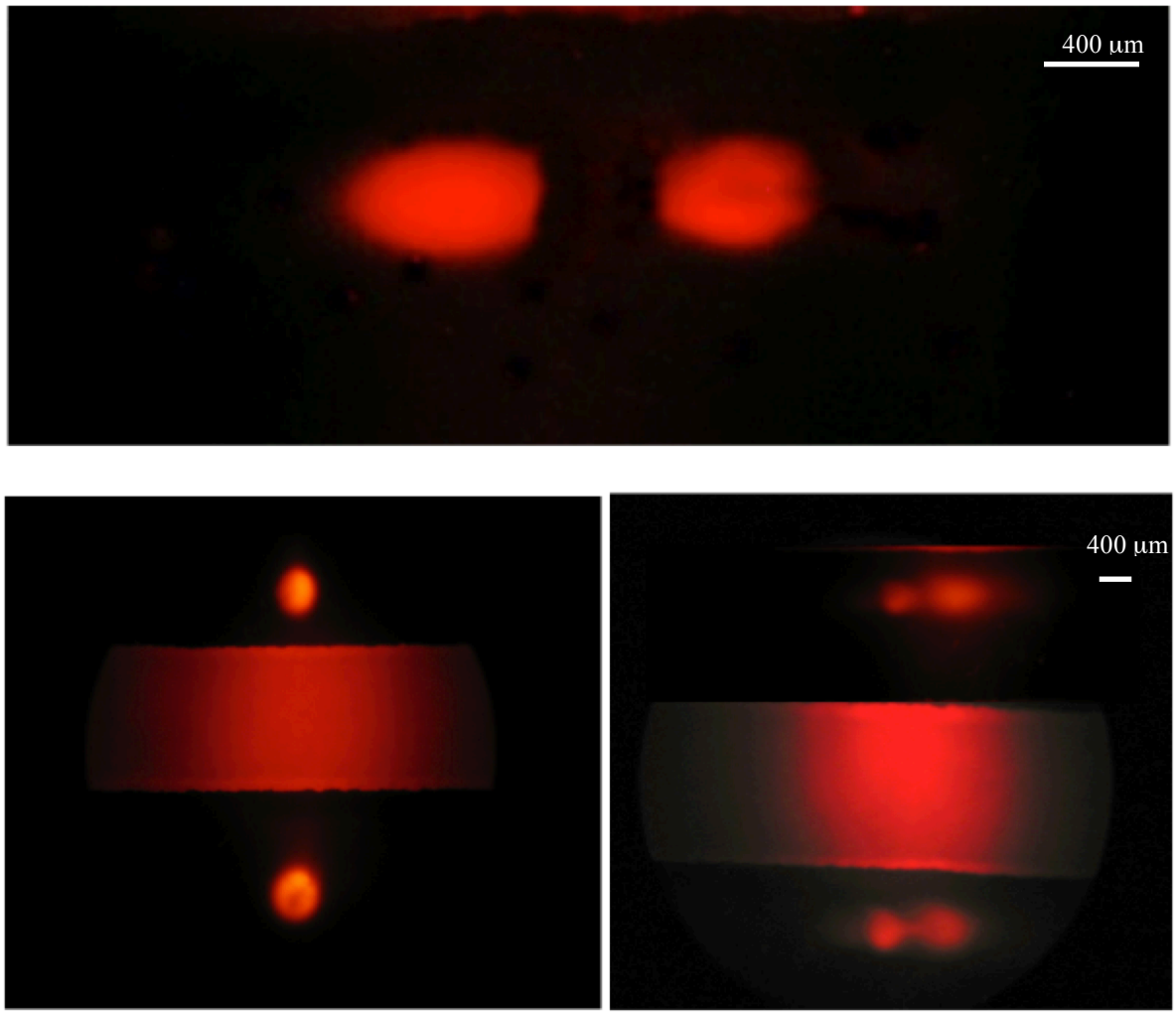

Figure 30. Top . Top view of two bands of Alexa Fluor 532 Goat anti-rabbit IgG after 3 minutes of separation containing 25kDa and 50kDa. Bottom: two lane protein injection and protein separation indicating no cross-talk between the lanes.

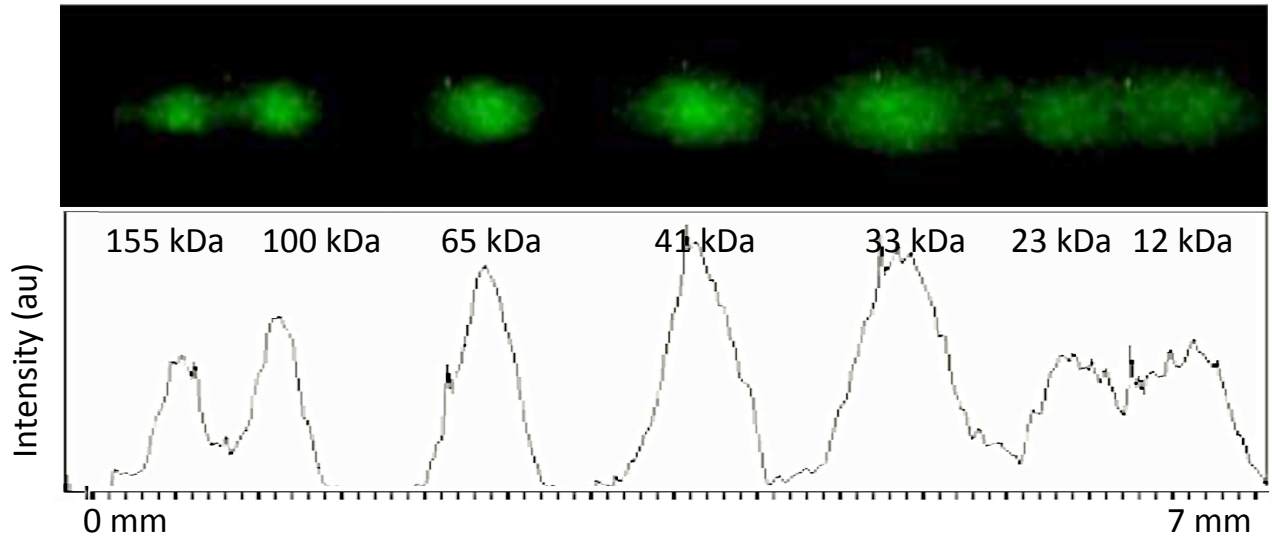

Figure 31. Imaging of running gel after separation experiment. All seven bands of the protein ladder are visibly separated in the gel. The intensity of the small proteins appears lower than the other proteins which may be an indication that the smaller proteins are leaking through the track etched membrane, and being depleted from the injection plug.

5.3 Conclusion

In this study, we demonstrated the development and utility of a general-purpose laminate technology that utilizes microfluidic coupons to integrate multiple materials and technologies together into a small platform for doing micro-scale assays. The microfloupons are manufactured separately, then laminated together to form a final integrated device that can perform a bioassay on a small size scale. In this work, our microfloupons were made from gel and paper, silicone rubber, track-etched membrane, and photosensitive polymer, resulting in low cost laminates with high functionality. We demonstrated this technology for a gel-based application (gel electrophoresis). Gels are typically difficult to integrate into microfluidic devices, and layer-to- layer functionality is particularly difficult. However,

with the microfloupon approach, gels are readily integrated, and functionality between layers (such as use of apertures, electrical vias, filtration) is readily included.

The application described in this paper was for injecting and separating proteins in a gel, following the SDS-PAGE protocol. Injection was accomplished through the use of shaping electric fields, apertures built into the microfloupons, and a nanoporous membrane built into a microfloupon. We demonstrated that 10 ng of protein can be collected into a small plug in the microfloupon with reasonable efficiency. We used a track-etched membrane, which slowed down the protein transport in the gel, but ultimately did not capture all the proteins. However, it did allow us to explore the use of protein injection using field shaping and lithographic patterning of apertures, such as the use of a 100 lm aperture patterned directly on the track-etched membrane. Future versions of this strategy should use membranes with smaller pore sizes, or use ionic membranes such as dialysis membranes—both of which are hard to integrate into conventional microfluidics, but easy to incorporate into a microfloupon stack. By changing the direction of the electric fields, we demonstrated that injection could be followed by electrophoretic separation of the proteins, with protein masses ranging from 25kDa to 50kDa in one experiment and 12 kDa to 155 kDa. The gel microfloupon was easily removed, handled, and transported to another sys- tem for imaging. If desired, this gel

microfloupon could be placed in a second cassette for electroblotting, suggesting that this system can be designed for a full Western analysis with small protein samples. A major benefit of the microfloupon approach is that different technologies can be combined together as needed to produce an assay of interest.

Chapter 6

Microvalve Systems

6.1 Introduction

Microvalves, which have proven to be important components in current microfluidic technology, are widely used in MEMS applications and are very useful in fluidic manipulation and delivery. The challenging requirements for microvalves have been to reduce the overall size, leakage and price while improving performance and reliability.

One of the driving forces behind designing microvalves in microfluidic systems has been the transition from single lane microfluidic devices to advanced sophisticated parallel multistep operational process. Consequently, precise controlling of fluid flow and successfully manipulating the flow in microchannels is an essential part of the operation. Therefore, integration of microvalves and micropumps on Lab-On-a-Chip devices is of major interest. Development of precise and reliable microvalve would be an important step to achieve this goal. However, from a practical solution standpoint, the successful miniaturization and commercialization of fully integrated microfluidic systems have been delayed due to the lack of reliable microfluidic components, i.e., micropumps and microvalves and the lack of reliable mass production methods which has left the prototype microvalves

and micropumps in the research labs. Therefore there is a need to address the above challenge and that was the deriving force behind this part of the research to be able to demonstrate a microvalve using microfloupon technology.

A variety of microvalves have been developed for on-chip fluidic manipulation and control. Most microvalves found today roughly fall into one of two major categories: passive microvalves, using mechanical and non-mechanical moving parts and active microvalves, using mechanical and non-mechanical moving parts, as well as external systems. A passive microvalve is often a check valve or a capillary valve that allows fluid flow in a forward direction while preventing the flow in the reverse direction[121–123]. These passive valves are often used in micro-pump applications and route fluid flow in the desired direction, but lack the ability to precisely control flow rate. Active microvalves are composed of a flow channel, a membrane or flexure, and an actuator; there are no actuator components in passive microvalves. Active microvalves can be categorized into three groups based on their actuation method. Traditionally, (1) mechanical active microvalves are accomplished using the MEMS-based bulk or surface micromachining technologies, where mechanically movable membranes are coupled to magnetic, electric, piezoelectric or thermal actuation methods. (2) mechanical active microvalves can be operated by the use of smart or intelligent materials. These non-mechanical active microvalves may hold

movable membranes, which are, however, actuated due to their functionalized smart materials such as phase change or rheological materials. In addition, (3) external active microvalves are actuated by the aid of external systems such as built-in modular or pneumatic means. Additionally, based on their initial mode, microvalves can be divided into normally open, normally closed and bistable microvalves.[124]

Based on the actuation method, microvalves can handle different pressure range and different time response

As far as the materials and methods of microvalves go, borrowing micromachining techniques from semiconductor industry, the first microvalves were built on silicon[125,126]. Later due to the biocompatibility of silicon with biological assays, devices were made mostly in glass and polymers. A variety of microvalves and micropumps have been demonstrated using polymers, and glass-silicon. In the next section, the mechanisms for actuation of active microvalves is explained and discussed.

6.2 Active Valves Actuation Methods

Active valves are critical components of a microfluidic system in controlling the fluid flow. The active microvalves usually incorporate a moving membrane to open and close the valve. These microvalves have employed several actuation methods including pneumatic[127–129], piezoelectric[130–133], electromagnetic[134–137] thermal[138–140], and other actuation methods[141–144].

For characterization of microvalves, a few specifications are always considered. The major specification bases for microvalves are leakage, valve capacity, power consumption, closing force (pressure range), temperature range, response time, reliability, biocompatibility, and chemical compatibility.

The leakage ratio L_{valve} is defined as the ratio between the flow rate of the closed state $\dot{Q}$ closed and of the fully open state $\dot{Q}$ open at a constant inlet pressure:

Eq. (5) $$L_{valve} = \frac{\dot{Q}\ \text{closed}}{\dot{Q}\ \text{open}}$$

Additionally, based on their initial mode, microvalves can be divided into normally open, normally closed and bistable microvalves.

Figure 32 illustrates several methods of active microvalve actuation, which are explained in the subsequent sections.

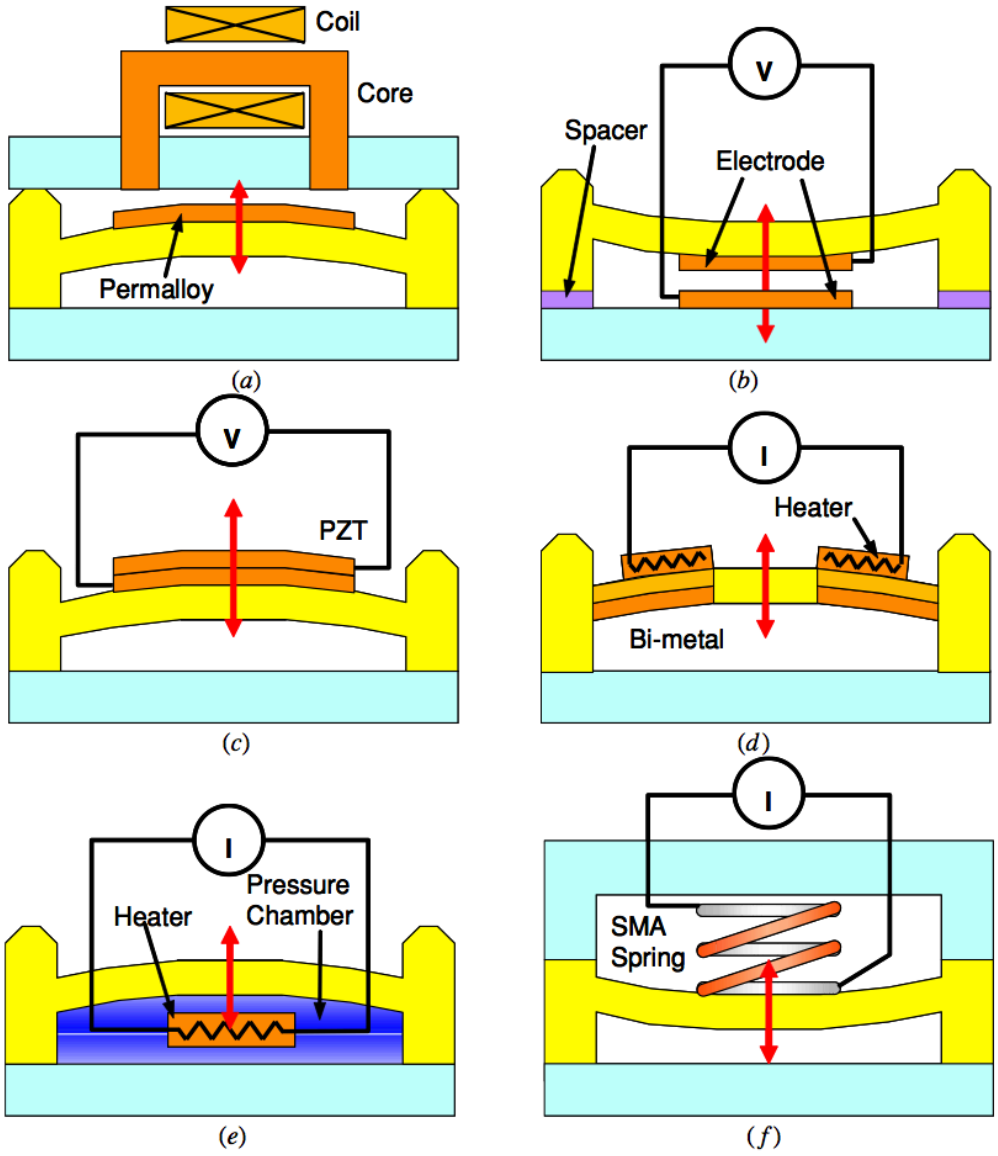

Figure 32. Illustrations of actuation principles of active microvalves with mechanical moving parts: (a) electromagnetic; (b) electrostatic; (c) piezoelectric; (d) bimetallic; (e) thermopneumatic and (f) shape memory alloy actuation.[124]

6.2.1 Pneumatic Actuation

Pneumatic microvalves are the most common and simplest kind of valves in which the air pressure usually provides the force for actuation of the membrane, which means this technique, requires external precise air

pressure and vacuum, making the devise operation bulky. The response time of pneumatic valve depends on external switching which are much slower than the microvalve itself and because of large external supply systems the response time is in the order of several hundred milliseconds to several seconds.

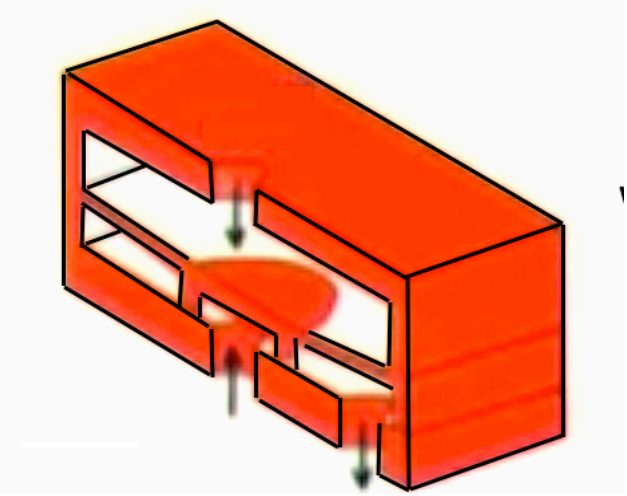

Figure 33. Illustration of a pneumatic actuation of a microvalve where an external pressure controls the movement of the membrane to open and close the microvalve.

6.2.2 Thermal Actuation

As the name calls for, thermal actuation is a method in which the thermal heat energy is converted to mechanical movement causing displacement of the membrane. Among the microvalves, thermo-pneumatic, and shape memory alloy actuations use thermal properties of materials to generate displacements. These actuation schemes generally produce a considerable amount of force while simultaneously achieving large strokes.

Thermo-pneumatic microvalves are operated by volumetric thermal expansion or phase-change phenomena coupled to membrane deflection. Thermo-pneumatic actuators use a combination of thermal and pneumatic techniques to provide the force for the membrane actuation, which depends on high temperature operation and an external pneumatic device. The actuation method can provide relatively large deflection. However, this type of valve typically has a longer response time and the fabrication process is often complicated due to the necessity to fill the chamber with fluid and to provide a hermetic seal. Takao et al. employed PDMS as a diaphragm material for a long stroke actuation in microvalve operation and high sealing performance.[145] At 50kPa inlet pressure, a micro-heater power of 100 mW was required to cut-off the flow, and a flow-rate of 17 mL/min was achieved when fully open. The transient time necessary to open the valve was about 23 s and the transient time necessary to close the valve was 1.5 s. Rich et al. also developed a high-flow thermopneumatic microvalve, which is constructed from a three-wafer stack with a corrugated diaphragm.[138] In general, thermal actuation schemes can provide large force to withstand large pressure but as they require current for heating elements, these methods have relatively high power consumption, and generally have slow response time

Memory alloy microvalve actuation is a less popular method of microvalve actuation for liquid controlling and more popular for gas handling. The

operation principle of the microvalves is based on the use of a SMA micro-device for deflection control of a membrane, which thus opens or closes the valve port. The valves are designed for operation in a normally open condition, where the pressure acts as a biasing force against the actuation force generated by the SMA device. Kohl et al. were able to actuate a gas microvalve in a normally open state and allow control pressure differences below 2500 hPa at gas flows below 360 standard ccm.[146]

6.2.3 Electrostatic Actuation

In this method, by using the electric field, an electrode membrane is actuated. Electrostatic microvalves often require relatively high applied voltages (> 100 V) to generate sufficient force to open and close the valves against even a modest pressure (1 kPa), since the electrostatic force is inversely proportional to the square of the gap between the electrodes. The electrostatic force generated between two conductors depends on the separation distance (d) and the applied voltage (V):

Eq. (6)
$$F = \frac{\partial E}{\partial d} = -\frac{1}{2}\frac{\varepsilon A}{d^2}V^2$$

where ε is the electric permittivity, and A is the overlap area of the two parallel plates. Assuming the actuation voltage stays constant, the electrostatic force $F \propto [D^0]$. This indicates the force is independent of the characteristic length, D, and would become a dominant force in micro-

domain. However, unless the separation distance is very small, the force is generally small. In general, electrostatic actuation is adequate for the low force and energy density requirements and has been used successfully in many MEMS applications. Nonetheless, in some cases, this small displacement may hinder the microvalve performance by limiting flow rate, and to obtain significant forces, large form factors maybe required.

Similar to memory alloy microvalve, most electrostatic microvalves have been employed for gas flow regulations rather than liquid flow controls due to electrolysis of liquids at high voltages. However, some researchers have been able to use touch-mode capacitance to close the valve in a modest voltage range of around 50V.[147,148] A touch-mode actuator consists of a flexible membrane and a fixed electrode. The membrane starts out touching the fixed electrode at one side of the membrane. When a voltage is applied, a zipping action is created that pulls the membrane onto the rest of the electrode. An advantage of a touch-mode capacitance actuator is that the electrostatic force can be maintained or increased by using the zipping action, even though the initial gap between electrodes is larger than the one of a typical electrostatic actuator.

6.2.4 Piezoelectric Actuation

In piezoelectric microvalve, the electrical energy is directly converted to linear motion. Certain crystals have the ability to produce a mechanical

deformation by a change in the electrical polarization of the crystal. This is called piezoelectricity. This effect has been widely used in microvalve and micropump fabrication, because it can generate large force. There are several commercially available MEMS-based micropumps based on these piezoelectric principles (from thinXXS Microtechnology, Zweibrucken, Germany and Star Micronics, Shizuoka, Japan). One of the earliest works on fabrication of piezoelectric microvalves was presented by Esashi et al[125]. The valve is constructed from silicon mesa suspended with a flexible silicon diaphragm pressing against a glass plate by a stack piezo-actuator with dimensions of 3×1.4×9 mm3. The valve is capable of modulating a gas flow from 0.1 to 85 mL/min with 73.5kPa inlet pressure in less than 2 ms response time. Although large force is available using piezoelectric actuators, large stroke is a challenging issue even for large voltages. This issue has been compensated through the use of hydraulic amplification and piezo bimorph or stacked piezoelectric disks.

6.2.5 Electromagnetic Actuation

Electromagnetic actuation utilizes the force generated between interactions of current-carrying conductors and a magnetic field. According to the Lorentz force law, the electromagnetic force acting on a test charge is represented as:

Eq. (6) $$F = qv \times B$$

Where q is the electrical charge of the particle, v is the velocity of the particle, and B is the magnetic field. The main advantage of magnetic actuation is the ability to create a relatively large force and thus large deflections with low driving voltages. However, this force does not scale favorably in the micro-domain. Electromagnetic actuators, unlike the other types, operate under low voltage and low power consumption. In this type of valves, the change in the magnetic flux density in the displacement direction dB_z/dZ provides the actuation force (F_z). The electromagnetic field can originate from an electromagnetic coil, a permanent magnet or combinations of the two. Since an electromagnetic drive can apply force over a comparatively long range and can easily control conductive fluid, it would be useful in many applications.

One of the first active micro-machined valves was reported by Terry et al. in 1979, to be used in an integrated gas chromatography system.[149] The valve consists of an etched silicon orifice, a nickel diaphragm, and a solenoid actuator and plunger assembly. When the solenoid was energized, the plunger was pulled, allowing the diaphragm to relax and gas to flow. Other examples of works in magnetically actuated microvalves have been explained.[134,136,141] Most of the designed valve have been manufactured in silicon. The fabrication techniques for these microvalves are complicated,

require cleanroom facilities and are expensive to manufacture which means they can't be scalable. In addition they require continuous current consumption. The process that will be explained in the following chapters are the process of making a microvalve that is electromagnetically actuated and has the capability to latch up and down. Using a bistable technique can reduce the energy consumption of the electromagnetic microvalve. In addition, since the effective range of electromagnetic forces is comparatively long, the valve driver can be located outside the fluid flow being controlled. This also relieves the driver of restrictions on its coil dimension, which would normally apply if the driver were integrated with the valve

In the systems where latching and unlatching is not present, a continuous current consumption can raise the temperature at the valve operating point causing heat and degradation of the sample. A few groups have successfully made electromagnetic actuated microvalves with latching/unlatching systems[134,150], nevertheless, to our knowledge no groups has attempted to make a microvalve in paper with actual channels using conventional lab equipment and tools making a scalable manufacturing process.

Chapter 7

μFloupon Technology in Microvalve System

7.1 Concept and Design:

Figure 34 shows a schematic design representing the paper microvalve. The microvalve was constructed using five main microfloupon layers all made out of paper-PDMS. To actuate the microvalve we chose to use electromagnetic actuation method. This actuation scheme was the best option for this design since other actuation methods did not satisfy our requirements. With pneumatic actuation, although simple, there needs to be an external channel to change the pressure externally and the design required having no need for external pressure system. As far as thermal actuation goes, nearby heater fabrication can introduce unwanted parasitic heat want to raise the temperature, so to avoid any complication caused by heat in the channels where reagents and solutions are present, any actuation methods that would cause overheating were not considered. SMA actuation also needs high temperature and also consumes high power usage. An electromagnetically driven microvalve can be designed to provide large force and stroke but this method might require relatively large power. To overcome this challenge, a latching method was incorporated in the design to avoid continuous flow of current and to actuate the valve with just a pulse where the membrane will be in a closed or open state. The design involved incorporating different

microfloupon layers each composed from different materials as it is shown in figure 34.

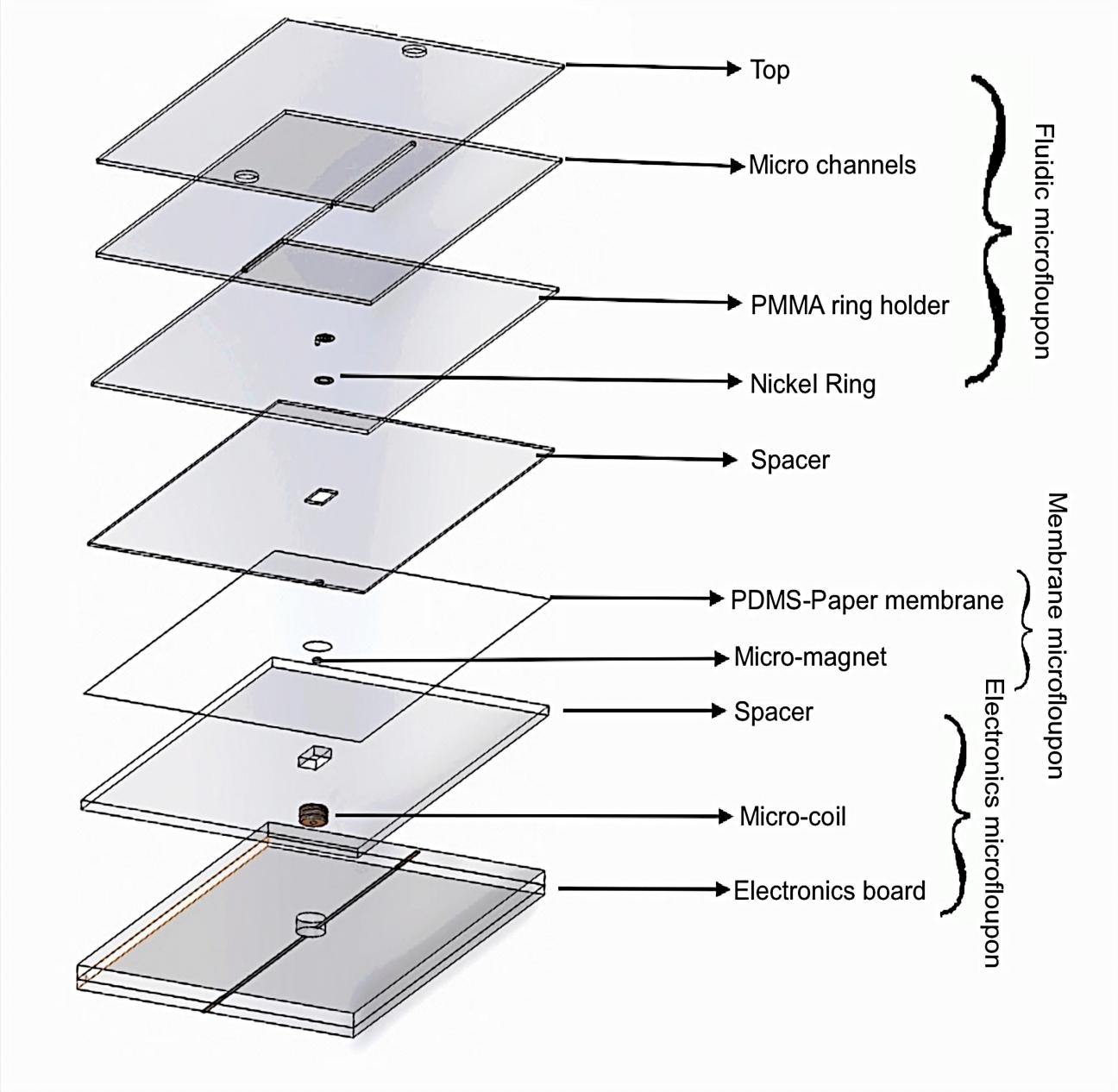

Figure 34. A simplified model of electromagnetically bistable microvalve with latching/unlatching mechanism components. The components are composes to make different microfloupon layers in the system.

Total of three major microfloupons were designed and fabricated separately using different materials and techniques and then combined to make the whole system: electronics microfloupon, membrane microfloupon, and fluidic microfloupon.

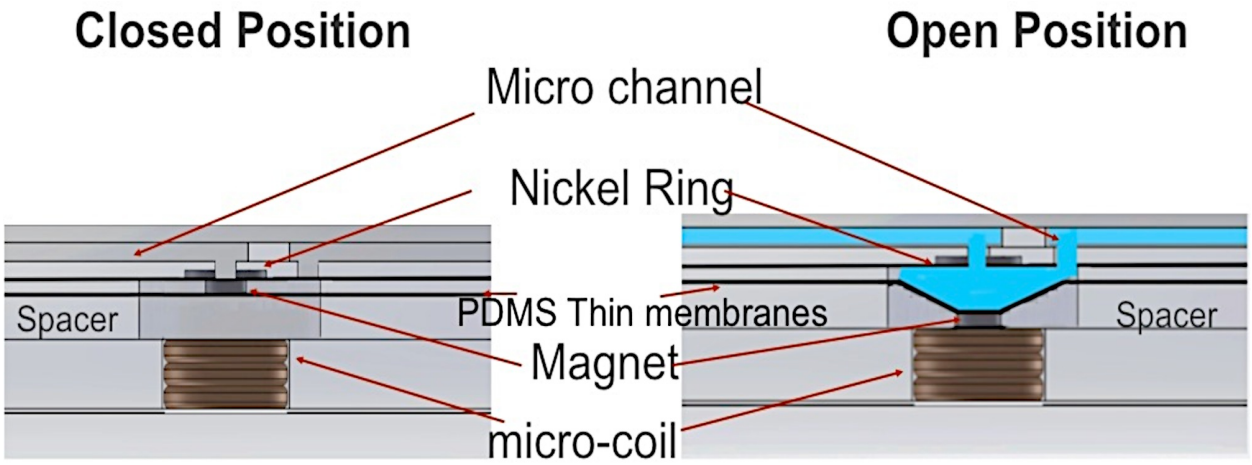

Figure 35. Side view of the microvalve. left: Valve in the closed state latched up using a nickel ring. Right: Valve in the open state latched down using an Iron core.

By applying voltage and controlling the direction of the current, the membrane was triggered to move vertically opening and closing the microvalve. When the valve is electromagnetically actuated, the membrane moves up or down latching to the top and the bottom. This has become possible by attaching a micro magnet to the membrane. A micro core is attached inside the coil. As the coil is actuated, the current induced in the coil creates a magnetic field. This field at one point moves the magnet towards the coil while at the opposite direction of current it moves the magnet away from the coil. As it moves away from the coil, it gets attracted

to the nickel ring causing the magnet and as a result the membrane to close the channel. As the current direction changes by a switching mechanism, the magnetic force from the coil attracts the magnet causing it to move down and attaches to the Iron core and stays latched down.

In the next sections the fabrication process and the function of each microfloupon is explained.

7.2 μFloupon Fabrication

In the final design, a total of three microvalves were incorporated. The following manufacturing sections are based on the final design of the three microvalves system.

7.2.1 Electronics microfloupon

All the layers were designed in Adobe Illustrator first in able to align them perfectly at the assembly time. Electronics microfloupon is composed of a PCB board, a micro-coil, Iron core and the connection cables. To manufacture the PCB board, first the Adobe Illustrator file was transferred to Eagle CAD software. Figure36 top shows the final schematic of the PCB board. Three signal paths and one ground path was generated next to where the micro-coil opening was. After drawing the board, the board was sent to an outside vendor, smartprototyping.com to get manufactured. The final product is shown in figure 35 bottom. The thickness of the board was chosen

to be 500μm, however, later the empirical value for the thickness turned out to be 1 mm. This thickness was accomplished by stacking two boards on top of each other.

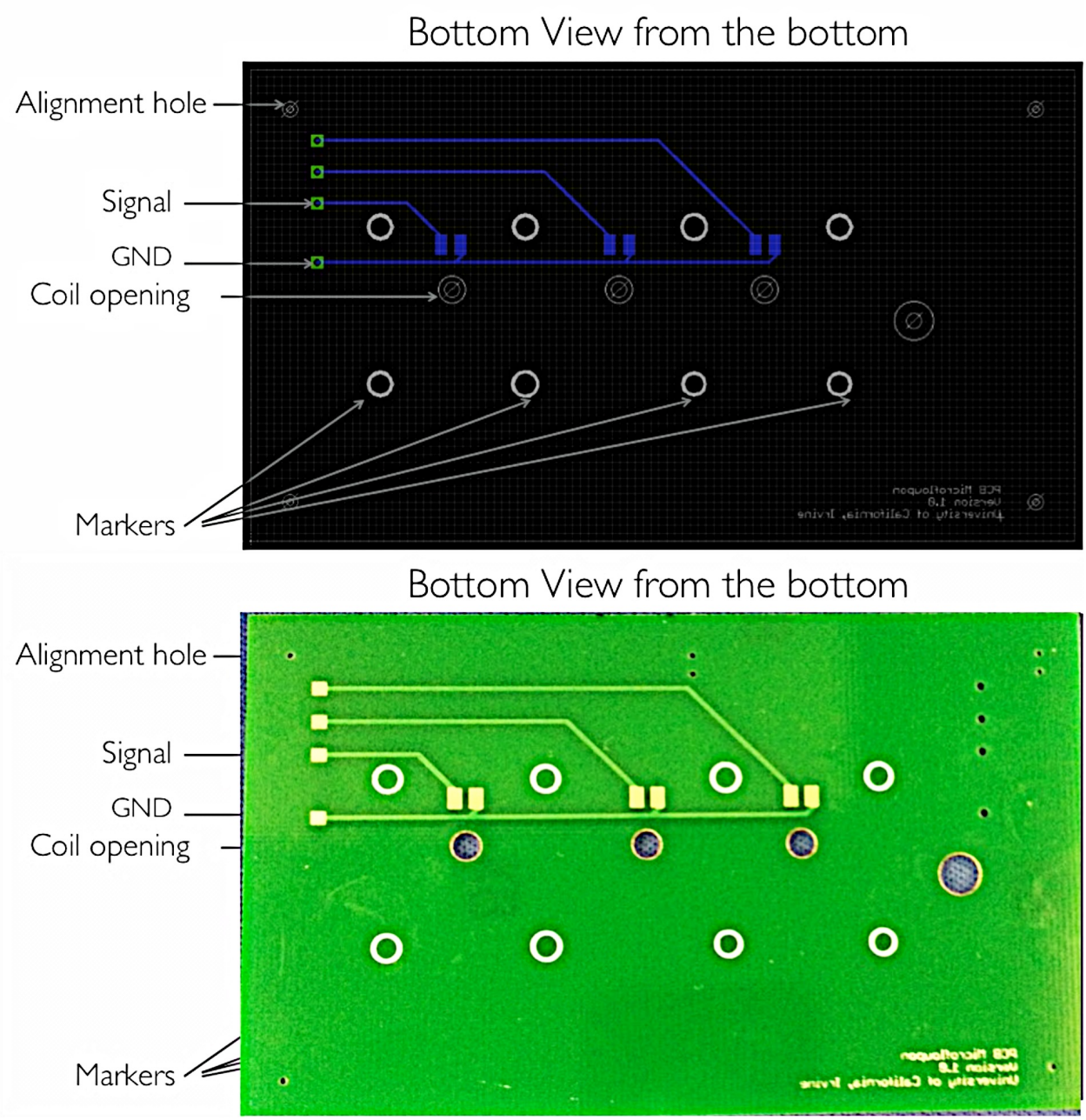

Figure 36. Top. Schematic of the PCB board in eagle CAD software. Bottom: Final PCB board with 500μm thickness. The design included three holes for incorporating micro-coils and also an opening on the right for reaction chamber.

To fabricate the micro-coil an in-house coiling machine was employed. The wire thickness was chosen to be 78μm with 200 turns. After manufacturing the dimension of the coil was measured to be 3.5mm diameter and 1.5mm height. The diameters of holes in the PCB boards were designed to match the diameter of the coils. One hole with diameter of 5mm was designed to give a full view of the reaction chamber. Iron cores were manufactured by an outside vendor to match the coils inside dimension and height and were placed inside the coils. Super glue was used to secure the cores inside the coils and then the coils were adhered to the board. Each two ends of the coils were stripped carefully using flux and the coils were soldered to enable the electrical connection. The resistances of the coils were measured to be around 6.5Ω.

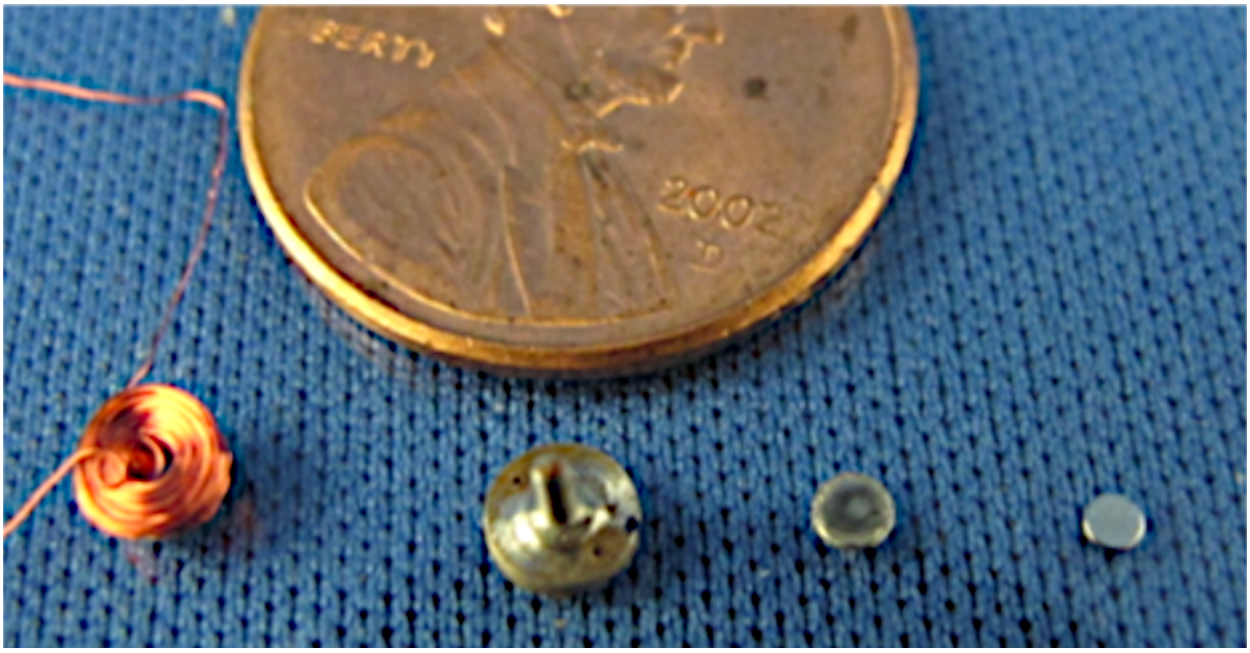

Figure 37. Image comparison between the different components of the microvalve and a penny. From left to right: micro-coil, Iron core, nickel ring, and micro magnet.

7.2.2 Membrane μFloupon

To actuate the valve properly, a thin flexible membrane was needed. To fabricate the thin membrane with thickness around 50-70μm, a unique manufacturing technique was invented and utilized. Since the goal was to able to move the membrane in and out of the system to assemble and dissemble the valve, only using thin PDMS membranes was not suitable. For this reason, a hybrid of paper and PDMS was chosen to be able to carry the membrane around.

First, a thin sheet of paper with the thickness of 30μm was patterned using CO2 laser cutting machinery. The pattern was drawn in Adobe Illustrator. This pattern included 3 circular windows with diameter of 3.5mm and 4 alignment holes for future assembly. To be able to cut the paper without burning the paper, the lowest setting on the laser cutting machinery was chosen.

After cutting the paper, a mixture of PDMS (1:10) ratio was prepared and degassed for 10 minutes. Meanwhile, a polymer surface was treated with soap and air-dried untouched in order not to remove any of the solvent from the surface to facilitate the release of membrane at the assembly time. After degassing PDMS, around 5g of PDMS was dispensed over the paper and the PDMS was pushed and distributed inside the paper to impregnate the paper entirely. The excess PDMS was removed from the top of the paper and the paper is degassed for another 10 minutes. Then, the paper-PDMS was

placed on the treated surface. The membrane was then carefully covered with another treated surface and the remaining air bubbles were pushed out. A Weight was placed on top of the sandwiched paper and it was placed under the pressing machine for a couple of hours. The sandwich was then taken out and placed in a 40°C oven over night to polymerize and set. After polymerization of PDMS, the sandwich was opened and the top layer was removed.

Gold-coated magnets with 500μm thickness and 1mm diameter were secured to a 50μm paper with super glue and then the paper was manually cut carefully around the magnets. Then, the magnet-papers were placed in the middle of each PDMS circle with a drop of uncured PDMS. Then the combination was again placed back in the 40°C oven for a few hours for the PDMS to cure where PDMS was acting as a glue to bond the paper to PDMS irreversibly. The paper acted as a facilitator to bond the magnet securely to the PDMS membrane. This technique was created since the hydrophobicity of PDMS doesn't allow any material to bond to it. Figure38 shows the process of bonding the magnet to the PDMS membrane. As it is shown, it is difficult to cut the paper around the magnet perfectly if it is done manually. This process can be improved in the future by using machinery to cut the paper automatically.

At the end, this process resulted in a PDMS membrane that could be actuated electromagnetically. This process was unique in a sense that the

solution would not be in direct contact with magnet at any time and would not be contaminated by metal. In this case, gold-coated magnets were used, but one can use any type of material without any solution contamination.

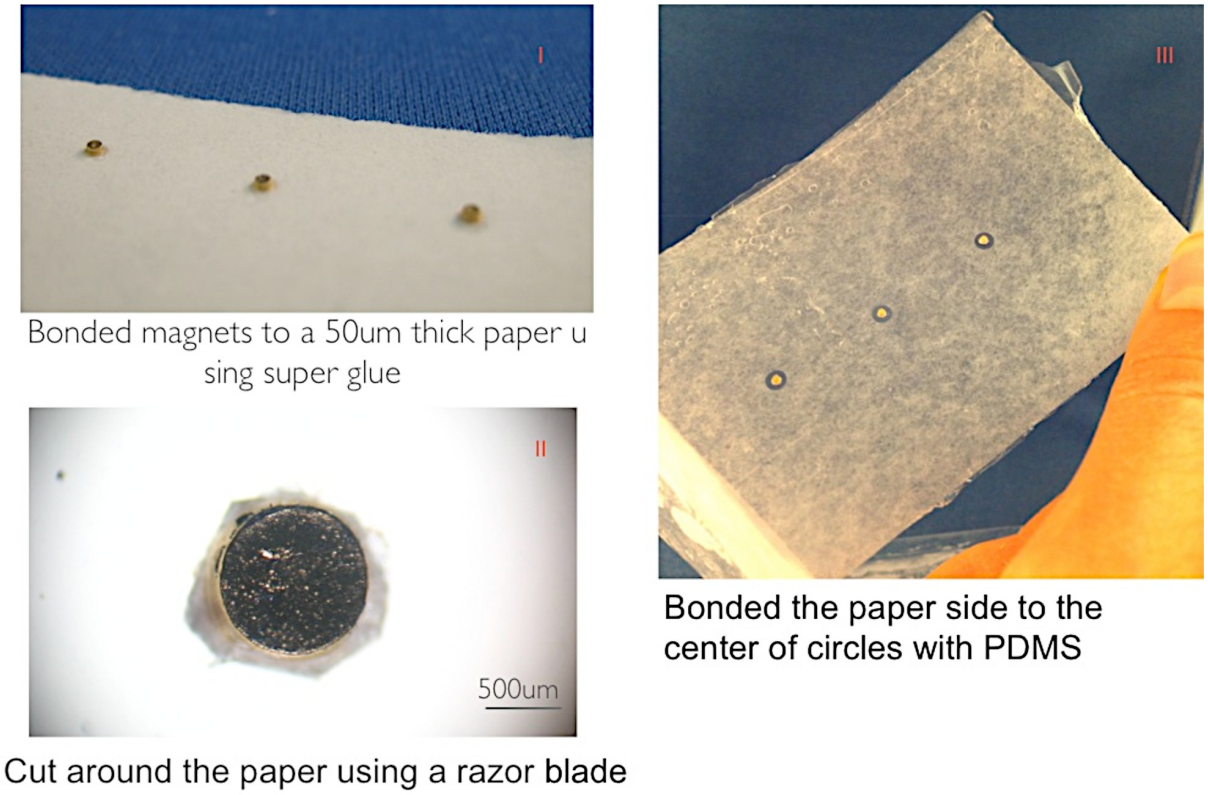

Figure 38. Process of bonding the micro magnet to the PDMS membrane. I. micro magnets are attached to a 50μm paper. II. The paper is cut around the magnet manually with a razor blade. III. The magnets with paper are bonded to the PDMS membrane by using uncured PDMS and curing it to create the bond.

7.2.3 Fluidic μFloupon

The fluidic microfloupon can be made using paper-PDMS or using other polymers such as PMMA. In our experiments, we used PMMA to be able to characterize the valve and to visually be able to monitor the function of the device.

To fabricate the fluidic layer, first the design was drawn on Adobe Illustrator and then it was exported to Eagle CAD where we were able to use the program to generate the G-Code to use with CNC machinery.

After generating the G-Code, two 500μm thick PMMA sheets where used to make each layers. One layer was made to hold the nickel ring and the access holes, one layer to make the micro channels. After fabricating the two layers, each layer was carefully cleaned with isopropanol and air-dried. The two layer were then bonded together permanently with isopropanol, heat and pressing machine as it was described in earlier chapters.

The nickel rings were electroformed following standard nickel electroplating technique. SU8 negative photoresist was used to make a positive mold on copper substrate. A 270μm layer of photoresist was hot laminated on the copper and patterned by photolithography in the lab. Next nickel was electroplated inside the mold, starting from the copper substrate. The mold was immersed in TECHNI NICKEL HT-2 Nickel-plating solution from Technic Inc. The mold served as the cathode while a rod of nickel was used for the anode. The solution temperature was controlled at 50 °C and it was mechanically agitated by blowing nitrogen gas into the solution. The mechanical agitation is important to remove bubbles forming at the nickel deposition sites, which otherwise would affect the quality of the electroformed surface. Pulsated current was supplied to the electrodes with pulse amplitude of 10 mA, pulse width of 350ms and off time of 50ms

between pulses. The plating period was 12 hours. The electroformed nickel rings were mechanically released from their mold for further integration with the microfloupon microvalve system.

The nickel rings were placed in the ring holders of PMMA layer and bonded to the board using super glue. Figure39 shows the nickel rings and the final results of fluidic microfloupon.

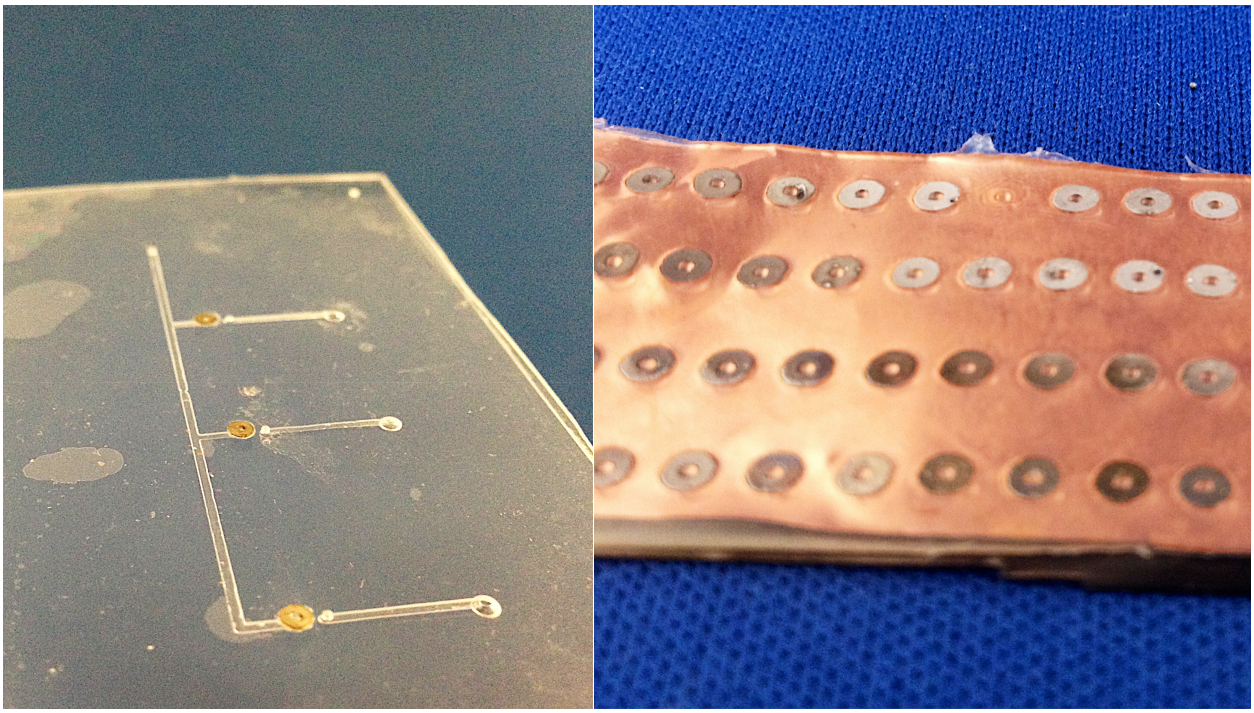

Figure 39. Left: fluidic microfloupon layer containing the rings and micro-channels. Right: Electroplated Nickel rings

7.3 Microvalve Assembly And Automation/Control

As discussed earlier, all the major microfloupons were fabricated separately. To assemble the device, the microfloupon layers were aligned and the corresponding microfloupons were stacked from bottom to top. electronics, membrane, and fluidic microfloupons on top of each other. PDMS spacers

were placed on each side of the membrane to act as a gasket. The hydrophobic surfaces of fully cured PDMS form an easily reversible seal and assure a leakage-free device. Figure40 demonstrate the assembled total microvalve system from the top and from the bottom view. This system is another example of microfloupon system where different materials and techniques were used to make each microfloupon separately and then easily assembled at the final step.

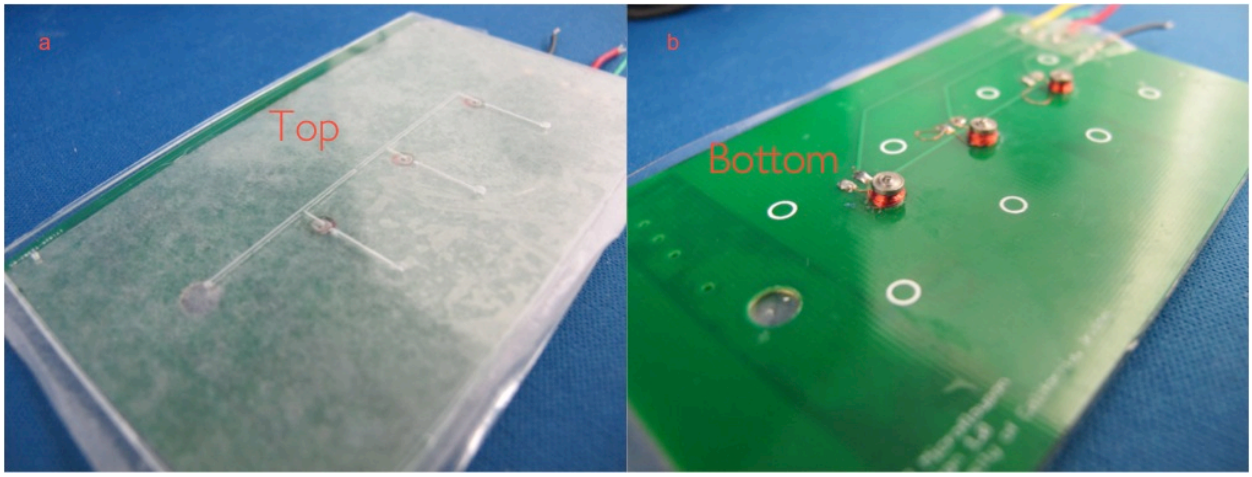

Figure 40. Assembled microfloupon valve system from the top and bottom view.

Top reservoirs were made separately using laser cutting machinery and were bonded to the top fluidic microfloupon using 5-minute epoxy.

In addition, to enforce the seal between the layers and to avoid any leakage a housing was made for the device using CNC machinery. The housing material was chosen to be PMMA since this material is easy to work with and is transparent. Using screws at different locations, the system can have equal pressure or different pressure at each point as the user desired to

avoid any leakage. The final device under test is shown in figure41. Tubes were added to the system at each access point after de device was placed in the housing for further testing the device.

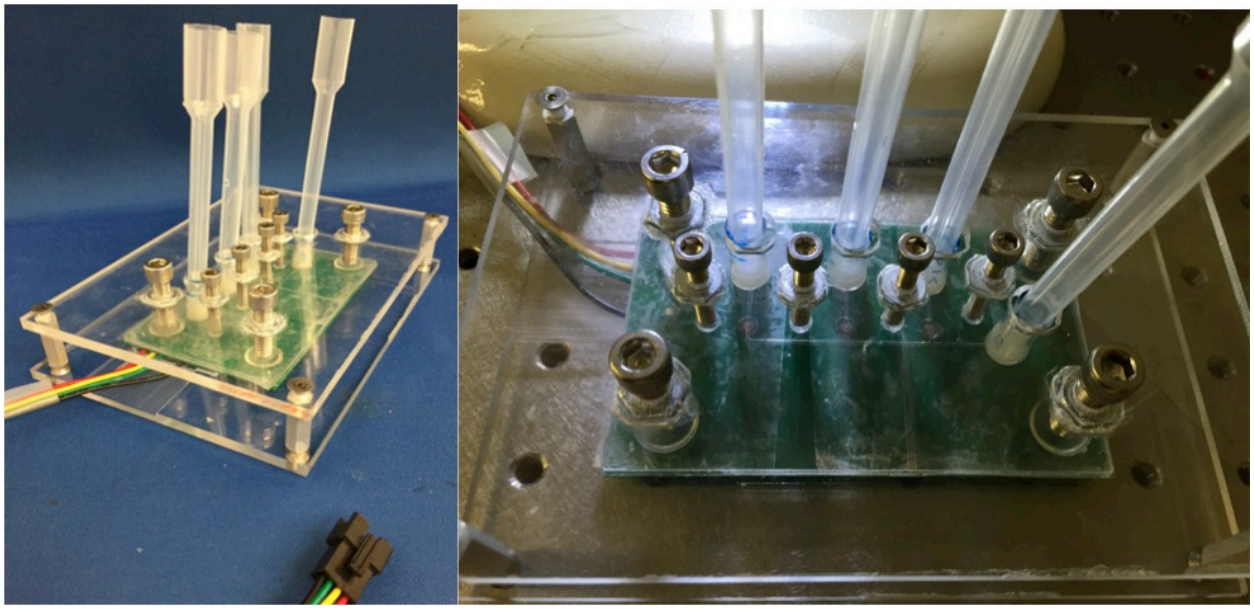

Figure 41. Microfloupon valve system in the housing case.

In order to automate switching between the microvalves, a computer-controlled system was designed. In order to control the microvalves, a microcontroller system was required. For this project, Arduino board along with solid state switches were utilized. Arduino software doesn’t contain any graphical user interface. Therefore, to make the user interface, another programing language was needed. Processing software was chosen and utilized to interact with the user through computer screen. The Arduino code was written as following to send a pulse to open and close the solid state switch.

```
char valueOfserial;
void setup() {
  //start serial connection
  Serial.begin(9600);
  pinMode(2, OUTPUT);
  pinMode(3, OUTPUT);
  pinMode(4, OUTPUT);
  digitalWrite(2, LOW);
  digitalWrite(3, LOW);
  digitalWrite(4, LOW);
 }
void loop() {
  // send data only when you receive data:
  if (Serial.available() > 0) {
                // read the incoming byte:
                valueOfserial = Serial.read();
  }
  if (valueOfserial == 'A'){
    digitalWrite(2, HIGH);
   }
  if (valueOfserial == 'Z'){
    digitalWrite(2, LOW);
  }
if (valueOfserial == 'B'){
    digitalWrite(3, HIGH);
  }
  if (valueOfserial == 'Y'){
    digitalWrite(3, LOW);
  }
if (valueOfserial == 'C'){
    digitalWrite(4, HIGH)
  }
  if (valueOfserial == 'X'){
    digitalWrite(4, LOW);
}
}
```

The processing code was written as following to create six buttons on the computer screen where the user could press to send the data to Arduino and from Arduino to the solid state switches where the voltage would be applied to open and close the microvalves.

```
Import processing.serial.*;
Serial myPort;  // Create object from Serial class
int val;        // Data received from the serial port
PFont f;
void setup(){
  size (600, 300);
  String portName = Serial.list()[2];
  myPort = new Serial(this, portName, 9600);
  println(portName);
}
```

```
void draw(){
  background(35,191,222);
  fill(100,180,220);
  rect(40,50,450,150);
// Draw first rectangle and check to see if it is clicked then write A to serial port
  fill (255,0,0);
  rect(80,120,50,25);
  if (mouseOverRect1() == true && mousePressed == true) {
     myPort.write('A');
     delay(1000);
     myPort.write('Z');
  }
// Draw second rectangle and check to see if it is clicked then write B to serial port
  fill(35,222,47);
  rect(140,120,50,25);
 if (mouseOverRect2() == true && mousePressed == true) {
     myPort.write('B');
     delay(500);
     myPort.write('Y');
  }
// Draw third rectangle and check to see if it is clicked then write C to serial port
  fill (255,0,0);
  rect(210,120,50,25);
  if (mouseOverRect3() == true && mousePressed == true) {
     myPort.write('C');
     delay(500);
     myPort.write('X');
  }
// Draw forth rectangle and check to see if it is clicked then write D to serial port
  fill(35,222,47);
  rect(270,120,50,25);
  if (mouseOverRect4() == true && mousePressed == true) {
     myPort.write('D');
     delay(500);
     myPort.write('W');
  }
// Draw fifth rectangle and check to see if it is clicked then write E to serial port
  fill (255,0,0);
  rect(340,120,50,25);
    if (mouseOverRect5() == true && mousePressed == true) {
     myPort.write('E');
     delay(500);
     myPort.write('V');
  }
// Draw fifth rectangle and check to see if it is clicked then write E to serial port
  fill(35,222,47);
  rect(400,120,50,25);
   if (mouseOverRect6() == true && mousePressed == true) {
     myPort.write('F');
     delay(500);
     myPort.write('U');
  }
  f=createFont("Arial",12,true);
  textFont(f,12);
  fill(0);
  text("Valve1",85,100);
```

```
  text("close",85,110);
  text("Valve1",150,100);
  text("open",150,110);
  text("Valve2",220,100);
  text("close",220,110);
  text("Valve2",280,100);
  text("open",280,110);
  text("Valve3",350,100);
  text("close",350,110);
  text("Valve3",410,100);
  text("open",410,110);
}
boolean mouseOverRect1()  {// Test if mouse is over square
  return ((mouseX >= 80) && (mouseX<=130) && (mouseY>=120) && (mouseY<=145));
}

boolean mouseOverRect2()  {// Test if mouse is over square
  return ((mouseX >= 140) && (mouseX<=190) && (mouseY>=120) && (mouseY<=145));
}

boolean mouseOverRect3()  {// Test if mouse is over square
  return ((mouseX >= 210) && (mouseX<=260) && (mouseY>=120) && (mouseY<=145));
}

boolean mouseOverRect4()  {// Test if mouse is over square
  return ((mouseX >= 270) && (mouseX<=320) && (mouseY>=120) && (mouseY<=145));
}

boolean mouseOverRect5()  {// Test if mouse is over square
  return ((mouseX >= 340) && (mouseX<=390) && (mouseY>=120) && (mouseY<=145));
}

boolean mouseOverRect6()  {// Test if mouse is over square
  return ((mouseX >= 400) && (mouseX<=450) && (mouseY>=120) && (mouseY<=145));
}
```

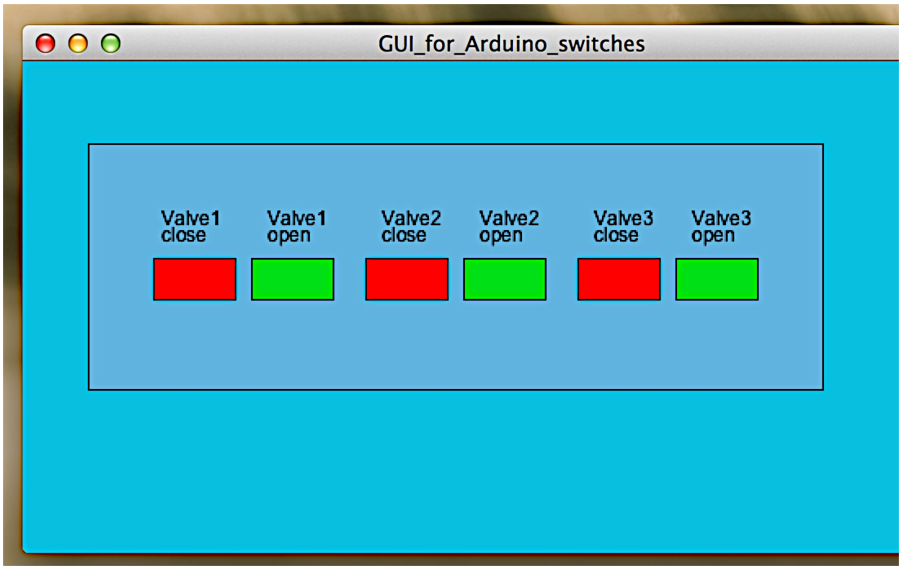

Figure 42. Graphical User Interface for microvalve system using processing.

7.4 μFloupon Valve Characterization

All the characterization data has been collected based on room-temperature data and using one valve only. To characterize the valve, the isolation pressure, breakout pressure, time response and pressure response were measured. In the following sections, the experimental setup and the results of each test are reported.

7.4.1 Flow/Leakage Rate vs. Pressure

To measure the flow rate vs. pressure the following tests were setup. The results were indication of the isolation and breakout pressure as well.

First, relatively large reservoirs were setup at the inlet and outlet of the microvalve. The reservoir at the inlet was attached to a vertical stand to be able to move it up and down to change the pressure. Then, colored water was added to the reservoirs and the tubing and the microvalve to fill out the whole system. Then carefully a drop of oil was added to the outlet of the microvalve. The tube at the outlet was marked with units in order to monitor the movement of the oil drop through the tubing. Then flow rate of the oil drop was measured at specific pressures. By changing the height of the inlet reservoir, the pressure was kept as a variable. At each pressure, the microvalve was switched closed were the isolation rate was measured and then it was kept open and the flow rate was measured based on how much

the oil drop has moved through the tube. Figure43 shows the experimental setup for this test.

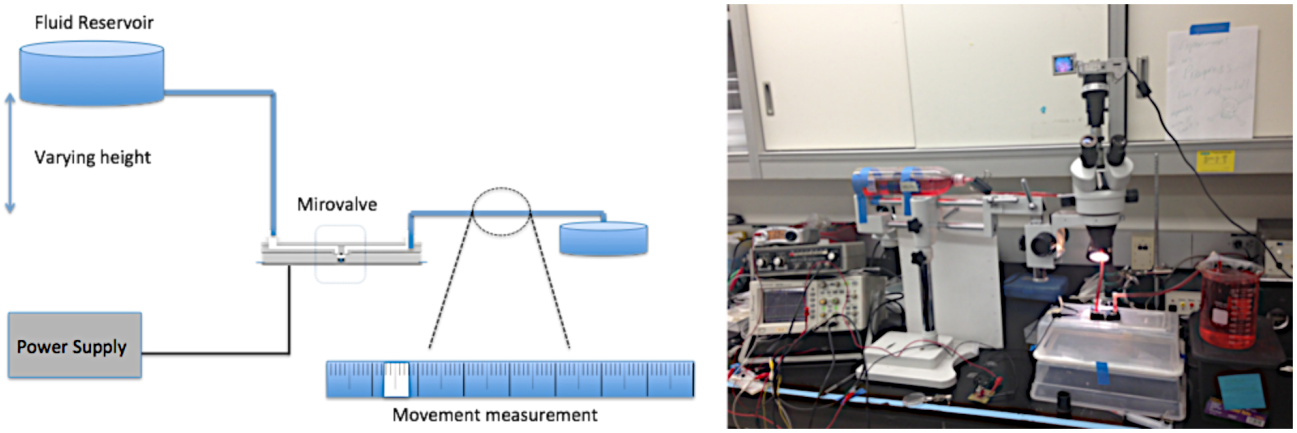

Figure 43. Experimental set up for flow rate measurement.

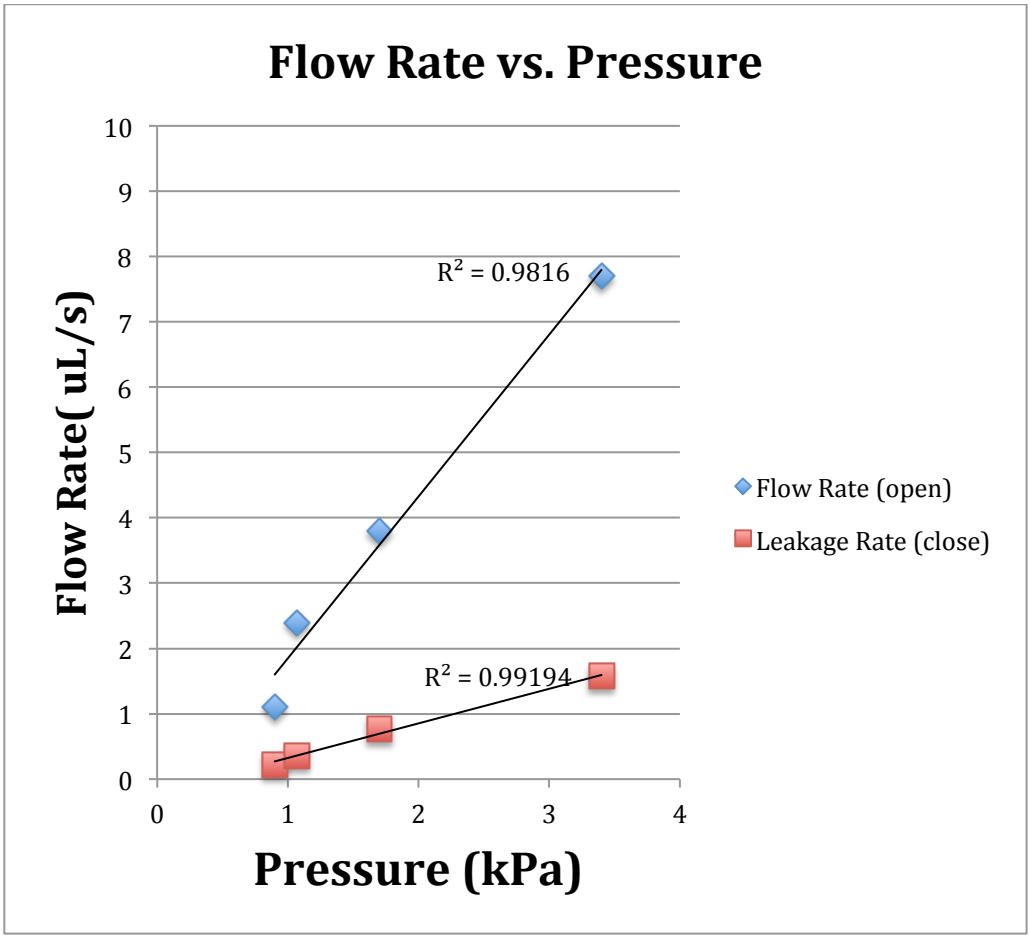

Graph2. Flow rate vs. pressure for an open and closed valve.

To calculate the pressure at each height, the pressure difference between the two end reservoirs was measured. This was done simply by using the following pressure formula:

Eq. (7) $$\Delta P = \rho . g . \Delta h$$

Where, *P* is pressure, ρ is density, g is acceleration of gravity, and *h* is height. So, by measuring the height difference, we were able to calculate the pressure.

To calculate the flow rate of the oil drop, the time it took for the oil drop to move from one specific point to another was monitored Then the volume of that section in which the oil drop was move through was calculated and divided by the measured time. This gave the flow rate measuring in μL/s and then the data was graphed which is shown for a closed and open valve on graph2. It is shown that above 3.5kPa the valve would break open and the seal between the magnet and the nickel ring would break. Since this valve is designed for simple lab tests, this pressure is sufficient for low-pressure lab applications where the concern is mostly to control the fluidic flow at low pressure.

7.4.2 Time Response

To measure the dynamic response of the microvalve, an oscilloscope and a pulse generator were utilized. The test set up for this test is shown in figure 44. In this test set up the pressure was kept constant at 900Pa and the time response of the valve was measured by varying pulses.

Since the valve incorporates latching mechanism, just single pulses are sufficient to activate the valve making this valve as an attractive valve for low power application.

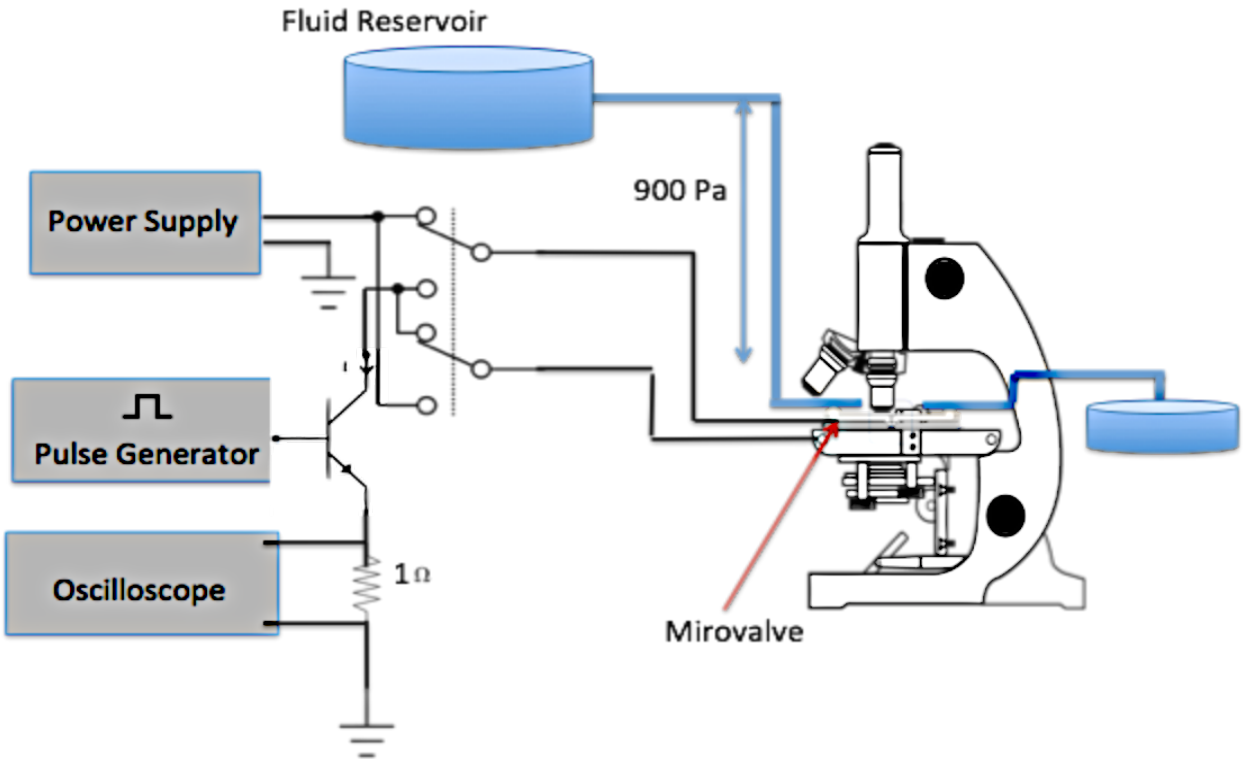

Figure 44. Microvalve time response test setup using an oscilloscope and a pulse generator.

To measure the time response, a predetermined pulse was sent to the microvalve while monitoring the activity of the microvalve under the microscope. The microvalve was able to successfully open and close as fast as 6 ms by applying 611mA of current. The functionality of the valve was also tested for the threshold of the current. The valve was functional with 150ms of response time as low as 222mA of current. Below this threshold the valve was not functional anymore. The time response data was collected vs. current and plotted as it is shown on graph3.

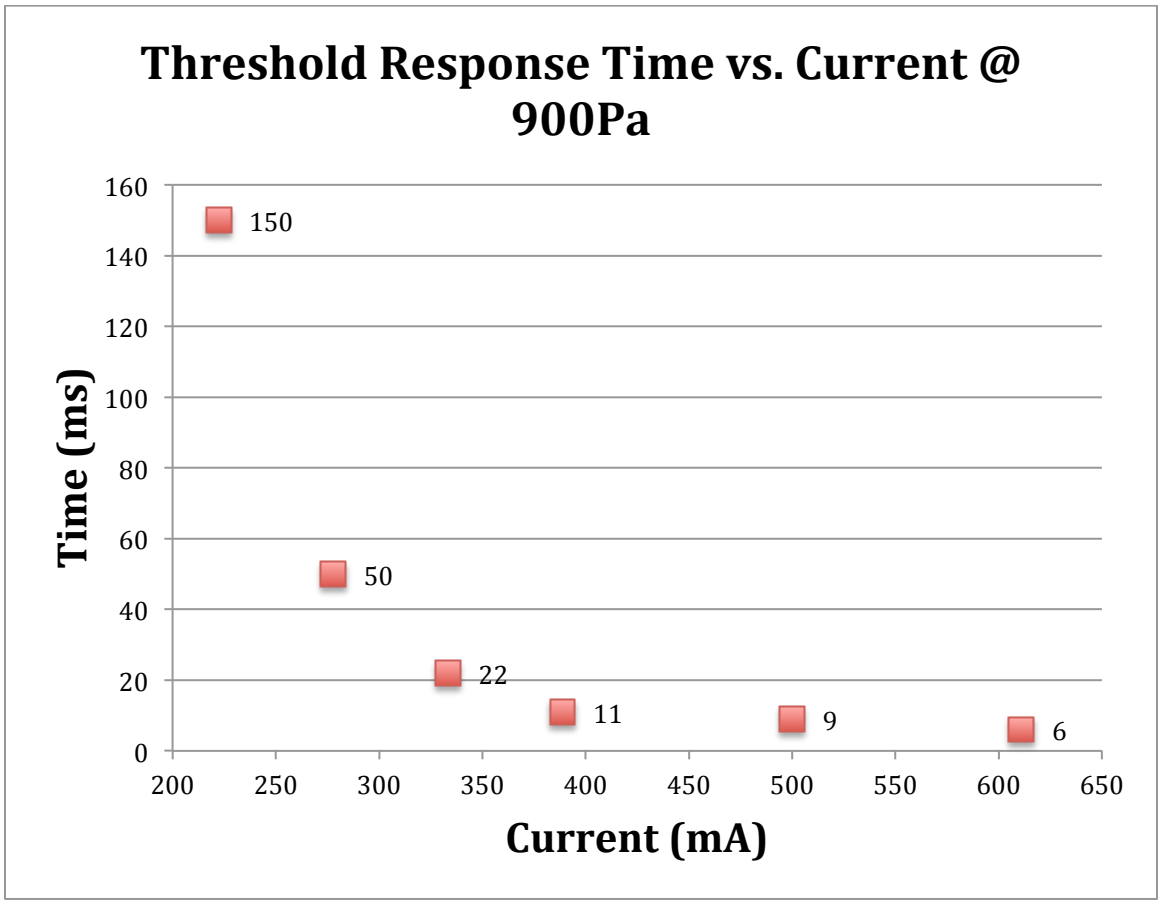

Graph3. Threshold response time vs. current at 900Pa.

As a result, the valve power consumption was calculated. At 6ms , the valve consumed 25.8W while at 150ms consumed 9.38W. These numbers make for a sufficient valve for high-speed switching applications as well as low-power applications.

7.5 Conclusion

The above work demonstrated the design, microfabrication and testing of a novel low-cost easy to manufacture high-speed bistable electromagnetically actuated microvalve. This shows another application of coupon-based

approach " microfloupons"[151] where each layer was made out of different materials from paper impregnated with Polydimethylsiloxane (PDMS) to PCB board, and PMMA material using conventional manufacturing techniques which are laminated together. All the layers of the system were manufactured separately and stacked on top of each other to make the microvalve system. The electronic layer, which contains the micro-coil, can be easily integrated into the system as a layer without any additional complicated manufacturing technique. The membrane layer incorporates a permanent magnet, which allows the membrane to move vertically with electromagnetic force. Actuating the permanent magnet drives the normally closed microvalve PDMS membrane to open and close. Not only this is a simple low-cost design, but also the latching and unlatching mechanism makes for a low-power system where the temperature doesn't change from the ambient temperature, which is an advantage compare to the valves with thermal actuation scheme.

Chapter 8

Conclusion and recommend future work

8.1 Conclusion

Microfluidics biochips have become an important field of work that can enable tremendous advances in chemistry and biology. These composite microsystems, also known as lab-on-a-chip or bio-microelectromechanical system (MEMS), offer a number of advantages over conventional laboratory procedures. They automate highly repetitive laboratory tasks by replacing cumbersome equipment with miniaturized and integrated systems, and they enable the handling of small amounts, e.g.,micro- and nanoliters, of fluids. Thus, they are able to provide ultrasensitive detection at significantly lower costs per assay than traditional methods, and in a significantly smaller amount of laboratory space.

Although they can be a powerful solution to many problems, the microfluidic field has not yet found its way in industry. The root cause of this problem stems from the way the manufacturing of these products is based on. Conventional manufacturing methods typically involve expensive cleanroom facilities and they are usually application-based solutions that cannot be applied to multiple problems, so the manufacturing techniques cannot be scaled up. In addition, the systems are usually made as a whole and cannot

be easily integrated together. In addition, the complexities of assays are increasing and the current solutions are not economically sufficient nor can be integratable with different functionality.

The general objective of this dissertation is to propose a novel manufacturing technology platform where different parts of a bio-chip are manufactured separately in house or by outside vendors using different technologies and material and then stacked on top of each other. This technology is called 'microfloupon' or micro-fluidic coupon where each layer acts as a coupon where the coupons can be stacked to form a whole integrated system. This technology is a holistic approach where it can be applied to different applications and not limited to one specific application.

To demonstrate this technology as a universal platform to do be adapted in many areas, two applications were shown that are commonly used in biological assay experiments: electrophoresis biochip and a microvalve biochip.

In the electrophoresis microfloupon system, the microfloupons were made out of different polymers such as PMMA, 1002F photoresist, PDMS, and polycarbonate as well as paper and biological reagents such as polyacrylamide gel and SDS buffer. With the help of microfloupon technology, a 300μm polyacrylamide gel could be manufactured and handled separately by impregnating a paper with polyacrylamide gel. Also, the

polyacrylamide gel could be removed and imaged after the test and could be transferred to other systems for further analysis.

With this technology, we were able to concentrate small sample of protein and move the proteins in two-dimensional space which is a much difficult task using conventional microfluidic manufacturing techniques.

In the second part of the report, a completely different application of microfloupon technology was introduced. Since controlling the flow of reagents in microchannels has become an integral part of μTAS systems, the choice became obvious to make a microvalve based on microfloupon technology.

This system consists of three major microfloupons: the electronics, membrane and fluidics microfloupons. Each of these microfloupons was manufactured separately using different technologies and materials and then integrated together as a stack to form the complete system.

Electronics microfloupon was built by an outside vendor while the components of the board were built in-house and soldered to the board. Making a 50μm thick PDMS membrane where the membrane can be moved from place to place could not be possible without using the microfloupon technology where a thin sheet of paper could be impregnated with PDMS and the paper to act as a carrier for PDMS membrane.

Both of the explained applications' microfloupons were built in the lab with low-cost materials and components where we were able to integrate them to a whole functional module.

This novel technology is not limited to just the above applications and several other areas may benefit from this technology. This technology can be expanded to be used in cell sorting or micro-pumps and DNA analysis chips.

8.2 Recommended Future Work

This research is a start of a new manufacturing technology and has shown successful applications of microfloupon technology. However, there is room for optimization and future work.

The electrophoresis system can be further expanded to do Western Blotting analysis. Usually electrophoresis is the first step in analyzing protein samples and to quantify the result, further analysis such as Western Blotting is desired. To do so, another microfloupon cassette can be manufactured where the polyacrylamide micro-gel can be transferred to blot the separated protein and quantify the results.

To further improve the results, smaller size polycarbonate membrane or other types of nanoporous membrane can be utilized to capture all the protein sample to further improve the efficiency of the system.

Furthermore, with using some auxiliary boards, this system has the potential to become a low power system where there would be no need for high-power supply. This can be appealing where there is no access to high power voltage supplies.

In addition, imaging microfloupon can be built and integrated into the system for a whole complete μTAS where the test can be done in a lab environment or at point-of-care.

As far as the microvalve system goes, the performance of microvalve can be improved by tweaking the variables such as the distances between the magnet and the latching components or the thickness of the PDMS membrane to have a better bistable system with better isolation performance.

In addition, further applications of microfloupon system should be manufactured to further advance this technology and demonstrate its potential for applications such as DNA analysis, cell sorting, pumping and other essential assays.

At the end, this technology can be an economical solution to the current microfluidic manufacturing techniques and since it is low-cost, disposable applications can benefit from this technology as well.

List of References

1. Rivetb C, Leea H, Hirscha A, Hamiltona S, Lu H. Microfluidics for medical diagnostics and biosensors. *Chem Eng Sci*. 2011;66(7):1490–1507.

2. Erickson D, Li D. Integrated microfluidic devices. *Anal Chim Acta*. 2004;507(1):11–26.

3. Davis JJ, Morgan DA, Wrathmell CL, Axford DN, Zhaoa J, Wang N. Molecular bioelectronics. *J Mater Chem*. 2005;15:2160–2174.

4. Petersson F, Nilsson A, Holm C, Jonssonc H, Laurell T. Continuous separation of lipid particles from erythrocytes by means of laminar flow and acoustic standing wave forces. *Lab Chip*. 2004;5(20-22).

5. Majedi FS, Mahdi M, Hasani-Sadrabadi, et al. Microfluidic assisted self-assembly of chitosan based nanoparticles as drug delivery agents. *Lab Chip*. 2013;13:204–207.

6. Jiang H, Weng X, Li D. Microfluidic whole-blood immunoassays. *Microfluid Nanofluidics*. 2011;10(5):941–964.

7. Wang C-H, Lee G-B. Automatic bio-sampling chips integrated with micro-pumps and micro-valves for disease detection. *Biosens Bioelectron*. 2005;21:419–425.

8. Whitesides GM. The origins and the future of microfluidics. *Nature*. 2006;442(7101):368–73. doi:10.1038/nature05058.

9. De Dobbelaere P, Falta K, Gloeckner S, Patra S. Digital MEMS for optical switching. *Commun Mag IEEE*. 2002;40(3):88–5.

10. Tanaka M. An industrial and applied review of new MEMS devices features. *Microelectron Eng*. 2007;84(5-8):1341–1344.

11. Bogue R. MEMS sensors: past, present and future. *Sens Rev*. 1997;27(1):7–13.

12. Calvert P. Inkjet Printing for Materials and Devices. *Chem Mater*. 2001;3299-3305(13):10.

13. De Volder M, Reynaerts D. Pneumatic and hydraulic microactuators: a review. *J Micromechanics Microengineering*. 2010;20(4).

14. Auroux P-A, Iossifidis D, Reyes DR, Manz A. Micro total analysis systems. 2. Analytical standard operations and applications. *Anal Chem*. 2002;74(12):2637–52.

15. Lee SJ, Lee SY. Micro total analysis system (micro-TAS) in biotechnology. *Appl Microbiol Biotechnol*. 2004;64(3):289–99. doi:10.1007/s00253-003-1515-0.

16. Janasek D, Franzke J, Manz A. Scaling and the design of miniaturized chemical-analysis systems. *Nature*. 2006;442(7101):374–80. doi:10.1038/nature05059.

17. Pais A, Banerjee A, Klotzkin D, Papautsky I. High-sensitivity, disposable lab-on-a-chip with thin-film organic electronics for fluorescence detection. *Lab Chip*. 2008;8(5):794–800. doi:10.1039/b715143h.

18. Gravesen, P., Branebjerg, J., Jensen SJ. Microfluidics-a review. *J Micromech*. 1993;3:168–182.

19. Verpoorte E. Review Microfluidic chips for clinical and forensic analysis. *Electrophoresis*. 2007;23(5):677–712.

20. Fiorini GS, Chiu DT. Disposable microfluidic devices: fabrication, function, and application. *Biotechniques*. 2005;38:429–449.

21. Su F, Chakrabarty K, Member S, Fair RB. Microfluidics-Based Biochips : Technology Issues , Implementation Platforms , and Design-Automation Challenges. *IEEE Trans Comput Des Integr CIRCUITS Syst*. 2006;25(2):211–223.

22. Lin CH, Lee GB, Lin YH, Chang GL. A fast prototyping process for fabrication of microfluidic systems on soda-lime glass. *J Micromech Microeng*. 2001;(11):726–732.

23. McCreedy T. Fabrication techniques and materials commonly used for the production of microreactors and micro total analytical systems. *Trend Anal Chem*. 2000;19:396–401.

24. Brown L, Koerner T, Horton JH, Oleschuk RD. Fabrication and characterization of poly(methylmethacrylate) microfluidic devices

bonded using surface modifications and solvents. *Lab Chip*. 2005;6:66–73.

25. Muck A, Wang J, Jacobs M, et al. Fabrication of poly(methyl methacrylate) microfluidic chips by atmospheric molding. *Anal Chem*. 2004;76(8):2290–7. doi:10.1021/ac035030+.

26. Cheng J-Y, Wei C-W, Hsu K-H, Young T-H. Direct-write laser micromachining and universal surface modification of PMMA for device development. *Sensors Actuators B Chem*. 2004;99(1):186–196. doi:10.1016/j.snb.2003.10.022.

27. Kuncová-Kallio J, Kallio PJ. PDMS and its suitability for analytical microfluidic devices. *Conf Proc IEEE Eng Med Biol Soc*. 2006;1:2486–9. doi:10.1109/IEMBS.2006.260465.

28. Wu H, Odom TW, Chiu DT, Whitesides GM. Fabrication of complex three-dimensional microchannel systems in PDMS. *J Am Chem Soc*. 2003;125(2):554–9. doi:10.1021/ja021045y.

29. Sia SK, Whitesides GM. Microfluidic devices fabricated in poly(dimethylsiloxane) for biological studies. *Electrophoresis*. 2003;24(21):3563–76. doi:10.1002/elps.200305584.

30. Fujii T. PDMS-based microfluidic devices for biomedical applications. *Microelectron Eng*. 2002;61-62:907–914. doi:10.1016/S0167-9317(02)00494-X.

31. Y. Liu, D. Ganser, A. Schneider, R. Liu, P. Grodzinski NK. Microfabricated polycarbonate CE devices for DNA analysis. *Anal Chem*. 2001;73:4196–4201.

32. Mei-Ying Ye, Xue-Feng Yin Z-LF. DNA separation with low-viscosity sieving matrix on microfabricated polycarbonate microfluidic chips. *Anal Bioanal Chem*. 2005;381(4):820–827.

33. Fiorini GS, Jeffries GDM, Lim DSW, Kuyper CL, Chiu DT. Fabrication of thermoset polyester microfluidic devices and embossing masters using rapid prototyped polydimethylsiloxane molds. *Lab Chip*. 2003;3:158–163.

34. Coltro WKT, Silva JAF da, Silva HDT da, et al. Electrophoresis microchip fabricated by a direct-printing process with end-channel amperometric detection. *Electrophoresis*. 2004;(25):3832–3839.

35. Barker SLR, Tarlov MJ, Canavan H, Hickman JJ, Locascio LE. Plastic microfluidic devices modified with polyelectrolyte multilayers. *Anal Chem*. 2000;72:4899–4903.

36. Chen C-S, Breslauer DN, Luna JI, et al. Shrinky-Dink microfluidics: 3D polystyrene chips. *Lab Chip*. 2008;8:622–624.

37. Bai X, Roussel C, Jensen H, Girault HH. Polyelectrolyte-modified short microchannel for cation separation. *Electrophoresis*. 2004;25:931–935.

38. Castaño-Álvarez M, Ayuso DFP, Granda MG, Fernández-Abedul MT, Jose Rodríguez García AC-G. Critical points in the fabrication of microfluidic devices on glass substrates. *Sensors Actuators B Chem*. 2008;130(1):436–441.

39. Panaro N, Yuen P, Sakazume T, Fortina P, Kricka L, Wilding P. Evaluation of DNA Fragment Sizing and Quantification by the Agilent 2100 Bioanalyzer. *Clin Chem*. 2000;46(11):1851–1853.

40. Wallis G, Pomerantz DI. Field assisted glass–metal sealing. *J Appl Phys*. 1969;(40):3946–3949.

41. Xiao Z-X, Wu G-Y, Li Z-H, Zhang G-B, Hao Y-L, Wang Y-Y. Silicon–glass wafer bonding with silicon hydrophilic fusion bonding technology. *Sensors Actuators A Phys*. 1999;72(1):46–48.

42. Manz A, Harrison DJ, Verpoorte EMJ, et al. Planar chips technology for miniaturization and integration of separation techniques into monitoring systems. Capillary electrophoresis on a chip. *J Chromatogr*. 1992;593:253–258.

43. Becker H, Gartner C. Polymer microfabrication methods for microfluidic analytical applications General. *Electrophoresis*. 2000;21:12–26.

44. Steingoetter I, Fouckhardt H. Deep fused silica wet etching using an Au-free and stress-reduced sputter-deposited Cr hard mask. *J Micromech Microeng*. 2005;15:2130–2135.

45. Grosse A, Grewe M, Fouckhardt H. Deep wet etching of fused silica glass for hollow capillary optical leaky waveguides in microfluidic devices. *J Micromechanics Microengineering*. 2001;11:257–262.

46. Kawai K, Yamaguchi F, Nakahara A, Shoji S. FABRICATION OF VERTICAL AND HIGH-ASPECT-RATIO GLASS MICROFLUIDIC DEVICE BY

BOROSILICATE GLASS MOLDING TO SILICON STRUCTURE. In: *Miniaturized Systems for Chemistry and Life Sciences*.; 2010:1193–1195.

47. Raley NF, Davidson JC, Balch JW. Examination of Glass-Silicon and Glass-Glass Bonding Techniques for Microfluidic Systems. In: *Micromachining and Microfabrication*.; 1995.

48. Chiem N, Lockyear-Shultz, Andersson P, Skinner C, Harrison DJ. Room temperature bonding of micromachined glass devices for capillary electrophoresis. *Sensors Actuators B Chem*. 2000;63:147–152.

49. Harrison DJ, Manz JA, Fan Z, Ludi H, Widmer M. Capillary Electrophoresis and Sample Injection Systems Integrated on a Planar Glass Chip. *Anal chem*. 1992;64:1926–1932.

50. Beckera H, Locascio LE. Polymer microfluidic devices. *Talanta*. 2002;56(2):267–287.

51. Martynova L, LE L, M G, GW K, Christensen RG MW. Fabrication of plastic microfluid channels by imprinting method. *Anal Chem*. 1997;69(23):4783–4789.

52. Becker H, Rotting, Heim O. The fabrication of polymer high aspect ratio structures with hot embossing for microfluidic applications. In: *SPIE Conference on Microfluidic Devices and Systems II*.Vol 3877.; 1999:74–79.

53. Leea G-B, Chenb S-H, Huanga G-R, Sungb W-C, Lin Y-H. Microfabricated plastic chips by hot embossing methods and their applications for DNA separation and detection. *Sensors Actuators B Chem*. 2001;75(1-2):142–148.

54. Becker H, Dietz W, Dannberg P. Microfluidic Manifolds by Polymer Hot Embossing for μ-Tas Applications. In: *Micro Total Analysis Systems '98*.; 1998:253–256.

55. Tang G, Yan D, Yang C, Gong H, Chai JC, Lam YC. Assessment of Joule heating and its effects on electroosmotic flow and electrophoretic transport of solutes in microfluidic channels. *Electrophoresis*. 2006;27(3):628–39. doi:10.1002/elps.200500681.

56. Martinez AW, Phillips ST, Butte MJ, Whitesides GM. Patterned paper as a platform for inexpensive, low-volume, portable bioassays. *Angew Chem Int Ed Engl*. 2007;46(8):1318–20. doi:10.1002/anie.200603817.

57. LISOWSKI P, ZARZYCKI PK. Advances on paper-based analytical devices (μPADs) – literature review. *Camera Separatoria*. 2012;4(2):143–149.

58. Bruzewicz DA, Reches M, Whitesides G. Low-cost printing of poly(dimethylsiloxane) barriers to define microchannels in paper. *Anal chem*. 2008;80:3387–3392.

59. Abe K, Kotera K, Suzuki K, Citterio D. Inkjet-printed microfluidic multianalyte chemical sensing paper. *Anal chem*. 2008;80(18):6928–6934.

60. Carrilho E, Martinez AW, Whitesides GM. A simple micropatterning process for paper-based microfluidics. *Anal chem*. 2009;81:7091–7095.

61. Dungchai W, Chailapakul O, Henry C. A low-cost, simple, and rapid fabrication method for paper-based microfluidics using wax screen-printing. *Analyist*. 2011;136(1):77–82.

62. Olkkonen J, Lehtinen K, Erho T. Flexographically printed fluidic structures in paper. *Anal chem*. 2010;82(24):10246–10250.

63. Chitnis G, Ding Z, Chang CL, Savran CA, Ziaie B. Laser-treated hydrophobic paper: an inexpensive microfluidic platform. *Lab Chip*. 2011;11:1161–1165.

64. Li X, Tian J, Nguyen TH, Shen W. Paper-based microfluidic devices by plasma treatment. *Anal chem*. 2008;80(23):9131–9134.

65. Wang W, Wu WY, Zhu JJ. Tree-shaped paper strip for semiquantitative colorimetric detection of protein with self-calibration. J. *Chromatogr A*. 2010;1217(24):3896–3899.

66. Shi J, Tang F, Xing H, Zheng H, Bi L, Wang W. Electrochemical detection of Pb and Cd in paper-based microfluidic devices. *J Braz Chem Soc*. 2012;23(6):1124–1130.

67. Li X, Ballerini DR, Shen W. A perspective on paper-based microfluidics: Current status and future trends. *Biomicrofluidics*. 2012;6(1):11301–1130113. doi:10.1063/1.3687398.

68. Melin J, Gimenéz G, Roxhed N, van der Wijngaart W, Stemme G. A fast passive and planar liquid sample micromixer. *Lab Chip*. 2004;4(3):214–9. doi:10.1039/b314080f.

69. Werdich A a, Lima E a, Ivanov B, et al. A microfluidic device to confine a single cardiac myocyte in a sub-nanoliter volume on planar microelectrodes for extracellular potential recordings. *Lab Chip*. 2004;4(4):357–62. doi:10.1039/b315648f.

70. Lagally ET, Simpson PC, Mathies R a. Monolithic integrated microfluidic DNA amplification and capillary electrophoresis analysis system. *Sensors Actuators B Chem*. 2000;63(3):138–146. doi:10.1016/S0925-4005(00)00350-6.

71. Grover WH, Skelley AM, Liu CN, Lagally ET, Mathies R a. Monolithic membrane valves and diaphragm pumps for practical large-scale integration into glass microfluidic devices. *Sensors Actuators B Chem*. 2003;89(3):315–323. doi:10.1016/S0925-4005(02)00468-9.

72. Hou HW, Bhagat AAS, Lee WC, Huang S, Han J, Lim CT. Microfluidic Devices for Blood Fractionation. *Micromachines*. 2011;2(4):319–343. doi:10.3390/mi2030319.

73. Herrmann M, Roy E, Veres T, Tabrizian M. Microfluidic ELISA on non-passivated PDMS chip using magnetic bead transfer inside dual networks of channels. *Lab Chip*. 2007;7(11):1546–52. doi:10.1039/b707883h.

74. Anderson GJ, M Cipolla C, Kennedy RT. Western blotting using capillary electrophoresis. *Anal Chem*. 2011;83(4):1350–5. doi:10.1021/ac102671n.

75. Hughes AJ, Herr AE. Microfluidic Western blotting. *Proc Natl Acad Sci U S A*. 2012;109(52):21450–5. doi:10.1073/pnas.1207754110.

76. Towbin H, Staehelin T, Gordon J. Electrophoretic transfer of proteins from polyacrylamide gels to nitrocellulose sheets: procedure and some applications. 1979. *Biotechnology*. 1992;24(9):145–9.

77. He M, Herr AE. Automated microfluidic protein immunoblotting. *Nat Protoc*. 2010;5(11):1844–56. doi:10.1038/nprot.2010.142.

78. Herr AE, Hatch A V, Throckmorton DJ, et al. Microfluidic immunoassays as rapid saliva-based clinical diagnostics. *Proc Natl Acad Sci U S A*. 2007;104(13):5268–73. doi:10.1073/pnas.0607254104.

79. Macbeath G, Schreiber SL. Printing Proteins as Microarrays for High-Throughput Function Determination. *Science (80-)*. 2000;289(2000):1760–1763. doi:10.1126/science.289.5485.1760.

80. Rissin DM, Kan CW, Campbell TG, et al. Single-molecule enzyme-linked immunosorbent assay detects serum proteins at subfemtomolar concentrations. *Nat Biotechnol*. 2010;28(6):595–9. doi:10.1038/nbt.1641.

81. Swank, R T, Munkres KD. Weight with Analysis Sodium of Oligopeptides Gel Sulfate by Electrophoresis in Polyacrylamide Dodecyl. *Anal Biochem*. 1971;39:462–477.

82. Affymetrix GeneChip. Available at: http://www.affymetrix.com.

83. Alvankarian J, Bahadorimehr A, Davaji B, Majlis BY, Member S. Issues and Challenges in Microfluidic Research Studies. In: *IEEE-ICSE*.; 2012:333–335.

84. Bahadorimehr A, Majlis BY, Kebangsaan U. FABRICATION OF GLASS-BASED MICROFLUIDIC DEVICES WITH PHOTORESIST AS MASK. *Inf MIDEM*. 2011;41(3):193–196.

85. Jr JTS, Cima MJ, Langer R. A controlled-releasemicrochip. *Lett to Nat*. 1999;397:335–338.

86. Martinez AW, Phillips ST, Whitesides GM. Three-dimensional microfluidic devices fabricated in layered paper and tape. *Proc Natl Acad Sci U S A*. 2008;105(50):19606–11. doi:10.1073/pnas.0810903105.

87. Anderson JR, Chiu DT, Jackman RJ, et al. Fabrication of topologically complex three-dimensional microfluidic systems in PDMS by rapid prototyping. *Anal Chem*. 2000;72(14):3158–64. Available at: http://www.ncbi.nlm.nih.gov/pubmed/10939381.

88. Kovacs GTA. *Micromachined Transducers Sourcebook*. New York: McGraw-Hill; 1998.

89. Sechi D, Greer B, Johnson J, Hashemi N. Three-Dimensional Paper-Based Micro fl uidic Device for Assays of Protein and Glucose in Urine. *Anal Chem*. 2013;85:10733–10737.

90. Liao Y, Song J, Li E, et al. Rapid prototyping of three-dimensional microfluidic mixers in glass by femtosecond laser direct writing. *Lab Chip*. 2012;12(4):746–9. doi:10.1039/c2lc21015k.

91. Ford SM, Davies J, Kar B, Qi SD, Mcwhorter S, Soper SA. Micromachining in Plastics Using X-Ray Lithography for the Fabrication of IVIicro- Electrophoresis Devices. *J Biomech Eng*. 1999;121:13–21.

92. Roberts M a, Rossier JS, Bercier P, Girault H. UV Laser Machined Polymer Substrates for the Development of Microdiagnostic Systems. *Anal Chem*. 1997;69(11):2035–42. doi:10.1021/ac961038q.

93. Espy HH. Mechanism The mechanism of wet-strength development in paper : a review. *Tappi J*. 1995;(April):90–99.

94. Ren X, Bachman M, Sims C, Li GP, Allbritton N. Electroosmotic properties of microfluidic channels composed of poly(dimethylsiloxane). *J Chromatogr B Biomed Sci Appl*. 2001;762(2):117–25.

95. Hu Y, Zhou S, Wu L. Surface mechanical properties of transparent poly(methyl methacrylate)/zirconia nanocomposites prepared by in situ bulk polymerization. *Polymer (Guildf)*. 2009;50(15):3609–3616. doi:10.1016/j.polymer.2009.03.028.

96. Klank H, Kutter JP, Geschke O. CO(2)-laser micromachining and back-end processing for rapid production of PMMA-based microfluidic systems. *Lab Chip*. 2002;2(4):242–6. doi:10.1039/b206409j.

97. McCormick RM, Nelson RJ, Alonso-Amigo MG, Benvegnu DJ, Hooper HH. Microchannel electrophoretic separations of DNA in injection-molded plastic substrates. *Anal Chem*. 1997;69(14):2626–30. Available at: http://www.ncbi.nlm.nih.gov/pubmed/9341052.

98. Carrozza MC, Menciassi a, Tiezzi G, Dario P. The development of a LIGA-microfabricated gripper for micromanipulation tasks. *J Micromechanics Microengineering*. 1998;8(2):141–143. doi:10.1088/0960-1317/8/2/024.

99. Jillek W, Yung WKC. Embedded components in printed circuit boards: a processing technology review. *Int J Adv Manuf Technol*. 2005;25(3-4):350–360.

100. Wright, Therese Lawlor Gallagher C. Development of a printed circuit board design for in-circuit test advisory system. *Comput Ind*. 1997;33(2-3):253–259.

101. Wu LL, Babikian S, Li G-P, Bachman M. Microfluidic printed circuit boards. In: *2011 IEEE 61st Electronic Components and Technology Conference (ECTC)*. Ieee; 2011:1576–1581. doi:10.1109/ECTC.2011.5898721.

102. Merkel T, Graeber M, Pagel L. A new technology for fluidic Microsystems based on PCB technology. *Sensors and Actuators*. 1999;77:98–105.

103. Wego A, Richter S, Patel L. Fluidic Microsystems based on printed circuit board technology. *J Micromechanics Microengineering*. 2001;11:528–531.

104. Fair RB. Digital microfluidics: Is a true lab-on-a-chip possible? *Microfluid Nanofluidics*. 2007;3:245–281.

105. Shapiro AL, Vinuela E, Maizel J V. Molecular weight estimation of polypeptide chains by electrophoresis in SDS-polyacrylamide gels. *Biochem Biophys Res Commun*. 1967;28:815–820.

106. Hames B. *Gel Electrophoresis of proteins practical approach*. 2nd ed. (Hames B, Rickwood D, eds.). IRL Press; 1983:1.

107. Baldomero O, Baine P, Davidson N. Electrophoresis of the Nucleic Acids. *Biopolymers*. 1964;2(3108):245–257.

108. Raymond S, Weintraub. L. Acrylamide gel as a supporting medium for zone electrophoresis. *Science (80-)*. 1959;130(711).

109. Smith BJ. SDS Polyacrylamide gel electrophoresis of proteins. In: *Methods in molecular biology*. Humana Press; 1984:41–55.

110. Ferguson KA. Starch-gel electrophoresis-application to the classification of pituitary proteins and polypeptides. *Metabolism*. 1964;13(10):985–1002.

111. Wu D, Qin J, Lin B. Electrophoretic separations on microfluidic chips. *J Chromatogr A*. 2008;1184(1-2):542–59. doi:10.1016/j.chroma.2007.11.119.

112. Liu J, Yang S, Lee CS, DeVoe DL. Polyacrylamide gel plugs enabling 2-D microfluidic protein separations via isoelectric focusing and multiplexed sodium dodecyl sulfate gel electrophoresis. *Electrophoresis*. 2008;29(11):2241–50. doi:10.1002/elps.200700608.

113. Hatch A V, Herr AE, Throckmorton DJ, Brennan JS, Singh AK. Integrated preconcentration SDS-PAGE of proteins in microchips using photopatterned cross-linked polyacrylamide gels. *Anal Chem*. 2006;78(14):4976–84. doi:10.1021/ac0600454.

114. Song S, Singh AK, Kirby BJ. Electrophoretic concentration of proteins at laser-patterned nanoporous membranes in microchips. *Anal Chem*. 2004;76(15):4589–92. doi:10.1021/ac0497151.

115. Okada H, Kaji N, Tokeshi M, Baba Y. Poly(methylmethacrylate) microchip electrophoresis of proteins using linear-poly(acrylamide) solutions as separation matrix. *Anal Sci*. 2008;24(3):321–5.

116. Bousse L, Mouradian S, Minalla A, Yee H, Williams K, Dubrow R. Protein sizing on a microchip. *Anal Chem*. 2001;73(6):1207–12.

117. Kuschel M, Neumann T, Barthmaier P, Kratzmeier M. Use of lab-on-a-chip technology for protein sizing and quantitation. *J Biomol Tech*. 2002;13(3):172–8.

118. Goetz H, Kuschel M, Wulff T, et al. Comparison of selected analytical techniques for protein sizing, quantitation and molecular weight determination. *J Biochem Biophys Methods*. 2004;60(3):281–93. doi:10.1016/j.jbbm.2004.01.007.

119. Pai J-H, Wang Y, Salazar GT, et al. Photoresist with low fluorescence for bioanalytical applications. *Anal Chem*. 2007;79(22):8774–80. doi:10.1021/ac071528q.

120. KEESOM, W.H., ZELENKA, R.L. CJR. A Zeta-Potential Model for Ionic Surfactant Adsorption on an Ionogenic Hydrophobic Surface. *J Colloid Interface Sci*. 1988;125(2):575–585.

121. Smith L, Hok B. A silicon self-aligned non-reverse valve. In: *TRANSDUCERS '91 International Conference on Solid-State Sensors and Actuators*.; 1991.

122. Wang XQ, Tai YC. A normally closed in-channel micro check valve. In: *Thirteenth Annual International Conference on Micro Electro Mechanical Systems*.; 2000:68–73.

123. Xie J, Yang X, Wang XQ, Tai YC. Surface micromachined leakageproof Parylene check valve. In: *14th IEEE International Conference on Micro Electro Mechanical Systems*.; 2001:539–542.

124. Oh KW, Ahn CH. A review of microvalves. *J Micromechanics Microengineering*. 2006;16(5):R13–R39. doi:10.1088/0960-1317/16/5/R01.

125. Esashi M, Shoji S, Nakano A. Normally closed microvalve and mircopump fabricated on a silicon wafer. *Sensors and Actuators*. 1989;20(1-2):163–169.

126. Esashi M. Integrated micro flow control systems. *Sensors Actuators A Phys*. 1990;21(1-3):161–167.

127. Kelly RT, Wang C, Rausch SJ, Lee CS, Tang K. Pneumatic microvalve-based hydrodynamic sample injection for high-throughput, quantitative zone electrophoresis in capillaries. *Anal Chem*. 2014;86(13):6723–9. doi:10.1021/ac501910p.

128. Cooksey G a, Atencia J. Pneumatic valves in folded 2D and 3D fluidic devices made from plastic films and tapes. *Lab Chip*. 2014;14(10):1665–8. doi:10.1039/c4lc00173g.

129. Zhang W, Lin S, Wang C, et al. PMMA/PDMS valves and pumps for disposable microfluidics. *Lab Chip*. 2009;9(21):3088–94. doi:10.1039/b907254c.

130. Li H., Roberts DC, Steyn JL, et al. Fabrication of a high frequency piezoelectric microvalve. *Sensors and Actuators*. 2004;(111):51–56.

131. Rogge, T, Rummler, Z. Schomburg W. Polymer micro valve with a hydraulic piezo-drive fabricated by the AMANDA process. *Sensors and Actuators*. 2004;(110):206–12.

132. Shao P, Rummler Z, Schomburg WK. Polymer micro piezo valve with a small dead volume. *J Micromech Microeng*. 2004;14:305–09.

133. Yang E-H, Lee C, Mueller J, George T. Leak-tight piezoelectric microvalve for high-pressure gas micropropulsion. *Micropropuls J Microelectromech Syst*. 2004;13:799–807.

134. Sutanto J, Hesketh PJ, Berthelot YH. Design, microfabrication and testing of a CMOS compatible bistable electromagnetic microvalve with latching/unlatching mechanism on a single wafer. *J Micromechanics Microengineering*. 2006;16(2):266–275. doi:10.1088/0960-1317/16/2/011.

135. Su Y, Chen W, Cui F, Zhang W. Analysis and Fabrication Process of an Electro-Magnetically Actuated Valveless Micropump With Two Parallel Flexible Diaphragms. *Proc Inst Mech Eng Part C J Mech Eng Sci*. 2005;219(9):1007–1014. doi:10.1243/095440605X31841.

136. Yanagisawa K, Kuwano H, Tago a. Electromagetically driven microvalve. *Microsyst Technol*. 1995;2(1):22–25. doi:10.1007/BF02739524.

137. Sadler DJ, Liakopoulos TM, Cropp J, Ahn CH, Henderson HT. Prototype microvalve using a new magnetic microactuator. 1998;3515(September):46–52.

138. Rich CA, Wise KD. A high-flow thermopneumatic microvalve with improved efficiency and integrated state sensing. *J Microelectromechanical Syst*. 2003;12:201–208.

139. Takao H, Miyamura K, Ebi H, Ashiki M, Sawada K, Ishida K. A MEMS microvalve with PDMS diaphragmandtwo-chamberconfigurationof thermo-pneumatic actuator for integrated blood test system on silicon. *Sensors Actuators A Phys*. 2005;(119):468–75.

140. Ho C-M, Yang X, Grosjean C, Tai Y-C. A MEMS thermopneumatic silicone rubber membrane valve. *Sensors Actuators A Phys*. 1995;64:101–8.

141. Bosh D, Heimhofer B, Muck G, Seidel H, Thumser U, W W. A silicon microvalve with combined electromagnetic/electrostatic actuation. *Sensors Actuators A Phys*. 1993;37:684–92.

142. Hua S., Sachs F, Yang D., Chopra HD. Microfluidic actuation using electrochemically generated bubbles. *Anal chem*. 2002;74:6392–6.

143. Liu R, Yu Q, Beebe D. Fabricationand characterization of hydrogel-based microvalves. *JMicroelectromechSyst*. 2002;11:45–53.

144. Richter, A, Kuckling D, Howitz S, Gehring T, K-F A. Electronically controllable microvalves based on smart hydrogels: magnitudes and potential applications. *J Microelectromechanical Syst*. 2003;12:748–753.

145. Takao H, Miyamura K, Ebi H, Ashiki M, Ishida M. A MEMS microvalve with PDMS diaphragm and two-chamber configuration of thermo-pneumatic actuator for integrated blood test system on silicon. *Sensors Actuators A Phys*. 2005;119:468–475.

146. Kohl M, Dittmann D, Quandt E, Winzek B. Thin film shape memory microvalves with adjustable operation temperature. *Sensors Actuators A Phys*. 2000;83(1-3):214–219. doi:10.1016/S0924-4247(99)00386-6.

147. Bae B, Han J, Masel RI, Shannon MA. A bidirectional electrostatic microvalve with icrosecond Switching Performance. *j mi*. 2007;16(6):1461–1471.

148. Legtenberg R, Gilbert J, Senturia SD, Elwenspoek M. Electrostatic curved electrode actuators. *J Microelectromechanical Syst*. 1997;6(3):257–265.

149. Terry SC, Jerman JH, Angell JB. A Gas Chromatographic Air Analyzer Fabricated on a Silicon Wafer. *IEEE Trans Electron*. 1979;26(12):1880–1886.

150. Capanu M, Boyd JG, Hesketh PJ. Design, fabrication, and testing of a bistable electromagnetically actuated microvalve. *J Microelectromechanical Syst*. 2000;9(2):181–189. doi:10.1109/84.846698.

151. Saedinia S, Nastiuk KL, Krolewski JJ, Li GP, Bachman M. Laminated microfluidic system for small sample protein analysis. *Biomicrofluidics*. 2014;8(1):014107–1–01407–15. doi:10.1063/1.4865675.